The Dissertation Committee for Jacob Cole Claussen
certifies that this is the approved version of the following dissertation:

The Deconstruction of Orbifold Fixed Points in Heterotic M-theory

Committee:

Vadim Kaplunovsky, Supervisor

Jacques Distler

Willy Fischler

Andrew Neitzke

Sonia Paban

The Deconstruction of Orbifold Fixed Points in Heterotic M-theory

by

Jacob Cole Claussen, B.A.

DISSERTATION

Presented to the Faculty of the Graduate School of

The University of Texas at Austin

in Partial Fulfillment

of the Requirements

for the Degree of

DOCTOR OF PHILOSOPHY

THE UNIVERSITY OF TEXAS AT AUSTIN

August 2016

Dedicated to my wife and best friend Blair.

Acknowledgments

This material is based upon work supported by the National Science Foundation under Grant Number PHY-1316033.

I should start with my debt of gratitude to the theory group faculty. I'd obviously like to thank my supervisor Vadim Kaplunovsky for getting this project off the ground in the first place and laying the foundation from which I could work. I'd also like to thank Jacques Distler for introducing me to string theory, M-theory, and the oddities of attempting to dualize phenomena between the two. To Willy Fischler, I want to say that it has been a pleasure owning the halls of RLM together in the hours before eight o'clock in the morning. To Sonia Paban, I am grateful that your door has always been open to me when I needed to talk to you, a courtesy you selflessy extend to anyone in need your assistance. And to Andrew Neitzke, it is through you that I got my first taste of quantum field theory in the context of geometry, without which I would have been lost all of these years. Along with the rest of the faculty here, you have provided the entire theory group with your sage advice when we inevitably hit a wall in our work and we are all extremely grateful for your leadership.

Throughout my years here, I have also had the pleasure of meeting many people who have lent me tremendous support in my times of dire need

and helped me bear the burden of my other duties so that I could focus on my research. I am forever grateful to Matt Ervin for everything he's done; some day I will convince him that I actually do my own hair and not my wife. Lisa Gentry, the fixture of my morning copy runs, has always been there to help me with my instructing duties, and I am glad she waited till I was leaving to do so herself. Of course no day is complete without my regular "good morning" from Jan Duffy, nor is it complete without running to her at least ten times with some silly problem with which she is always more than happy to assist. Finally, in this regard I would like to thank Austin Gleeson, who throughout my graduate studies has managed to be an instructor, manager, advocate, mentor, and dear friend.

I have enjoyed this time with my nose buried in my research, but I know that it is difficult on the people in my personal life, so I also think it is important to thank them for putting up with my relative absence all of these years. My friends have always been a gift to me, and I am thankful that they have stuck it out with me, even after long periods of telling them I was just too busy. But most importantly, my family at home in Illinois deserves my appreciation for all that they have done for me. Over the course of my studies, I have lost some of these wonderful people who I have known my whole life and raised me in my tight-knit community. As difficult as this has been on the entire family, there has always been an outpoor of support for me. And now, with a pile of little ones on the way, I look forward to spending more time with them in the years to come.

Finally, I would probably get in trouble if I didn't have a paragraph set aside for my wife, Blair, to whom I have dedicated this. Before agreeing to file our taxes jointly, we were best friends and have been since. Where I go, she goes. Where she goes, I go. She has understood what this means to me and has accommodated my needs far beyond what is reasonable at times. As this experience comes to a close, I think it would be appropriate to recite a beautiful line of prose for her about the things to come in our future together. However, as that is not the style of our relationship, I will instead recite a quote by Frank Costanza from the hit TV show Seinfeld: *"Serenity now, serenity now..."*

The Deconstruction of Orbifold Fixed Points in Heterotic M-theory

Publication No. _____

Jacob Cole Claussen, Ph.D.
The University of Texas at Austin, 2016

Supervisor: Vadim Kaplunovsky

The compactification of $E_8 \times E_8$ heterotic string theory on orbifolds of the form $T^6/\mathbb{Z}_N$ produces a 4D spectrum of untwisted states and twisted states. Unlike the untwisted states, the twisted states are confined to the fixed points of the $\mathbb{Z}_N$ action and can be charged under subgroups of both E_8 gauge groups simultaneously. While insignificant in the string theory case, dualizing to heterotic M-theory yields a peculiar phenomenon. Specifically, in heterotic M-theory the E_8 gauge groups are isolated from each other by an extra dimension with 11D supergravity in the bulk between them. Determining how states can be charged across this bulk becomes a highly nontrivial problem to solve. We propose a procedure that utilizes deconstruction to probe these fixed points and build the appropriate states in the continuum limit. We then analyze and apply this procedure to the $\mathbb{Z}_3$, $\mathbb{Z}_4$, $\mathbb{Z}_{6-I}$, and $\mathbb{Z}_7$ orbifolds.

Table of Contents

Acknowledgments **v**

Abstract **viii**

Chapter 1. Introduction **1**

Chapter 2. Orbifolds **6**
2.1 Untwisted Sector 9
2.2 Twisted Sector 12

Chapter 3. Heterotic M-theory **14**
3.1 Orbifold limits of Calabi-Yau manifolds 16
3.2 Gauge mediation across the bulk 18

Chapter 4. Heterotic Orbifold Models in 6D **20**
4.1 Type-I' String Theory 22
4.2 (Multi-)Taub-NUT Geometry 24
4.3 Brane-Engineering the Fixed Points 25

Chapter 5. 5D Field Theory **30**
5.1 5D Gauge Theories from Type-I' String Theory 33
5.2 M-theory and Calabi-Yau Threefolds 37
5.3 Brane Webs 38

Chapter 6. Deconstruction **47**
6.1 Deconstructing SQCD on S^1 47
6.2 Deconstructing SQCD on $S^1/\mathbb{Z}_2$ 52

Chapter 7. $\mathbb{Z}_3$ Orbifold **54**
7.1 Deriving the Brane Web 58
7.2 The E_0 SCFT 59
7.3 Deconstructing the Fixed Point Theory 61
7.4 Spectrum at Blow-down 65
7.5 Interpretation 70

Chapter 8. $\mathbb{Z}_4$ Orbifold **74**
8.1 Deriving the Brane Web 80
8.2 Deconstructing the Fixed Point Theory 81
8.3 Spectrum at Blow-down 83
8.4 Interpretation 86

Chapter 9. $\mathbb{Z}_{6-I}$ Orbifold **89**
9.1 Deriving the Brane Web 94
9.2 Deconstructing the Fixed Point Theory 95
9.3 Spectrum at Blow-down 97
9.4 Interpretation 99

Chapter 10. Z_7 Orbifold **104**
10.1 Deriving the Brane Web 105

Chapter 11. Future Directions **109**

Bibliography **111**

Chapter 1

Introduction

There has long been a rich history of dualities between string theories. These connections manifested fully, however, with the seminal work of Edward Witten [1]. Here he introduced the concept of M-theory, a mysterious theory of which all string theories and 11D supergravity are limiting cases. The dualities are then simple underlying transforms in this mysterious theory. Under this proposal, type-I and $SO(32)$ heterotic string theories are S-dual, so that the weak-coupling limit of one is the strong-coupling limit of the other. Type-IIB string theory is actually self-dual in this respect, though it's relationship with type-IIA string theory was well established [2, 3] and type-I is simply an orientifold projection of type-IIB. One of the biggest surprises, however, was that the strong coupling limit of type-IIA string theory was found to be dual to 11D supergravity compactified on a circle, where the size of this extra dimension was related to the coupling. Despite all of this, the paper concluded without a proper conjecture for the strong coupling limit of the last remaining theory, $E_8 \times E_8$ heterotic string theory.

In subsequent work by Hořava and Witten [14, 15], this strong coupling limit was explored in more depth and it was found to be related to 11D super-

gravity again. This time, however, they found that the 11D theory needed to be compactified on an interval with particular boundary conditions on the supergravity multiplet fields. Consistency with anomalies due to these boundary conditions then forced the presence of 10D E_8 gauge fields fixed at each of the boundaries. This theory reduces to heterotic supergravity as the size of the interval vanishes, so yet again the size of this extra dimension can be related to the string coupling. To be consistent, one would expect phenomena in one of the theories to have a dual explanation in the other. One such example of particular interest here is the compactification of the heterotic string on orbifolds and the resulting spectrum.

Orbifolds are interesting compactification structures [4, 5]. Constructed by twisting a torus by some group action, orbifolds carry most of the conveniences of tori in terms of compactification but with many more desirable features, such as a realistic amount of supersymmetry. Furthermore, they can also be interpreted as singular limits of Calabi-Yau manifolds, so that much of the associated machinery for them can be applied directly or adapted to orbifolds. As advantageous as these compactifcation schemes are in string theory, and specifically $E_8 \times E_8$ heterotic string theory, one major point of interest would be to translate them to the dual 11D supergravity theory and study the theory across this transition.

As it turns out, this transition is fairly clean for much of the theory. This is a reflection of the relative simplicity of the geometry and the resulting ease in solving the string worldsheet theory to generate the perturbative

spectrum for such models. Much of the geometry in the string theory simply carries over to the 11D supergravity theory and so their is little to explore. However, upon inspection of the individual models, there are certain instances in which states are produced in the string picture that do not have trivial dualizations into the 11D supergravity theory. These states have gauge charges under subgroups of each E_8, a unimpressive feat in the string theory interpretation. However, upon dualization to the 11D theory, the E_8 gauge groups become separated by the extra dimension, and so any state charged under both must somehow be charged across the bulk of the interval. The bulk theory is simply 11D supergravity, and so one is forced to conclude that either supergravity is able to mediate between the gauge groups at these points of singular curvature to charge states locally across the bulk, or else the local states on the string theory side have nonlocal origins on the 11D supergravity side. As it turns out, both of these options will end up holding some validity, depending on the dimension of the orbifold.

This work is organized as follows. First, we will discuss some general features of these orbifolds, including the procedure for forming them and the resulting spectra. Next, we will present a more detailed account of the duality between the heterotic string and 11D supergravity, which we will simply refer to as M-theory and the compactified theory as heterotic M-theory for convenience. Our main goal throughout this work will be to reverse the order of compactification so that we first compactify on the orbifold, then the interval. As is often the case, this is simpler when compactified to 6D rather than 4D, so

we next introduce this case with a pertinent example and describe the solution in terms of brane engineering. We will find that this machinery does not easily translate to 4D, as the effective theory being compactified on an interval is no longer simply a 7D gauge theory. Instead, it will be a 5D superconformal field theory, as we will discuss. Throughout our discussion of 5D field theory, we will begin building our procedure for forming the twisted states in question, bringing in toric diagrams and dual brane webs to develop 5D gauge theories at the resolved fixed points. To compactify these theories, we will introduce another method, deconstruction, that lends itself quite well to this. We then have a standard method with which to tackle each orbifold fixed point: resolve the singularity, look at the resulting toric diagram, dualize to a brane web, deconstruct the resulting gauge theory, set the deconstruction quiver on an interval rather than a circle, and observe the resulting 4D spectrum as we approach the appropriate limits of parameter/moduli space. We then apply this to the $\mathbb{Z}_3$, $\mathbb{Z}_4$, $\mathbb{Z}_{6-I}$, and $\mathbb{Z}_7$ orbifolds.

Before we proceed however, there are two main caveats to this work that we must address. First, it is important to note that there are additional consistent orbifolds to which we will not apply this procedure. The $\mathbb{Z}_{6-II}$, $\mathbb{Z}_{8-I}$, $\mathbb{Z}_{8-II}$, $\mathbb{Z}_{12-I}$, and $\mathbb{Z}_{12-II}$ orbifolds have the unfortunate property that, unlike the orbifolds we do consider, they all have multiple resolutions of their fixed points. These resolutions are all related to each other by flop transitions, and flops are captured by the deconstruction procedure, so it seems reasonable that these theories could be described within our framework. However, one

must crawl before they can walk, and so we restrict ourselves to the simpler analyses.

The second major caveat has to deal with the presence of anomalous $U(1)$'s in the compactified 4D theories. These anomalies are canceled by a 4D remnant of the Green-Schwarz mechanism [6]. However, the presence of this term in 4D causes a quadratically-divergent Fayet-Iliopoulos term to arise at one-loop order [7]. This introduces D-terms which can force VEV's on fields and actually drive us away from the very fixed points we are trying to study, rendering our analysis inapplicable [8]. As a result, we will only focus on models that present twisted states of interest and have no anomalous $U(1)$'s.

Chapter 2

Orbifolds

The orbifolds of interest for our model building are constructed from 6D tori. Starting with $\mathbb{C}^3$, we ask that its coordinates z^m, $m = 1, 2, 3$, be invariant under a specific set of complex translations,

$$z^m \to z^m + v^m. \tag{2.1}$$

We will be considering specific examples in which these translations form 6D root lattices Λ of (combinations of) Lie groups, so that we are essentially modding by Λ,

$$T^6 = \mathbb{C}^3/\Lambda. \tag{2.2}$$

This is important to the construction, because only a few root lattices can consistently lend themselves to our orbifolds. When performing the orbifolding procedure to follow, we will assume that we have already identified the correct root lattice for a specific orbifold.

Given the proper torus, we can now attempt to "fold" it. This is achieved by twisting the torus by the action of some group G, known as the point group. The twists θ (along with the tori translations v) act on the coordinates of $\mathbb{C}^3$ as

$$z^m \to \theta^{mn} z^n + v^m, \tag{2.3}$$

and so an orbifold must necessarily be invariant under this action. This requires that we mod the torus by G,

$$T^6/G = (C^3/\Lambda)/G. \tag{2.4}$$

In this manner, it is clear to see why not just any Λ will work; Λ and G must be consistent to ensure that their actions are not coprime on $\mathbb{C}^3$.

The orbifolds considered here have point groups

$$G = \mathbb{Z}_N = \{h \in \mathbb{C} : h^N = 1\}. \tag{2.5}$$

We can choose the coordinate basis so as to diagnolize the corresponding twists θ. They then take the rather simple form

$$\theta^{mm} = \theta^m = e^{(2\pi i \phi_m)}, \quad \phi_m = \frac{r_m}{N} \tag{2.6}$$

for some vector of integers $\vec{r}$. This vector is known as the twist vector for the point group, while $\vec{\phi}$ is known as the normalized twist vector. A specific choice of this twist vector for given $\mathbb{Z}_N$ does not seem obvious from what we have done so far. In fact, there is no specific choice from a geometric point of view. However, consistency with heterotic string theory will impose some very tight constraints on the forms allowed for $\vec{r}$, and limit us to only a few viable cases. Since we must discuss the heterotic string theory implications, let's first discuss how this twisting can act on the gauge group present.

The heterotic string is a combination of a right-moving type-II superstring and a left-moving bosonic string. The extra sixteen dimensions in the

left-moving string are wrapped on an $E_8 \times E_8$ root lattice to form a 16D torus, so we can imagine the twisting group acting on these dimensions as well. While it can act on it trivially, preserving the whole $E_8 \times E_8$ gauge symmetry, in general it will break this gauge symmetry to some subgroup. We can use the generators λ^K of the Cartan subalgebra $U(1)^{16}$ as coordinates in $\mathbb{C}^{16}$, then ask that they be invariant under $\mathbb{Z}_N$ gauge twists:

$$\lambda^K \to e^{2\pi i \beta_K} \lambda^K, \quad \beta_K = \frac{s_K}{N} \tag{2.7}$$

for some 16-vector of integers $\vec{s}$ known as the gauge shift vector ($\vec{\beta}$ would be the normalized gauge shift vector).

We now have two piece of information to parametrize the action of the point group on a torus: a twist vector $\vec{r}$ and a gauge shift vector $\vec{s}$. These must act similarly on the worldsheet fields z^m, $\widetilde{\psi}^m$, and λ^K, as well as their resulting modes. Specifically, for the modes of the R sector of $\widetilde{\psi}^m$, the mode numbers altered by these shifts[1]:

$$\widetilde{\psi}^m : n \to n - \phi_m, \quad \widetilde{\psi}^{\overline{m}} : n \to n + \phi_m. \tag{2.8}$$

Because the R sector is in the spinor representation, it will have eigenvalue

$$\frac{1}{2} \sum_{m=1}^{3} \phi_m. \tag{2.9}$$

[1]This shift in mode numbers actually extends across all worldsheet oscillators, but we are only concerned with the R sector for our purposes. Consult [5] for a fuller treatment.

A similar argument for the R sector of λ^K in the current algebra yields an eigenvalue in each E_8:

$$\frac{1}{2}\sum_{K=1}^{8}\beta_K, \quad \frac{1}{2}\sum_{K=9}^{16}\beta_K. \tag{2.10}$$

For $\mathbb{Z}_N$ to properly twist the theory, we must demand

$$\frac{1}{2}\sum_{m=1}^{3}\phi_m = \frac{1}{2}\sum_{K=1}^{8}\beta_K = \frac{1}{2}\sum_{K=9}^{16}\beta_K = 0 \text{ mod } 1. \tag{2.11}$$

Without getting too far into the underlying string theory, a slightly more intensive argument involving the level-matching condition [5] gives another constraint on the allowed forms of $\vec{r}$ and $\vec{s}$:

$$\sum_{m=1}^{3}\phi_m^2 - \sum_{K=1}^{16}\beta_K^2 = 0 \text{ mod } 2N. \tag{2.12}$$

Equipped with these equations, eqs. (2.11) and (2.12), we can now define all possible orbifolds. Table 2.1 contains a full list of consistent $T^6/\mathbb{Z}_N$'s, along with the necessary root lattice for the corresponding T^6.

2.1 Untwisted Sector

To see how the gauge shift vectors act on each E_8 gauge group, we will first need to consider the root system. This can be generated in $\mathbb{R}^8$ as the set of all 8-vectors with length squared equal to 2, coordinates either all integers or all half-integers, and sum of the coordinates even. The case with all integer

Point Group	Normalized Twist Vector	Root Lattice Group
$\mathbb{Z}_3$	$\left(\frac{1}{3}, \frac{1}{3}, -\frac{2}{3}\right)$	$SU(3) \times SU(3) \times SU(3)$
$\mathbb{Z}_4$	$\left(\frac{1}{4}, \frac{1}{4}, -\frac{2}{4}\right)$	$SO(5) \times SO(5) \times SU(2) \times SU(2)$
$\mathbb{Z}_{6-I}$	$\left(\frac{1}{6}, \frac{1}{6}, -\frac{2}{6}\right)$	$G_2 \times G_2 \times SU(3)$
$\mathbb{Z}_{6-II}$	$\left(\frac{1}{6}, \frac{2}{6}, -\frac{3}{6}\right)$	$G_2 \times SU(3) \times SU(2) \times SU(2)$
$\mathbb{Z}_7$	$\left(\frac{1}{7}, \frac{2}{7}, -\frac{3}{7}\right)$	$SU(7)$
$\mathbb{Z}_{8-I}$	$\left(\frac{1}{8}, \frac{2}{8}, -\frac{3}{8}\right)$	$SO(5) \times SO(9)$
$\mathbb{Z}_{8-II}$	$\left(\frac{1}{8}, \frac{3}{8}, -\frac{4}{8}\right)$	$SO(9) \times SU(2) \times SU(2)$
$\mathbb{Z}_{12-I}$	$\left(\frac{1}{12}, \frac{4}{12}, -\frac{5}{12}\right)$	$F_4 \times SU(3)$
$\mathbb{Z}_{12-II}$	$\left(\frac{1}{12}, \frac{5}{12}, -\frac{6}{12}\right)$	$F_4 \times SU(2) \times SU(2)$

Table 2.1: The point group, normalized twist vector, and root lattice group for each allowable orbifold. Technically, there are actually more root lattices allowed for some of the $\mathbb{Z}_N$ point groups. However, these can be seen as specific subcases with tighter constraints on the Wilson lines [37]. The root lattices listed here are the most general.

coordinates must have the form

$$\begin{aligned} \text{Root}_{D_8}: \quad & (\underline{+1, +1, 0^6}), \\ & (\underline{+1, -1, 0^6}), \\ & (\underline{-1, +1, 0^6}), \\ & (\underline{-1, -1, 0^6}), \end{aligned} \tag{2.13}$$

where the underline denotes permutations of the entries. This generates $4 \times \binom{8}{2} = 112$ roots, which form the root system for $D_8 = SO(16)$. The remaining roots must have all half-integer coordinates that sum to an even number. This

is only achieved if there is an even number of positive entries, so these must have the form

$$\begin{aligned}\text{Spinor}_{D_8}: \quad & (+\frac{1}{2}^8), \\ & (+\frac{1}{2}^6, -\frac{1}{2}^2), \\ & (+\frac{1}{2}^4, -\frac{1}{2}^4), \\ & (+\frac{1}{2}^2, -\frac{1}{2}^6) \\ & (-\frac{1}{2}^8).\end{aligned} \tag{2.14}$$

There are $\binom{8}{8} + \binom{8}{6} + \binom{8}{4} + \binom{8}{2} + \binom{8}{0} = 128$ of these roots[2] for a total of 240 roots. Along with the $\text{rank}(E_8) = 8$ Cartan generators, these form the 248-dimenstional adjoint representation of E_8 under which the 10D gauge fields transform.

The 16D gauge shift vector can actually be broken up into two 8D shift vectors, one corresponding to each E_8. Taking one of these vectors, $\vec{s}_1$, we can now act on all of the roots $\vec{R}$ of the E_8 root system by

$$\vec{s}_1 \cdot \vec{R} = \sum_{i=1}^{8} s_{1,i} R^i. \tag{2.15}$$

From a geometric point of view, we generically have no preferential direction in $\mathbb{R}^8$ for the E_8 root system. The shift vector establishes a preference and then asks how much of each root vector is along that direction by using the dot product. This now distinguishes the roots from each other and breaks the

[2]These actually form the spinor representation of $SO(16)$.

gauge symmetry based on the values of this dot product. Resulting products that are integers are perpendicular to this direction and so survive as the remaining gauge symmetry. Roots with products that are not integers project onto the shift vector direction, and form chiral fields that are charged under the preserved gauge symmetry. These chiral fields are not twisted by the orbifold, simply projected down onto the preferential direction that the orbifold established by acting on the gauge bundle nontrivially. As a result, these states are referred to as the untwisted sector of the spectrum.

2.2 Twisted Sector

In addition to untwisted matter descended from the 10D theory, there are states that are true, lower-dimensional states generated by the orbifolding procedure. From a physical point of view, this can be viewed as open strings on the torus. The point group of the orbifold identifies points on the torus, so an open string on the torus stretched between two points identified under the point group action will be a closed string on the orbifold. The closed string then generates massless states which we identify as the twisted sector of the spectrum.

From a string worldsheet point of view, this can be seen as the result of the modified mode numbers for the oscillators, allowing them to form new massless combinations that are normally not so with their original mode numbers. These states have zero momentum in the compactified directions of the orbifold because they are stuck at the fixed points, but propogate in the

noncompact dimensions. For a treatment of the calculation of the spectra for each orbifold, consult [38].

One natural extension of the above arguments is to k-twists. Specifically, consider an element $h \in \mathbb{Z}_N$. By definition, we know $h^N = 1$, but this implies that

$$h^{2N} = h^{3N} = h^{4N} = ... = h^{(N-1)N} = 1. \tag{2.16}$$

In other words, the twist can be applied multiple times and still maintain the necessary consistency condition. As it turns out, each k-twisted sector is capable of having its own spectrum for $k \in [1, N-1]$, though the k- and $(N-k)$-twisted sectors are chiral conjugates of each other. Also, the 0-twisted sector and N-twisted sector are equivalent and correspond to the untwisted sector.

We will see later in specific examples that these various twisted sectors can have complicated overlying fixed structures. On top of the fixed points that are invariant under the action a k-twist, there can be fixed tori or fixed lower-dimensional orbifolds under a different k-twist. These lower-dimensional orbifolds can have the fixed points of the original k-twist as its fixed points as well, introducing geometric complexity. From a string theory point of view, however, these are all equally simple spectra to calculate, and a brief investigation of the geometry reveals the multiplicity of each state.

Chapter 3

Heterotic M-theory

It has been well established that, similar to type IIA supergravity, the strong coupling limit of $E_8 \times E_8$ heterotic supergravity can be related to an 11D supergravity theory [14, 15]. The bosonic part of the action for this theory takes the simple form

$$S_{SG} = -\frac{1}{2\kappa^2} \int_{\mathcal{M}_{11}} \sqrt{-g} \left(R + G \cdot G + C \wedge G \wedge G \right), \tag{3.1}$$

where C is a 3-form in the graviton supermultiplet with field strength $G = dC$. This supergravity theory is interpreted as an effective field theory in the low-energy limit of M-theory, just as 10D supergravity theories correspond to string theories. Out of convenience, we will refer to this 11D supergravity theory as M-theory henceforth.

In order to make contact between M-theory and heterotic string theory, we must compactify the extra dimension present in M-theory. The choice of surface to compactify on must break half of the supersymmetry present, otherwise the 11D $\mathcal{N} = 1$ supersymmetry will compactify to 10D $\mathcal{N} = 2$ supersymmetry instead of $\mathcal{N} = 1$ as needed for heterotic supergravity. The simplest manner in which to achieve this is to compactify M-theory on an interval, $S^1/\mathbb{Z}_2$. Here $\mathbb{Z}_2$ acts on S^1 by $x^{10} \to -x^{10}$. For this to be a symmetry

of the action, it is required that C also be odd under the $\mathbb{Z}_2$ action, $C \to -C$, while the metric g must be even. In terms of components, these conditions take the form:

$$\begin{gathered} g_{IJ}, g_{10,10}, C_{IJ10} \to g_{IJ}, g_{10,10}, C_{IJ10}, \\ g_{I,10}, C_{IJK} \to -g_{I,10}, -C_{IJK}, \end{gathered} \tag{3.2}$$

where the indices $I, J, K, ... = 0, ..., 9$ denote the ten dimensions perpendicular to the compactified dimension, x^{10}.

The action of $\mathbb{Z}_2$ on S^1 has two fixed points, $\{0, \pi R\}$, corresponding to the ends of the interval. These 10D surfaces must have boundary conditions for the fields that are consistent with the the $\mathbb{Z}_2$ action on them. This implies that there will be 10D zero modes for the even fields, but not for the odd fields which must vanish at the boundaries. Unfortunately, the presence of these modes at the boundaries introduces anomalies to our theory, which we would hope to cancel with the addition of other fields. Since the theory in the bulk of the interval is just 11D supergravity, it is anomaly free there and there are no 11D fields that can be added to cancel the anomaly. Since the anomaly is concentrated at the 10D boundaries, it makes sense to try adding matter specifically to these boundaries, namely 10D vector multiplets. There are 248 vector multiplets needed at each boundary to cancel the anomaly, which is the dimension of the adjoint representation of E_8. Thus, we conclude that each boundary has an E_8 gauge multiplet present on it. Because these 10D surfaces are important and mentioned quite frequently, we will err on the side of convenience and refer to them as M9-branes, which will be slightly more in line with our discussion of M-branes below.

There are further complications that arise from this anomaly cancellation, requiring the mixing of gauge and gravity terms at the M9-branes, specifically in the Bianchi identity for G. However, as these considerations are beyond our scope, we can just focus on the relatively simple picture before us. At strong coupling, heterotic string theory looks like M-theory compactified on an interval. There are two 10D E_8 gauge multiplets, one at each boundary separated by the 11D bulk. As the coupling becomes weak, the size of this interval becomes small and the two boundaries become coincident. In this limit, the theory looks ten-dimensional with a gauge group $E_8 \times E_8$, as is required for the heterotic theory.

The orbifold models we have considered above now have an M-theory interpretation: we compactify it on an interval, drive the interval width to zero, compactify this theory on the 6D orbifold of our choice, and then observe the resulting spectrum. This interpretation need not be the only path to our spectrum, though. There is nothing to stop us from instead compactifying M-theory on the 6D orbifold first and then the interval. Our spectrum should not depend on the order in which these steps are taken, so it would be interesting to investigate this alternative method and confirm its consistency. This procedure comes with a two major issues, however, and we must address each one.

3.1 Orbifold limits of Calabi-Yau manifolds

The first major concern involves the orbifolds themselves. In string theory terms, orbifolds are simple geometries with well-defined worldsheet confor-

mal field theories and hence are perfectly consistent. However, geometrically we cannot compactify M-theory on an orbifold; since it has points of singular curvature, it does not even qualify as a manifold! Thus, in order to consider this situation we must first define what we even mean by "compactifying M-theory on an orbifold." Let's illustrate this with an example with which we will become quite familiar: the $\mathbb{Z}_3$ orbifold. The origin of this orbifold as a T^6 with some $\mathbb{Z}_3$ action suggests that it has zero curvature away from the fixed points, and 27 fixed points with singular curvature. Since the root lattice and point group actions commute, it is easy to see that the fixed points of $T^6/\mathbb{Z}_3$ have the same structure as the single fixed point of $\mathbb{C}^3/\mathbb{Z}_3$, namely that of a complex projective plane $\mathbb{CP}^2$ blown down to a point (for a good review and applications, see [32]). Blowing this point back up to a $\mathbb{CP}^2$ has the effect of smearing the singular curvature, and blowing up all of the points of the orbifold in this manner results in a smooth Calabi-Yau threefold on which we can geometrically compactify M-theory. The sizes of these blown-up $\mathbb{CP}^2$'s are tunable parameters, and driving them back down to zero returns our original orbifold. Thus, as we discuss "compactifying M-theory on an orbifold" what we actually mean is "compactifying M-theory on a Calabi-Yau threefold that has as an orbifold as its singular limit when certain parameters are varied appropriately." We shall return to this topic in more depth later, after having discussed some of the features of the resulting 5D theories that can arise.

3.2 Gauge mediation across the bulk

The other major issue to consider is how the emergence of this bulk dimension at strong coupling will effect the gauge charging of states. Specifically, anomaly cancellation requires that their be an E_8 gauge theory confined to each M9-brane at the end of the interval, while in the bulk between these theories we simply have 11D supergravity. Therefore, the gauge fields are completely isolated from each other, with only gravity playing mediator between them. Any state charged under one of the E_8's or some subgroup of it will reasonably be localized to that end of the interval, as is clear when considering the untwisted sectors of the orbifold models. However, when we attempt to transfer this logic to the twisted sector of these same orbifold models, we find an immediate obstruction: there are states present that are charged under (subgroups of) both E_8's! On which end are these states localized? Are they localized at all? and how are they capable of being mysteriously charged across the bulk? These are the questions that we seek to answer as we carry on through this work.

It is worth noting one important feature of this interpretation. Just like its string theory counterparts, M-theory has extended objects, or branes, that couple to the 3-form C and it's dual 6-form $*C$, namely the M2-brane and M5-brane. The M2-branes are capable of wrapping on any (real) 2-cycles in the blown-up fixed point geometry to create electrically-charged particles with masses proportional to the size of the blow-up. Similarly, the M5-branes are capable of wrapping on the entire 4-cycle of the blown-up fixed point to create

magnetically-charged strings with tension proportional to the square of the size. Thus, as we approach the orbifold limit, the particles become massless and the strings become tensionless. The presence of these massless states is interesting, but they are not capable of accounting for the curious states in the spectra that we find in the string theory case.

As it turns out, the case of M-theory compactified on $T^4/\mathbb{Z}_N$ and its corresponding 6D theory has already been studied in [21, 22]. Due to its ease and the relevence of some of its results, we will review this presentation for the specific case where $N = 2$. For more examples, see the references.

Chapter 4

Heterotic Orbifold Models in 6D

4D orbifolds start with a rank-4 root lattice acting on $\mathbb{C}^2$ to produce a torus. This torus is then acted on by a twist to further identify points. For a $\mathbb{Z}_2$ twist, we need the $SU(2)^4$ root lattice, and normalized twist vector $\vec{\phi} = (\frac{1}{2}, \frac{1}{2})$. Each complex dimension has four fixed points under this twist and root lattice action, for a total of $4 \times 4 = 16$ fixed points on the whole orbifold.

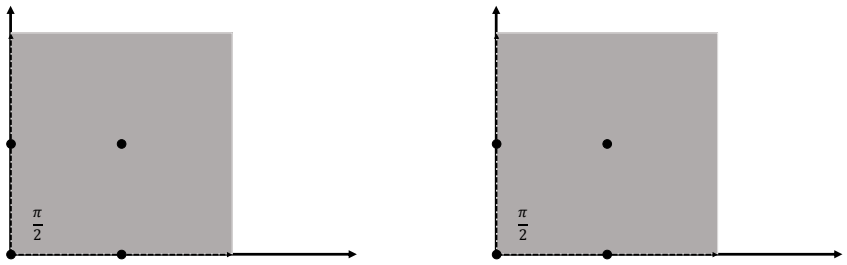

(a) $SU(2) \times SU(2)$ (b) $SU(2) \times SU(2)$

Figure 4.1: The root lattice for each coordinate z^i. The gray region signifies the fundamental domain of the torus in each complex dimension. The solid points are the fixed points of the $\mathbb{Z}_2$ action.

The only consistent E_8 gauge symmetry breaking patterns are $E_8 \to E_7 \times SU(2)$ and $E_8 \to SO(16)$. The gauge shift vectors and modular invariant

combinations of gauge groups are listed in Table 4.1, along with the twisted and untwisted spectra for each model. From this table we can see that there is a state charged under both E_8's, meaning it will somehow need to be charged across the bulk in the heterotic M-theory picture.

Normalized Shift Vector	Gauge Group	Untwisted Spectrum	Twisted Spectrum
$\frac{1}{2}(1^2,0^6),\frac{1}{2}(0^8)$	$E_7\times SU(2)\times E_8'$	$(\mathbf{56},\mathbf{2};\mathbf{1})$	$\frac{1}{2}(\mathbf{56},\mathbf{1};\mathbf{1})+4(\mathbf{1},\mathbf{2};\mathbf{1})$
$\frac{1}{2}(1^2,0^6),\frac{1}{2}(2,0^7)$	$E_7\times SU(2)\times SO(16)'$	$(\mathbf{56},\mathbf{2};\mathbf{1})+(\mathbf{1},\mathbf{1};\mathbf{128}_s)$	$\frac{1}{2}(\mathbf{1},\mathbf{2};\mathbf{16})$

Table 4.1: The gauge shift vectors and modular invariant combinations of gauge groups. The twisted and untwisted spectra for each model are also included.

In M-theory, it is known that compactification on a K3 surface with type A_{N-1} singularity, such as $T^4/\mathbb{Z}_N$, results in an $SU(N)$ gauge theory on the resulting 7D theory. Compactification of these theories on $S^1/\mathbb{Z}_2$ forces one to impose boundary conditions unnaturally on the resulting fields in order to acquire the proper spectra [21]. Fortunately, there is a chain of dualities that prove to be quite useful in this case and allows a more natural derivation of the twisted states charged across the bulk.

Specifically, up to this point we have mentioned two compactifications of M-theory related to string theory. We know that M-theory compactified on an S^1 has type-IIA supergravity as a small radius limit [1, 9]. We have also discussed at length that M-theory compactified on an $S^1/\mathbb{Z}_2$ yields $E_8\times E_8$

heterotic supergravity as a small radius limit. What if instead we were to consider the case in which M-theory is compactified on $S^1_1 \times S^1_2/\mathbb{Z}_2$? For $R_1 \gg R_2$, We would simply see the $E_8 \times E_8$ heterotic theory compactified on S^1_1, which is a relatively simple model to investigate. However, in the limit that $R_1 \ll R_2$, we have what appears to be the type-IIA theory compactified on $S^1_2/\mathbb{Z}_2$. This theory, known as type-I' string theory [33], is a much less trivial model to investigate, so let's look at some of the qualitative features.

4.1 Type-I' String Theory

In type-I' string theory, the $S^1_2/\mathbb{Z}_2$ acts as an orientifold of the theory (due to the boundary conditions imposed on the Kalb-Ramond 2-form B descending from the boundary conditions imposed on the parent 3-form C). As a result, the boundary surfaces of the interval must be orientifold 8-planes. These two O8-planes have D-brane charge -8, for a total charge of -16. The theory necessarily needs to be charge-neutral, so to counter this charge we must insert 16 D8-branes along the interval. The positions of these branes is arbitrary in the sense of charge neutrality, but the configuration of the D8-branes has nontrivial effects on the resulting gauge symmetry of the theory. For instance, if all of the branes are in distinct locations in the bulk, then each D8-brane contributes its own $U(1)$ gauge symmetry and we have $U(1)^{16}$. This is the equivalent of turning on Wilson lines and breaking the $E_8 \times E_8$ gauge symmetry down to its Cartan subgroup in the heterotic picture. As we continue to vary the positions of the D8-branes, we similarly vary the Wilson line

parameters in the heterotic picture, allowing us to reach points of enhanced gauge symmetry. For instance, when k of the D8-branes are coincident at a point in the bulk, then the gauge symmetry is enhanced,

$$U(1)^k \to U(k). \tag{4.1}$$

There are additional symmetry enhancements when D8-branes are coincident with one of the O8-planes. Specifically, for k D8-branes coincident on an O8-plane, the resulting gauge symmetry is enhanced,

$$U(1)^k \to SO(2k). \tag{4.2}$$

These two conditions properly summarize all attainable E_8 subgroups except for the exceptional ones: E_6, E_7, and E_8 itself. To account for these groups, it is necessary for the gauge coupling at the O8-plane in question to be infinite. This is achievable when the D8-branes away from the O8-plane are arranged in specific, fixed configurations. At these critical positions, the coupling at the boundary becomes infinite, and the fixing of the center of mass of the specifically arranged D8-branes effectively removes a $U(1)$ from their relative gauge group, which is then used to enhance the gauge group at the boundary:

$$SO(2k) \to E_{k+1}. \tag{4.3}$$

Thus, by considering $E_8 \times E_8$ heterotic string theory compactified on a circle, we are able to use M-theory and some duality arguments to transform our nontrivial questions into questions of brane dynamics in type-I' string theory.

4.2 (Multi-)Taub-NUT Geometry

The mission of this section is to investigate the twisted states of 6D orbifold theories. These twisted states are localized at the fixed points of the $\mathbb{Z}_N$ action on the T^4 under consideration, so for simplicity's sake let's focus on the spectrum at a single fixed point. Locally, any one of these fixed points is indistinguishable from the sole fixed point of $\mathbb{C}^2/\mathbb{Z}_N$, or any other geometry with a similar singularity structure, $SU(2)$ holonomy, and simple asymptotics. In order for us to make contact with the type-I' theory discussed previously, we are particularly interested in flat $\mathbb{R}^3 \times S^1$ asymptotics rather than $\mathbb{R}^4$, which is why we invoke the powerful multi-Taub-NUT geometry below.

The multi-Taub-NUT geometry of N Kaluza-Klein monopoles (denoted TN_N) has metric

$$ds^2 = V(\mathbf{x})d\mathbf{x}^2 + \frac{(dy - \mathbf{A}(\mathbf{x})d\mathbf{x})^2}{V(\mathbf{x})}, \tag{4.4}$$

where y is periodic with radius R, $y = y + 2\pi R$,

$$\nabla \times \mathbf{A} = \nabla V, \text{ and } V = 1 + \frac{R}{2}\sum_{i=1}^{N} \frac{1}{|\mathbf{x} - \mathbf{x}_i|}. \tag{4.5}$$

When all N monopoles are located at distinct $\mathbf{x}_i$, the geometry of the multi-Taub-NUT is smooth. However, when k of the monopoles coincide, there is a resulting $\mathbb{C}^2/\mathbb{Z}_k$ singularity located at that point. For the specific case in which all N monopoles are at the same point, we have a $\mathbb{C}^2/\mathbb{Z}_N$ singularity, and the multi-Taub-NUT geometry is simply an orbifolding of a basic Taub-NUT,

$$TN_N = TN_1/\mathbb{Z}_N. \tag{4.6}$$

In the limit that $R \to \infty$, the TN_1 curvature becomes negligible and $TN_1 \approx \mathbb{C}^2$. Thus, we see that in this limit

$$TN_N \approx \mathbb{C}^2/\mathbb{Z}_N. \tag{4.7}$$

4.3 Brane-Engineering the Fixed Points

Approximating our orbifold fixed point as a TN_N with its $\mathbb{R}^3 \times S^1$ asymptotics means that we can now consider M-theory with a dimension compactified on an S^1. For our approximation to be valid, we required that the radius of the S^1 be large, $R \to \infty$. However, in order for M-theory compactified on an S^1 to dualize to type-IIA theory, the opposite is actually necessary, $R \to 0$. The issue we hope to avoid is that everything we do in our type-IIA (or type-I') theory is invalidated when we try adapt it to the fixed point in question. Luckily, we know that the massless twisted spectrum is chiral and hence is independent of continuous parameters such as R. This assures us that the following construction will consistently describe states in the opposite regime of R.

We've now transformed our problem into one of brane engineering. The $E_8 \times E_8$ heterotic theory compactified on $T^4/\mathbb{Z}_N$ is dual to heterotic M-theory compactified on the same orbifold. The fixed points of this orbifold are locally indistinguishable from the fixed point of the TN_N discussed above, so we can use this geometry to explore the spectrum instead. By letting the radius of the TN_N become small (much smaller than the width of the $S^1/\mathbb{Z}_2$), we are able to dualize our theory once again, this time to type-I'

string theory. It was shown in [9] that the Kaluza-Klein monopoles introduced above dualize to D6-branes stretching across the bulk in the type-I' theory, and thus N coincident monopoles will similarly correspond to N coincident D6-branes. These D6-branes will have enhanced gauge symmetry, producing a 7D $U(N)$ SYM theory on the resulting world-volume. However, in this gauge symmetry there is a $U(1)$ that parametrizes the center-of-mass position. This is actually nothing more than an artifact of the fact that we are considering a non-compact geometry near the fixed point, when in fact the orbifold as a whole is compact. In the actual compact theory this $U(1)$ is absent, and so as we continue discussing the brane-engineering procedure, we will refer to the compact $SU(N)$ symmetry instead.

Now let's focus on the specific case of interest, the $T^4/\mathbb{Z}_2$ orbifold discussed above where the gauge symmetry is broken as

$$E_8 \times E_8' \to E_7 \times SU(2) \times SO(16)'. \tag{4.8}$$

This orbifold model has a simple interpretation in the type-I' picture, see Fig. 4.2. On the left O8-plane, there are 6 D8-branes stacked on top of each other, while away from the boundary there are 2 D8-branes coincident. Naively, this would yield a model with $SO(12) \times U(2)$ gauge symmetry. However, the two branes situated away from the boundary are in fact fixed at the critical point that causes infinite coupling at the O8-plane. Thus, the gauge symmetry is enhanced:

$$SO(12) \times U(2) \to E_7 \times SU(2). \tag{4.9}$$

The remaining 8 D8-branes are all coincident at the right O8-plane, and so the resulting gauge group on this boundary would be $SO(16)$, as we expect from the orbifold.

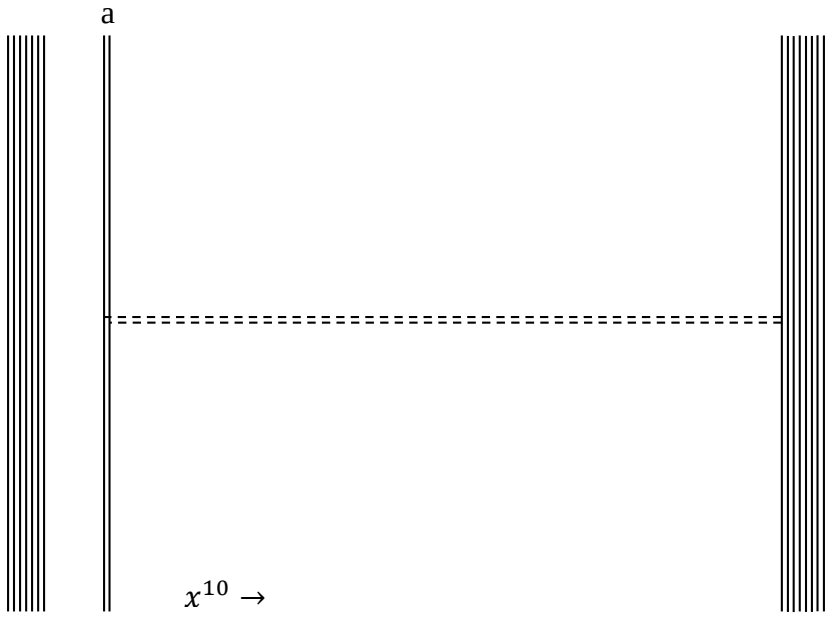

Figure 4.2: Type-I' brane configuration corresponding to the $T^4/\mathbb{Z}_2$ orbifold. The dashed lines correspond to D6-branes, while the solid lines correspond to D8-branes.

The $\mathbb{Z}_2$ fixed point corresponds to $N = 2$ coincident monopoles, and hence 2 D6-branes coincident at this point in the type-I' picture. The last consideration we must make is for the boundary conditions of these D6-branes when they reach the boundary on either side. On the $SO(16)$ side, the D6-

brane must terminate at the O8-plane since all D8-branes are coincident on it. Since the orientifold plane acts as a mirror, the gauge symmetry on a stack of N D6-branes at this junction must be broken as

$$SU(N) \to Sp(N/2). \tag{4.10}$$

For our simple case of $N = 2$, we have $SU(2) \to Sp(1) = SU(2)$, i.e., there is no gauge symmetry breaking (this should seem reasonable since $SU(2)$ is pseudoreal). At the D6-D8 junction, open strings form hypermultiplets with charges $(\mathbf{2}; \mathbf{16})$ under $SU(2) \times SO(16)$ (the intersection of the D6- and D8-branes has a 6D world-volume). Being at the O8-plane, half of the hypermultiplet is projected out, so the final state present is a half-hypermultiplet, $\frac{1}{2}(\mathbf{2}; \mathbf{16})$.

At the other boundary, there are a couple of possibilities for terminating the D6-branes. It is possible for the D6-branes to cross the bulk D8-branes and terminate on the O8-plane . However, the strings there are at infinite coupling so this is not a desirable option. Instead, we consider the two D8-branes away from the boundary as a terminus for the D6-branes. By locking the D6 gauge fields onto the D8 gauge fields via boundary conditions,

$$A_\mu^{(7D)}(x^{10} = a) = A_\mu^{(9D)}(\mathbf{x} = 0), \tag{4.11}$$

the combined gauge group $SU(2)_{D8} \times SU(2)_{D6}$ is broken to a diagonal subgroup $SU(2)_{diag}$[1]. Thus, the resulting half-hypermultiplet at the other boundary,

[1]there is an elegant derivation of this using T-duality in [22].

$\frac{1}{2}(\mathbf{2};\mathbf{16})$, is not charged under the initial $SU(2)_{D6}$ but under the surviving $SU(2)_{diag}$. In this way, the D6-branes carry the quantum numbers of one boundary across the bulk (in a mixed fashion) and create states localized at the other boundary. Dualizing back to heterotic M-theory and then going to weak heterotic string coupling so that the bulk vanishes, these states appear to be charged under just the original $SU(2) \times SO(16)$ subgroup of the $E_8 \times E_8$ gauge symmetry, as is calculated perturbatively.

In developing the machinery to solve the mystery of these mixed twisted states in 6D, we relied heavily on a few tools. It was absolutely necessary that we be able to find a geometry with similar fixed-point structure, $SU(2)$ holonomy, and $\mathbb{R}^3 \times S^1$ asymptotics, in order to dualize from heterotic M-theory to type-I' string theory. From here, we were able to use brane dynamics to prove the existence of 7D $SU(N)$ SYM theories at the fixed points stretched across the bulk. These SYM theories were able to carry quantum numbers across the bulk and create charged localized states on the opposite side. Unfortunately, there is no clear generalization of these tools from 6D to 4D. To start, there is no known 4D equivalent of the multi-Taub-NUT space (a geometry with orbifold fixed point structure, $SU(3)$ holonomy, and $\mathbb{R}^5 \times S^1$ asymptotics). What's worse, however, is that even if we were to find such a geometry, we already know that the 5D theories at these orbifold fixed points are highly nontrivial. As we will discuss in the next section, in the 4D case we will no longer be dealing with finitely coupled SYM theories at the fixed points as we did in 6D, but with infinitely-coupled 5D superconformal theories [17].

Chapter 5

5D Field Theory

As 5D gauge theory will be intricately involved in our solution to the 4D cases we consider, it is important that we discuss it in some detail. Minimal supersymmetry in five dimensions requires eight supercharges and, upon dimensional reduction, is related to the 4D $\mathcal{N} = 2$ superalgebra. There are two massless representations in 5D, corresponding to the vector multiplet, which has one real scalar field, and the hypermultiplet, which has four real scalar fields. When dimensionally reduced to 4D, the component of the vector field along the reduced dimension combines with the real scalar to form the complex scalar of a 4D $\mathcal{N} = 2$ vector multiplet, and the hypermultiplet reduces simply to a 4D hypermultiplet.

This relationship between 5D $\mathcal{N} = 1$ and 4D $\mathcal{N} = 2$ gauge theories is important because we know that the Lagrangian of the 4D theory along its Coulomb branch must satisfy special geometry, and thus the same applies to the 5D theory. Specifically, this Lagrangian must be derived by a prepotential that is locally a function of the vector superfields $\mathcal{A}^i$:

$$\mathcal{F} = c_0 + (c_1)_i \mathcal{A}^i + \frac{1}{2}(c_2)_{ij}\mathcal{A}^i\mathcal{A}^j + \frac{1}{6}(c_3)_{ijk}\mathcal{A}^i\mathcal{A}^j\mathcal{A}^k. \tag{5.1}$$

We know that the prepotential is at most cubic in the vector superfields be-

cause the 4D invariance condition on the scalars $A_4^i \to A_4^i + a^i$ translates to a similar condition in 5D, $\mathcal{A}^i \to \mathcal{A}^i + ia^i$. As c_0 and c_1 do not affect the Lagrangian, we will simply set them to zero and concern ourselves solely with c_2 and c_3.

Let's specialize to the case with gauge group $SU(2)$. It is clear to see that the coefficient of the quadratic term of the prepotential corresponds to the bare gauge coupling, $t_0 = \frac{1}{g^2}$. The cubic term corresponds to a Chern-Simons term, and it is important to note that for this term to be nonzero classically, the gauge group in question must have a cubic invariant. This is not the case for $SU(2)$, so classically $c_3 = 0$. However, there is the possibility of quantum corrections to this term at the 1-loop level. This calculation was performed for gauge group $SU(2)$ and N_f massless flavors in [10], and the resulting Chern-Simons coefficient takes the form:

$$c_3 = 2(8 - N_f). \tag{5.2}$$

We can then derive the gauge coupling of the effective theory on the Coulomb branch of the moduli space. At a generic point in the moduli space, the $SU(2)$ gauge group is broken to $U(1)$ and the Coulomb branch is parametrized by the VEV of a real scalar $\phi \in \mathbb{R}/\mathbb{Z}_2 = \mathbb{R}^+$. The coupling is then

$$t_{eff} = \frac{\partial^2 \mathcal{F}(\phi)}{\partial \phi^2} = t_0 + 2(8 - N_f)\phi \tag{5.3}$$

This theory has the common $SO(2N_f)$ global symmetry associated to $SU(2)$ gauge theory with N_f flavors.

The above expression can be generalized to include masses for the flavors, as well. It is worth discussing a few caveats about the parameters before doing so, however. First, as discussed in [10], the masses of these hypermultiplets in the effective Lagrangian can be analytically continued to include negative masses. The only importance is in preserving the relative sign of hypermultiplet masses. Their presence is significant, though, as it will in fact enrich the phase structure of our parameter/moduli space.

Second, the bare coupling parameter t_0 actually has a physical interpretation that should be considered. Specifically, there exists a current that is always conserved in 5D gauge theories,

$$j = *(F \wedge F). \tag{5.4}$$

This is the instanton current and corresponds to a $U(1)_I$ global symmetry. In 5D an instanton is a BPS state, and its mass depends on the bare coupling. Thus, we can interpret t_0 as the mass of a particle in some sense, and there is an additional $U(1)_I$ global symmetry as a result.

Now we can continue on toward generalizing eq. (5.3) to include massive flavors. However, with this generalization comes a complicated structure of global symmetries. In order to clearly illustrate this structure, let's use the familiar method of brane dynamics in type-I' string theory to discuss the different phases of the gauge theory.

5.1 5D Gauge Theories from Type-I' String Theory

In the section on 6D orbifold theories, we introduced the background of type-I' string theory. Consisting of an interval with O8-planes at the boundaries, the -8 D-brane charges associated to each O8-plane forces us to introduce 16 D8-branes to ensure D-brane charge neutrality. For the sake of interest, let's situate the D-branes so that N_r of them are near one boundary ($R = 0$) and $N_l = 16 - N_r$ are near the opposite boundary ($R = L$). We discussed the different possible arrangements of the D8-branes and resulting gauge groups earlier in this work, but what we'd like to do now is probe these brane configurations with a D4-brane (parallel to the D8-branes in the bulk direction) and study the resulting 5D gauge theory on the D4 world-volume. Most of this presentation is similar to that presented in [33, 34].

Consider the D4-brane in the vicinity of the $R = 0$ boundary, far from the $R = L$ boundary. In parameter terminology, the distance of the D4-brane from the boundary corresponds to the Coulomb branch scalar VEV, and the position of each D8-brane corresponds to the mass m_i of a hypermultiplet in the $SU(2)$ gauge theory (at $\phi = 0$) formed by open strings between it and the D4-brane. This implies that we will be considering configurations with general constraints

$$m_1, ..., m_{N_0}, \phi \ll m_{N_0+1}, ..., m_{16}, \tag{5.5}$$

so that $n = N_l$ of the flavors are very heavy and can be integrated out. The gauge symmetry of any given brane configuration manifests as a global symmetry on the D4 world-volume theory. Additionally, as the D4-brane approaches

the boundary ($\phi \to 0$), states due to open strings between it and its mirror image in the orientifold plane become light. When the D4-brane meets the boundary ($\phi = 0$), these states become massless and the $U(1)$ gauge symmetry on the world-volume is enhanced to $Sp(1) = SU(2)$, as expected.

To begin, let N_0 D8-branes be stacked on the O8-plane, $N_r - N_0$ of the D8-branes in the bulk away from the boundary, and ϕ small. Near the boundary the world-volume theory is $SU(2)$ gauge theory with N_0 flavors and from eq. (5.3), we know that the corresponding effective coupling is simply

$$t_{eff} = t_0 + 2(8 - N_0)\phi. \tag{5.6}$$

As ϕ increases and approaches the first D8-brane away from the boundary at m_1, the hypermultiplet associated to that D8-brane is becoming massless. For $\phi > m_i$, the effective coupling gains a linear correction based on the coupling at that D8-brane:

$$\begin{aligned} t_{eff} &= t_{eff}(m_1) + 2(8 - N_0 - 1)\phi \\ &= t_0 + 2(8 - N_0)m_1 + 2(8 - N_0 - 1)\phi. \end{aligned} \tag{5.7}$$

As the D4-brane continues to pass D8-branes, the effective coupling picks up corrections in a similar fashion. This behavior can be generally expressed as

$$t_{eff} = t_0 + 16\phi - \sum_{i=1}^{N_r} |\phi - m_i| - \sum_{i=1}^{N_r} |\phi + m_i|. \tag{5.8}$$

As a quick note, notice that for the case $N_r = 8$ and $\phi > m_{N_r}$, we have

$$t_{eff} = t_0, \tag{5.9}$$

so in a way we can view this bare coupling (the mass of the instanton) as the asymptotic value for large ϕ with eight flavors. Thus, in order to maintain $t \geq 0$, it is necessary for $t_0 \geq 0$. Beyond eight flavors, ϕ is necessarily bounded above by t_0.

Let's consider the specific case of N_f flavors on the boundary, and one flavor out in the bulk at m_0. For $\phi > m_0$, we know from eq. (5.8) that the effective coupling has the form

$$t_{eff} = t_0 + 2(8 - N_f - 1)\phi. \tag{5.10}$$

As we cross over the D8-brane in the bulk, so that $\phi < m_0$, we can use eq. (5.8) once again to generate the effective coupling,

$$t_{eff} = t_0 - 2m_0 + 2(8 - N_f)\phi = t_0' + 2(8 - N_f)\phi, \tag{5.11}$$

where we have define $t_0' = t_0 - 2m_0$ as a "corrected" bare coupling of sorts for the $SU(2)$ gauge theory at the boundary. This formalism sheds light on something mentioned above, namely that there is a critical position of the brane in the bulk such that the coupling diverges at the boundary, $m_0 = \frac{1}{2}t_0$. This divergence corresponds to an enhancement of the gauge symmetry in the brane configuration, i.e., an enhanced global flavor symmetry on the 4D world-volume theory near the boundary. At such strong coupling, the notion of a particle is not well-defined, and at $\phi = 0$ the theory is a nontrivial interacting conformal field theory with global symmetry $SO(2N_f) \times U(1)_I \to E_{N_f+1}$, where the $U(1)_I$ is the global symmetry for the instanton current. Put another way,

we can associate t_0' with (some simple redefinition of) the instanton mass, so the symmetry enhancement occurs when the instanton becomes massless, for a total of $N_f + 1$ massless states to generate the E_{N_f+1} global symmetry.

Finally, let's return to the idea that the masses need not be positive and specify $N_f = 1$ for our personal interests. The 5D theory at the boundary ($\phi = 0$) has trivial flavor symmetry for generic values of m_0, but the flavor symmetry is enhanced to $E_2 = SU(2) \times U(1)$ at the critical value of m_0. Allowing the flavor hypermultiplet to gain a mass $m > 0$ with m_0 fixed will result in a theory that is still infinitely coupled, now with $E_1 = SU(2)$ global symmetry and effective coupling

$$t_{eff} = t_0 - 2m_0 - 2m = -2m. \tag{5.12}$$

Allowing m to return to 0 and then go negative, we see that there is a new phase in the effective gauge coupling:

$$t_{eff} = (t_0 - 2m_0 - 2m) + 4m. \tag{5.13}$$

We now see an additional superconformal fixed point in the effective coupling along the locus in which $t_0 - 2m_0 - 2m > 0$ and $m < 0$ but $t_0 - 2m_0 + 2m_0 = 0$. At this fixed point the theory has an $\widetilde{E}_1 = U(1)$ global symmetry corresponding to this single parameter. If we additionally allow for $t_0' + 2m_0 < 0$, then the theory flows to an isolated superconformal fixed point with E_0, i.e. trivial, global symmetry.

The brane dynamics behind these theories involve a major change in the structure. In the regime $m_0 \geq 0$ studied thus far, we have been able

to consider the classic moduli space of the type-I' string theory, and left the infinite-coupling dynamics as limiting cases. The $\widetilde{E}_1$ and E_0 theories, however, require that we go beyond the classical limit and consider excited O8-planes [17], denoted O8*-planes. These have D-brane charge -9 instead of -8. As the mass parameter m approaches zero and then turns negative, the D8-brane enters the O8-plane and goes "behind it." Thus, its image exists on the actual physical interval. The image has mass parameter $m' = t_0 - 2m_0 + 2m$ and hence the $\widetilde{E}_1$ fixed point corresponds to the D8-brane and its image coinciding at the boundary, $m' = m = 0$. Open strings between the D6-brane and D8-brane thus create a massless hypermultiplet here. Allowing $m' < 0$ corresponds to dropping the original D8-brane further into the image, and hence its image D8-brane leaves the O8*-plane, the hypermultiplet gaining mass $|m'|$ in the process. The resulting theory at the O8*-plane is the E_0 SCFT.

5.2 M-theory and Calabi-Yau Threefolds

We mentioned previously that "compactifying M-theory on an orbifold" is really an abbreviation for "compactifying M-theory on a Calabi-Yau threefold and considering the singular limit in which it approaches an orbifold." In light of the above discussion of 5D field theory, consider such a compactification of M-theory. There is a wealth of literature on this topic, [11–13], but we will be concerned chiefly with the singular structures of these constructions [10, 17]. Specifically, we want to consider the case in which only a proper subset of the Calabi-Yau threefold vanishes. This subset forms an imbedded

surface of lower dimension in the threefold. In the proceeding, we are trying to make contact with the $SU(2)$ gauge theories discussed above. As the moduli space of these gauge theories are one-dimensional, we wish to only vary one parameter to shrink these surfaces. This limits us to complex codimension-one surfaces.

To illustrate, consider the case in which the subset of interest is the Hirzebruch surface $\mathbb{F}_1$, which is isomorphic to $\mathbb{CP}^2$ blown up at one point. This surface contains one 2-cycle corresponding to the blow-up $\mathbb{CP}^1$ and one 4-cycle, namely the entire $\mathbb{F}_1$. Wrapping an M2-brane on the 2-cycle creates a BPS state with mass proportional to its volume. Blowing this $\mathbb{CP}^1$ down then corresponds to a massless particle. At this wall of the Kähler cone there is a possible flop transition to "negative volume" under which the 4-cycle becomes a $\mathbb{CP}^2$. Shrinking this 4-cycle yields the E_0 SCFT from earlier, while instead shrinking the $\mathbb{F}_1$ yields the $\widetilde{E}_1$ SCFT. Each orbifold fixed point we will consider has a corresponding blown up 4-cycle in this general fashion that we wish to blow down, so we see that the complications associated to these 5D SCFT's will be prevelant going forward. The strategy we employ to make them more manageable begins with the brane web construction of 5D gauge theories.

5.3 Brane Webs

Part of the S-dual nature of type-IIB string theory is the existence of two extended objects of the same dimension: the D5-brane and the NS5-brane. We wish to study the resulting gauge theories of certain configurations

of these branes. These configurations, called brane webs [18, 19], are built out of D5-branes whose world-volumes fill $x^0, ..., x^4, x^5$ and NS5-branes filling $x^0, ..., x^4, x^6$. We will consider combinations of p of these D5-branes and q NS5-branes, referred to as (p, q)-branes. These branes' world-volumes share $x^0, ..., x^4$, where we will build our nontrivial 5D theories. The rest of the (p, q)-branes fill a plane whose coordinates we will label as (x, y).

Type-IIB also contains a complex scalar field that transforms under $SL(2, \mathbb{R})$,

$$\tau = \chi + ie^{-\Phi}, \tag{5.14}$$

where Φ is the dilaton whose exponentiated VEV gives the string coupling, $\langle e^{\Phi} \rangle = \lambda$, and χ is the RR scalar, also known as the axion. In this notation, the tension of a (p, q)-brane is written as

$$T_{(p,q)} = |p + \tau q| T_{D5}, \tag{5.15}$$

where T_{D5} is the D5-brane tension. Additionally, these (p, q)-branes are allowed to form vertices as long as the RR- and NSNS-charges are conserved,

$$\sum_i p_i = \sum_i q_i = 0. \tag{5.16}$$

As far as supersymmetry is concerned, it is possible to preserve 8 of the 32 supercharges (which we want for 5D $\mathcal{N} = 1$) by demanding [35]

$$\Delta x + \tau \Delta y \to p + \tau q, \tag{5.17}$$

i.e., the (p, q)-branes are required to "have a slope" in the (x, y)-plane parametrized by p and q. For ease of drawing, we will normalize so that $\tau = i$, meaning that a $(1, 1)$-brane will have a slope of 1.

Knowing that these (p, q)-branes can form vertices in the (x, y)-plane implies that they can be semi-infinite with one end terminating at a vertex or finite with both ends terminating at vertices. Combining (p, q)-branes in this fashion forms the basis of the brane webs we will be considering. Fig. 5.1 contains some examples of such configurations. Looking at these brane webs, we see two obvious forms of deformations that we would like to associate to parameters. Namely, we can think of deformations that have no effect on the asymptotic structure and deformations that do. For reasons that will soon become obvious, we will refer to these as local deformations and global deformations, respectively. This first type, local deformations, refers to breathing modes of closed surfaces on the (x, y)-plane, as is denoted with the dashed line in Fig. 5.1a. The parameter associated to this breathing mode corresponds to the VEV of a real scalar field in a BPS vector multiplet formed by a fundamental string stretched between two parallel D5-branes ($(1, 0)$-branes). These states are the familiar $U(1)$ gauge fields associated to strings on D-branes. When the VEV is zero so that the two D5-branes are coincident, we have gauge symmetry enhancement in the usual fashion.

For the second type of deformation, global deformations, we must be careful so as not to overcount actual relevant deformations. Naively, we count one generator for every semi-infinite (p, q)-brane; let's say there are n_{semi} of them. However, not all of these are linearly independent. For example, our resulting 5D theory should not care about relative translations of the brane web in the x- or y-directions, so two combinations of generators are in fact

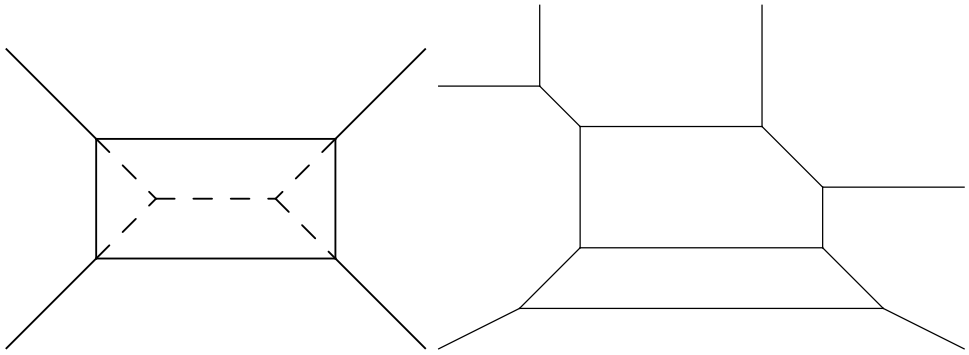

(a) (b)

Figure 5.1: Brane webs for flavorless $SU(2)$ SYM (a) and $N_f = 2$ $SU(3)$ gauge theory (b).

irrelevant. Additionally, charge conservation at each vertex has the global effect of fixing one vertex uniquely if all others are designated, so another generator is irrelevant. Thus, the number of generators of global deformations we end up with is

$$n_{global} = n_{semi} - 3, \tag{5.18}$$

and there is a corresponding global symmetry of rank n_{global}. Specifically, for the brane web in Fig. 5.1a, there is $n_{global} = 4 - 3 = 1$ generator corresponding to the width of the brane web. This $U(1)_I$ global symmetry is just the symmetry associated to the instanton current, and the BPS instanton state follows from stretching a D1-string to connect the two parallel NS5-branes ($(0,1)$-branes) in the web. As discussed earlier, the mass of the instanton is associated with the bare coupling of the 5D gauge theory, so we can thus associate the width of the brane web with this bare coupling.

The brane web in Fig. 5.1b has a significant increase in intricacy. First,

we have two closed surfaces in the (x, y)-plane, signifying a $U(1)^2$ gauge symmetry. Following the logic above, one should be able to see that when these surfaces both collapse so that 3 D5-branes are coincident, the gauge symmetry is enhanced to $SU(3)$. The semi-infinite D5-branes have a less immediate interpretation, however. We know from above that they should generate some global symmetry. The symmetry in question is actually a flavor symmetry, and thus these branes must generate BPS states, as well. These states correspond to strings that connect these semi-infinite branes to other D5-branes but are along the (p, q)-branes instead of in the empty space of the (x, y)-plane. These strings not fundamental strings or D1-strings, but instanton strings of the 6D world-volume theory on the (p, q)-brane. These are thus usually referred to as (p, q)-strips as opposed to strings [18].

Finally, we can have combinations of fundamental strings and D1-strings that can meet at vertices and form towers of BPS states. For instance, consider both brane webs in Fig. 5.2. They are two different phases of $SU(2)$ SYM that we will discuss below, but for now we just want to take notice that the BPS instanton-like state in Fig. 5.2b cannot be constructed as simply as the one in Fig. 5.2a, but must be a bound state from multiple (p, q)-strings.

The brane webs in Fig 5.2 demonstrate another key point about these configurations. Let's first consider a slightly different example in which we have $SU(3)$ gauge symmetry instead of $SU(2)$, as in Fig. 5.3. All of these models have the same Coulomb branch, but differ in their BPS spectra. This is a consequence of the Chern-Simons coupling in each model, and the differ-

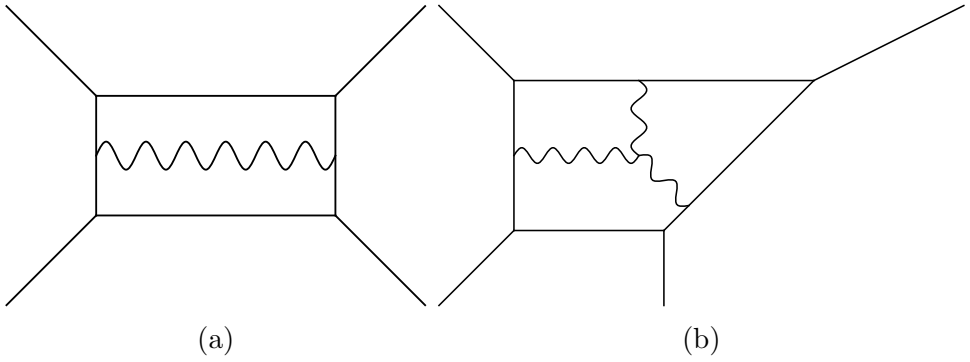

Figure 5.2: Instanton-like states for $SU(2)$ SYM, $\theta = 0$ (a) and $\theta = \pi$ (b).

ent brane webs correspond to a distinct Chern-Simons number, k [18]. Any additional brane webs are related to these by an $SL(2, \mathbb{Z})$ transformation or have negative k, which produces identical BPS spectra. Extending this rela-

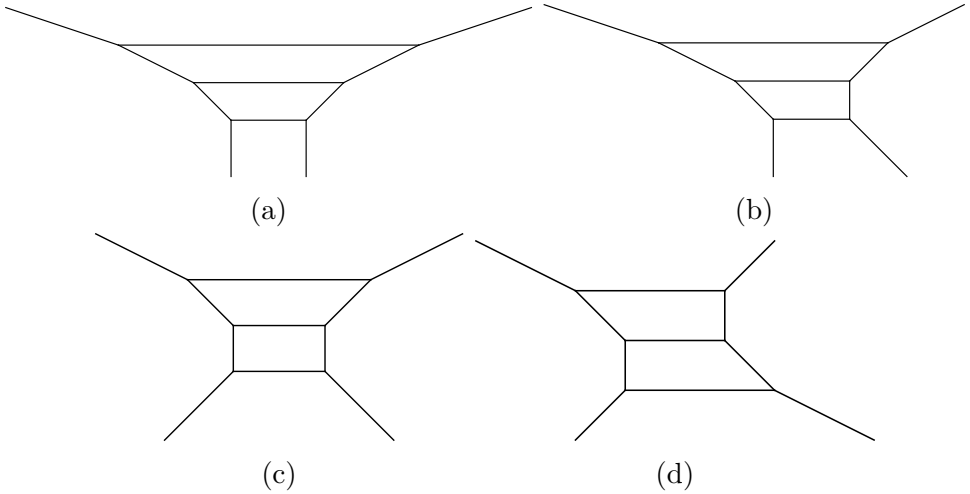

Figure 5.3: Brane webs for $SU(3)$ SYM with (a) $k = 3$, (b) $k = 2$, (c) $k = 1$, and (d) $k = 0$.

tionship to $SU(2)$ is met with some difficulty. On one hand, it is obvious that there are multiple pure $SU(2)$ SYM brane webs, as in Fig. 5.4. On the other

hand, $SU(2)$ has no cubic invariant, so it has no Chern-Simons term. However, similar to 4D where $\pi_3(SU(2)) = \mathbb{Z}$ leads to a vacuum θ-angle that can take values in $\{2\pi\mathbb{Z}\}$, in 5D we have $\pi_4(SU(2)) = \mathbb{Z}_2$ which leads to a θ-angle that can take values $\{0, \pi \bmod 2\pi\mathbb{Z}\}$. We thus have two $SU(2)$ SYM theories, differing by the value of a θ-angle. These different phases are represented in the various brane webs in Fig. 5.4. It's curious that from the field theory point of view, $\theta = 0$ and $\theta = 2\pi$ should be identical. However, the brane webs in Fig. 5.4a and Fig. 5.4c appear to be quite different. As it turns out, they do produce the same spectra as long as the bare coupling does not vanish. As it approaches zero, 6D strings stretched across the semi-infinite NS5-branes in Fig. 5.3a become tensionless, and the physics here is less understood [18].

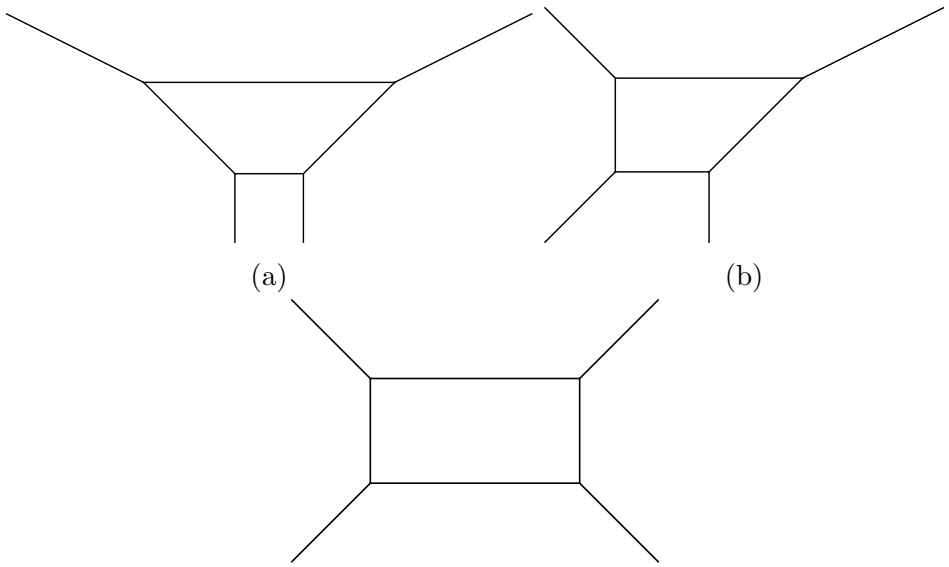

Figure 5.4: Brane webs for $SU(2)$ SYM with (a) $\theta = 2\pi$, (b) $\theta = \pi$, and (c) $\theta = 0$.

As demonstrated above, brane webs are extremely useful for constructing 5D $SU(N)$ gauge theories (though it is not explicitly presented, brane webs properly reproduce our results for the effective coupling). Their particular usefulness in our case, though, comes from their relationship to toric data [18]. Specifically, we will be able to make use of the toric diagrams associated to the resolution of singularities in each orbifold we consider[1]. Toric diagrams and brane webs are in some sense "dual" to each other. Consider, for example, the toric diagram in Fig. 5.5b. This can be derived from the brane web in Fig. 5.5a (and vice versa) by (1) replacing each face (open or closed) with a point, (2) replacing each vertex with a triangular face, and (3) rotating each line by 90° to connect the points and act as the edges of the triangular faces. With some resizing, you can see this overlayed in Fig. 5.5c

This translation between toric data and 5D gauge theories allows us to consider M-theory compactified on (blown-up) orbifolds. It is an important step for us to take, but it is still far from sufficient. As elegant as brane webs are for constructing 5D gauge theories, they are poorly suited for compactifying on $S^1/\mathbb{Z}_2$ to make contact with the heterotic theory. Luckily, we will see that there is another method for studying these theories, namely deconstruction, that lends itself quite well to compactification on an interval.

[1] A useful primer on toric diagrams and the "Inverse Algorithm" for extracting gauge theory information from toric data is [36].

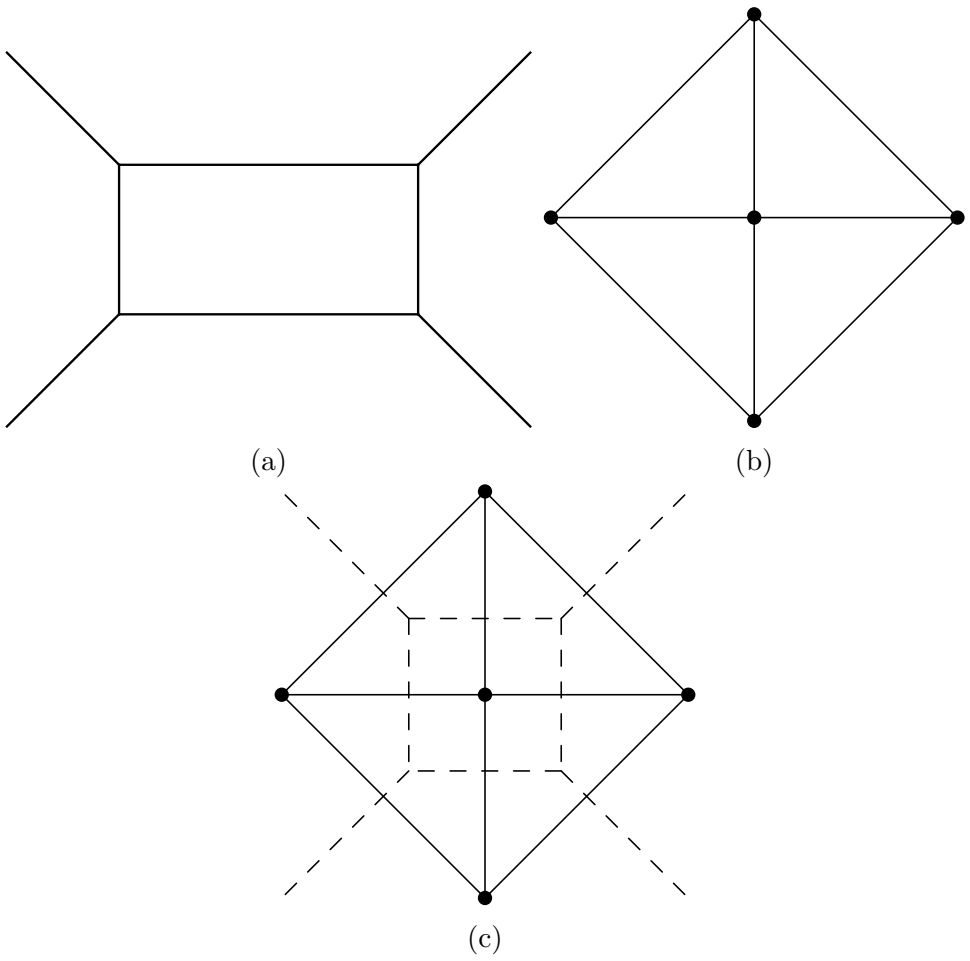

Figure 5.5: The brane web for $SU(2)$ SYM with $\theta = 0$ from above (a), its dual toric diagram (b), and the two overlayed (c).

Chapter 6

Deconstruction

In deconstruction, the 5D theory is compactified on a circle, and then this compactified dimension is latticized [31]. Being that 5D gauge theories are nonrenormalizable, this latticization acts as a necessary UV-cutoff. These lattice sites can be interpreted as nodes of a quiver, and the resulting description is a 4D $\mathcal{N} = 1$ quiver gauge theory. The quiver theory can be quite complicated, but enables the use of 4D calculation methods and (as we will discuss later) simplifies the process of compactifying on $S^1/\mathbb{Z}_2$. The deconstruction of general 5D $SU(N_c)$ SYM was derived in [23], and general SQCD with N_f flavors and Chern-Simons level k was derived in [25].

6.1 Deconstructing SQCD on S^1

We will begin with a 4D, $\mathcal{N} = 1$ quiver gauge theory with gauge group

$$G = \prod_{\ell=1}^{L} SU(N_c)_\ell. \tag{6.1}$$

At each node, there are N_f quark chiral superfields Q_ℓ^f in the fundamental representation of $SU(N_c)_\ell$ and N_f antiquark chiral superfields $\widetilde{Q}_\ell^f$ in the antifundamental representation. Between the nodes are bifundamental linking

chiral superfields Φ_ℓ in the fundamental representation of the $(\ell+1)$th node and the antifundamental representation of the ℓth node. Making the identification $\ell \to \ell + L$, we see that Φ_L links the Lth node to the first node. In this way, the quiver can be arranged in a circle as in Fig. 6.1. To complete the description of the quiver, we note that the gauge couplings at each node must be equal, $g_\ell = g \ \forall \ell$. This is necessary for translation invariance in the x^4-direction.

For this quiver theory to deconstruct 5D $SU(N_c)$ SQCD, it is necessary to introduce a couple of superpotential terms. The first of these is the usual "hopping" superpotential,

$$W_{hop} = \gamma \sum_{\ell=1}^{L} \sum_{f=1}^{N_f} \left(\widetilde{Q}^f_{\ell+1} \Phi_\ell Q^f_\ell - \mu_f \widetilde{Q}^f_\ell Q^f_\ell \right), \tag{6.2}$$

which allows the quark fields to propagate in the latticized x^4-direction. Here, to ensure that the speed of light for quarks and gluons is the same, it is necessary to impose that the Yukawa coupling γ be equal to the gauge coupling,

$$\gamma = g. \tag{6.3}$$

The second superpotential term that is needed is the O'Raifeartaigh superpotential

$$W_\Sigma = \beta \sum_{\ell=1}^{L} \sigma_\ell \left(\det\left(\Phi_\ell\right) - v^{N_c} \right) \tag{6.4}$$

where $v > 0$ is a constant and we have introduced the singlet chiral superfields σ_ℓ as Lagrange multipliers. Running along with the link fields in the quiver

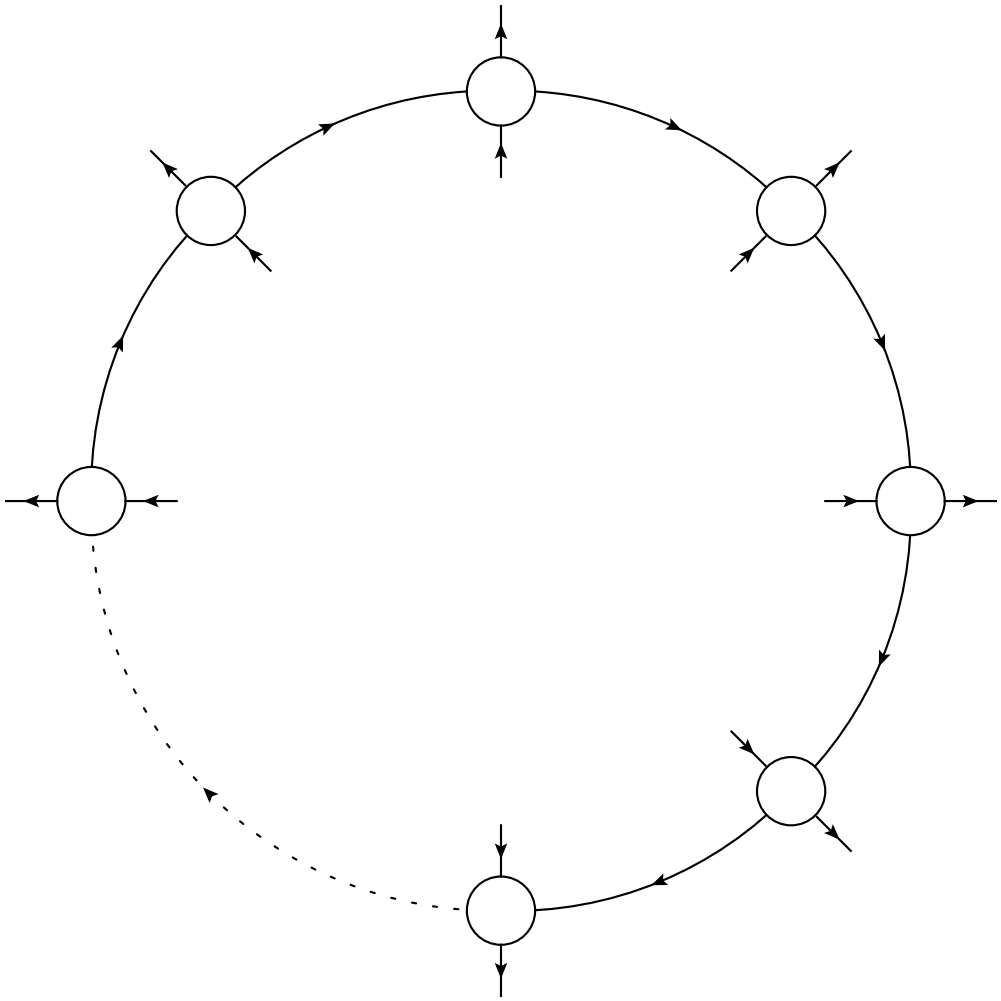

Figure 6.1: Deconstructive quiver. Each circle is a gauge group $SU(N_c)_\ell$ and each line is a chiral superfield. An ingoing arrow signifies that the chiral superfield is in the fundamental representation under $SU(N_c)_\ell$ and an outgoing arrow is in the antifundamental representation. Hence, the lines between nodes are the bifundamental link fields, while the ingoing (outgoing) arrows at each node represent the quarks (antiquarks); $N_f = 1$ above.

diagram, they have the effect of turning each link field into an $SL(N_c, \mathbb{C})$ linear

sigma model with the on-shell condition

$$\det\left(\Phi_\ell\right) = v^{N_c}. \tag{6.5}$$

Thus, we can define the scalar part of Φ_ℓ as

$$\Phi_\ell(x)|_{\theta=\bar{\theta}=0} = v \times \mathcal{P} \exp\left(\int_{a\ell}^{a(\ell+1)} dx^4 \left(iA_4(x) + \phi(x)\right)\right), \tag{6.6}$$

where ϕ is the real scalar superpartner of the 5D vector field A_μ, $\mu = 0, 1, 2, 3, 4$ and a is the lattice spacing. For $\phi = A_4 = 0$, eq. (6.5) constrains the VEV of the scalars in the Φ_ℓ fields to satisfy

$$\langle\Phi_\ell\rangle = v \times \mathbb{I}_{N_c \times N_c} \qquad \forall \ell \tag{6.7}$$

which breaks the 4D gauge symmetry to the diagonal $SU(N_c)$ of G. This quiver theory correctly reproduces the spectrum of 5D SQCD with gauge group $SU(N_c)$ and N_f flavors compactified on a circle with the conditions

$$a = \frac{1}{g|v|}, \qquad 2\pi R = La. \tag{6.8}$$

For the masses of the quarks to deconstruct properly, the quiver masses μ_f must be related to the 5D masses m_f as

$$\mu_f = ve^{am_f}. \tag{6.9}$$

Thus, for there to be light 5D quarks, it is necessary that $\mu_f \approx v$, and massless 5D quarks correspond to $\mu_f = v$.

The quiver theory also properly deconstructs the Coulomb branch of the 5D theory. To see this, note that the D-term constraints for each $SU(N_c)$

gauge group combine to give

$$\Phi_\ell^\dagger \Phi_\ell - \Phi_{\ell-1} \Phi_{\ell-1}^\dagger \propto \mathbb{I}_{N_c \times N_c}. \tag{6.10}$$

Along with eq. (6.5), these constraints force the Φ_ℓ VEV's to be equal (modulo an ℓ-dependent gauge transformation). These matrices can be simultaneously diagonalized to take the form

$$\langle \Phi_\ell \rangle = v \ \mathrm{diag}\,(e^{a\varphi_1}, e^{a\varphi_2}, ..., e^{a\varphi_{N_c}}) \tag{6.11}$$

with complex φ_k's subject to $\Sigma_k \varphi_k = 0$. From eq. (6.6), we conclude that the φ_k's can be identified as

$$\langle \phi \rangle + i \langle A_4 \rangle = \mathrm{diag}(\varphi_1, \varphi_2, ..., \varphi_{N_c}). \tag{6.12}$$

This is exactly as expected for a 5D vector multiplet compactified on a circle.

Finally, it is possible to deconstruct the Chern-Simons coupling of 5D SQCD. The details are tedious, but have been worked out in [25]. For our purposes, it is only necessary to consider the case where the masses of the 4D quarks are $\mu_f = 0$. As discussed earlier, it is necessary for $\mu_f \approx v$ for the 5D quarks to have light modes. When $\mu_f \gg v$, the 5D quarks have a large positive mass and actually decouple above the deconstruction threshold. However, when $\mu_f \ll v$, the 5D quarks are within the deconstruction threshold but have a large negative 5D mass and can be integrated out. This is the case for $\mu_f = 0$ ($m_f \to -\infty$), which has the benefit of decoupling the Φ_ℓ linear sigma models from each other. If this occurs, then the resulting Wess-Zumino

couplings of these link fields deconstruct the Chern-Simons coupling of the 5D theory, and we find

$$k = N_c - \#\{f : \mu_f \ll v\} - \frac{1}{2}\#\{f : \mu_f \approx v\} = N_c - \Delta F - \frac{1}{2}N_f, \qquad (6.13)$$

where ΔF symbolizes the number of quark flavors that have no light 5D modes but still affect k.

6.2 Deconstructing SQCD on $S^1/\mathbb{Z}_2$

The deconstruction procedure on S^1 above already highlights most of the machinery we need to extend to $S^1/\mathbb{Z}_2$. In fact, everything we discussed applies to the bulk nodes of our interval quiver. It is only the boundary nodes that need to be properly defined. Specifically, recall from eq. (3.2) that some of the components of the 3-form field C in M-theory have even boundary conditions under the $\mathbb{Z}_2$ action while others have odd:

$$\begin{aligned} C_{IJ10} &\to C_{IJ10}, \\ C_{IJK} &\to -C_{IJK}. \end{aligned} \qquad (6.14)$$

Wrapping this C on 2-cycles in the Calabi-Yau threefold on which we're compactifying produces the 5D gauge fields that we are deconstructing. We therefore must carry these boundary conditions down to the descendent gauge fields. The components perpedicular to the interval, C_{IJK}, compactify on the 2-cycles to produce the 4D gauge fields in the low-energy effective action. However, being odd under the $\mathbb{Z}_2$ action means that these gauge fields cannot have zero modes at the fixed points. We are thus forced to conclude that the gauge

symmetry vanishes at the boundaries. In terms of our quiver, it is necessary that there be no gauge symmetry on the boundary nodes. Instead, there is a surviving global symmetry acting on any chiral fields that were charged under the now-absent gauge symmetry. For example, consider the quiver associated to $SU(N_c)$ SQCD with $N_f = 1$ compactified on an S^1 in Fig. 6.1. The same theory compactified on $S^1/\mathbb{Z}_2$ would have a quiver of the form in Fig. 6.2.

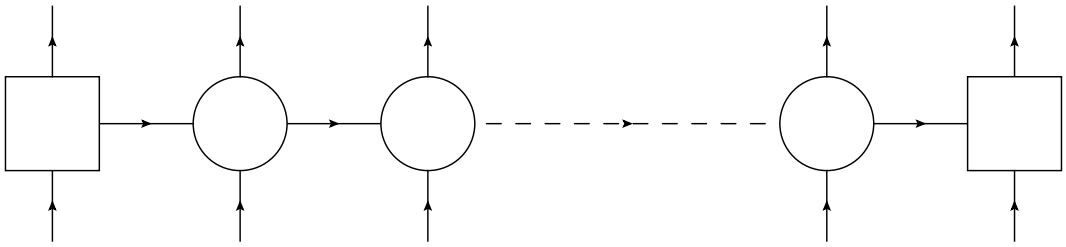

Figure 6.2: The deconstructive quiver for the model. The circular nodes are $SU(N_c)$ gauge groups and the square nodes are $SU(N_c)$ global groups. All nodes have $N_f = 1$.

The $\mathbb{Z}_2$-even part of C, C_{IJ10}, descends to the x^4-component of the 5D gauge field that gets compactified on the interval. Being even, this field does have zero modes on the boundary. It is also charged under the gauge symmetry of the immediate bulk mode, so it forms an $SU(N_c)_{gauge} \times SU(N_c)_{global}$ bifundamental chiral field. The superpotential terms that we introduced survive, also, and give these states nontrivial interactions with the gauge singlet states on the boundaries. Now that we have all of the necessary tools to begin handling some of these models, let's investigate the $T^6/\mathbb{Z}_3$ orbifold.

Chapter 7

$\mathbb{Z}_3$ Orbifold

As previously mentioned, the $\mathbb{Z}_3$ orbifold starts with a torus. The torus in this case is constructed by taking the complex three-plane $\mathbb{C}^3$ and modding by the $SU(3)\times SU(3)\times SU(3)$ root lattice $\Lambda_{SU(3)^3}$. This 6D root lattice can be decomposed into the product of three 2D root lattices $\Lambda_{SU(3)}\times\Lambda_{SU(3)}\times\Lambda_{SU(3)}$, where each identifies points on $\mathbb{C}$ by

$$z^i \sim z^i + 1, \quad z^i \sim z^i + e^{\frac{\pi i}{3}}. \tag{7.1}$$

Fig. 7.1 illustrates each individual complex dimension under this action. From here, we act on this torus with a $\mathbb{Z}_3$ twist. As discussed earlier, the consistent twist vector is $\vec{r} = (1, 1, -2)$[1]. This acts on the coordinates of the torus by identifying points under

$$z^i \to e^{(2\pi i)r_i/3} z^i. \tag{7.2}$$

[1]Since the twist vector components act on the coordinates as $z^i \to e^{(2\pi i)r_i/3}z^i$, they are invariant under shifts $r_i \to r_i + 3$. Thus, the shift vector could instead be written as $\vec{r} = (1, 1, 1)$, so we see that it actually acts identically on all complex coordinates of the torus.

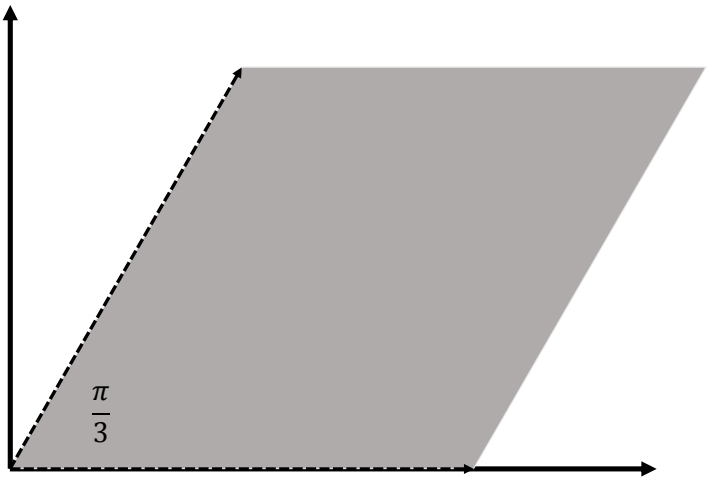

Figure 7.1: The $SU(3)$ root lattice on $\mathbb{C}$. The gray region signifies the fundamental domain of the torus in one complex dimension.

Looking at one complex coordinate of the torus, we see that there are three fixed points of the action on it[2]:

$$z^i_{fixed} = 0,\ \frac{1}{\sqrt{3}} e^{\frac{\pi i}{6}},\ \frac{2}{\sqrt{3}} e^{\frac{\pi i}{6}} \tag{7.3}$$

A fixed point on the $T^6/\mathbb{Z}_3$ must be a fixed point on each of the complex coordinates. This implies that there are $3^3 = 27$ fixed points of the twist on the T^6, one for each combination of fixed points on the torus coordinates. Table 7.2 shows the fundamental domain of each coordinate after orbifolding.

[2]There is only one fixed point on $\mathbb{C}$, $z^i_{fixed} = 0$. The other two fixed points on the torus require the action of the root lattice, eq. (7.1).

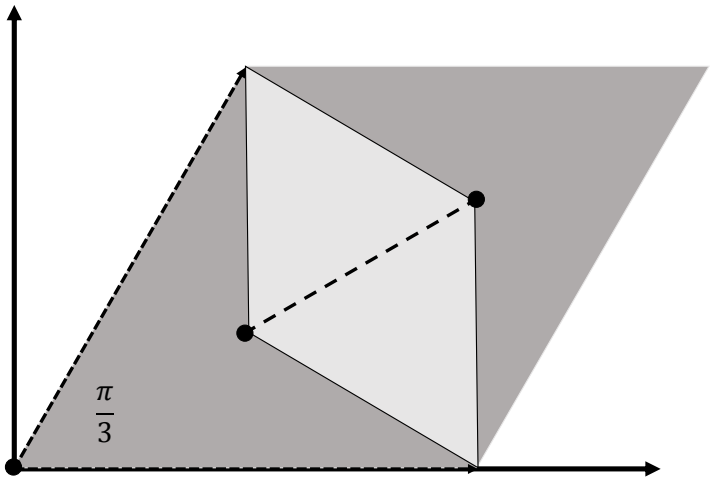

Figure 7.2: The orbifold action on a complex coordinate of the torus. The fixed points are labeled. The lighter region signifies the fundamental domain of the orbifold on the $SU(3)$ root lattice. The action of the point group of the torus identifies the fixed point at the origin with both of the remaining corners of this region, so they must be identified. The orbifold is folded across the dashed line as a result.

Next, we need to investigate the possible values for the gauge shift vector $\vec{s}$. Along with $\vec{r}$, this must satsify eqs. (2.11) and (2.12). Breaking $\vec{s}$ into two 8-vectors $\vec{s}_1$ and $\vec{s}_2$, eq. (2.11) limits the possible gauge shift vectors. We can check the roots of the E_8 root system to see which ones do not project onto this shift vector and preserve some of the gauge symmetry. We can also check to see which do project onto the shift vector, corresponding to the untwisted sector. The results of this are in Table 7.1. When the unbroken

gauge groups are (appropriately) combined, the untwisted sectors of the E_8 subgroups make up the total untwisted sector of the model.

Normalized Shift Vector	Gauge Symmetry	Untwisted Spectrum
(0^8)	E_8	$-$
$(\frac{1}{3}, \frac{1}{3}, -\frac{2}{3}, 0^5)$	$E_6 \times SU(3)$	$3(\mathbf{27}, \mathbf{3})$
$(\frac{1}{3}, \frac{1}{3}, 0^6)$	$E_7 \times U(1)$	$3(\mathbf{56}_2 + \mathbf{1}_{-4})$
$(\frac{1}{3}, \frac{1}{3}, \frac{1}{3}, \frac{1}{3}, -\frac{2}{3}, 0^3)$	$SU(9)$	$3(\mathbf{84})$
$(\frac{2}{3}, 0^7)$	$SO(14) \times U(1)$	$3(\mathbf{64}_{-1} + \mathbf{14}_2)$

Table 7.1: The allowable normalized shift vectors, along with their corresponding unbroken gauge symmetries and untwisted spectra. Subscripts denote $U(1)$ charges.

The breaking of $E_8 \times E_8$ must be consistent with eq. (2.12). This highly constrains which of the E_8 subgroups in Table 7.1 are able to combine with each other. The combinations that meet these criteria are listed in Table 7.2. The twisted spectra for these models are also given. A copy of each spectrum is localized at each fixed point, so the multiplicity of states is 27.

In the twisted spectra presented in Table 7.2, there is a pecularity in model 2 similar to what we alluded to earlier. Namely, there is a single state that is charged by subgroups of each E_8 group. This state is perfectly reasonable from the string theory point of view, but must somehow be charged across the bulk in the M-theory picture. This is an example of the situation

	Gauge Symmetry	Twisted Spectrum	Anamolous
1	$E_6 \times SU(3) \times E_8'$	$(\mathbf{27}, \mathbf{1}; \mathbf{1}) + 3(\mathbf{1}, \mathbf{3}; \mathbf{1})$	No
2	$E_6 \times SU(3) \times E_6' \times SU(3)'$	$(\mathbf{1}, \mathbf{3}; \mathbf{1}, \mathbf{3})$	No
3	$E_7 \times U(1) \times SO(14)' \times U(1)'$	$(\mathbf{1}; \mathbf{14})_{0;2} + (\mathbf{1}, \mathbf{1})_{0;-4} + 3(\mathbf{1}, \mathbf{1})_{4;0}$	Yes
4	$SU(9) \times SO(14)' \times U(1)'$	$(\overline{\mathbf{9}}; \mathbf{1})_{-4/3}$	Yes

Table 7.2: The Modular invariant models with $\mathbb{Z}_3$ twisted states charged under subgroups of both E_8's. For each model, there are 27 states (one at each fixed point). Subscripts denote $U(1)$ charges. The $U(1)$ gauge anomalies are also indicated.

we wish to explain. Our standard procedure as we investigate each orbifold with states posing this predicament will be to use the toric diagram for the resolved fixed point to build the corresponding brane web. We can then use this brane web to identify key details about the 5D gauge theory, such as the gauge group, matter content, and Chern-Simons number. This allows us to deconstruct this gauge theory, modify the boundaries to reflect compactification on $S^1/\mathbb{Z}_2$, and look at the spectrum as we drive the moduli/parameters toward the corresponding blow-down limit in the geometry.

7.1 Deriving the Brane Web

The blown-up fixed point of the $\mathbb{C}^3/\mathbb{Z}_3$ orbifold can be identified with a $\mathbb{CP}^2$, and has a toric diagram of the form in Fig. 7.3. We can see the procedure for finding the corresponding brane web in Fig. 7.4. Compared to our earlier examples, this brane web has a very peculiar structure. First, there are only

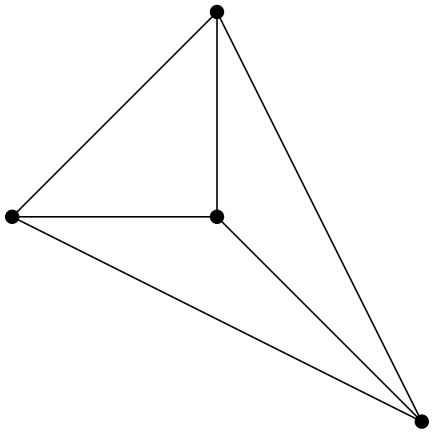

Figure 7.3: The toric diagram for the $\mathbb{C}^3/\mathbb{Z}_2$ (resolved) fixed point.

three external legs, so eq. (5.18) would imply that the rank of the global symmetry in the theory is $n_{global} = 3 - 3 = 0$, i.e., there is no global symmetry Second, we recognize a breathing mode for the closed surface in Fig. 7.4c, but since this closed face is a triangle, it collapes to a point rather than a line, and we find no gauge symmetry enhancement. At this point, the effective coupling diverges and we have the previously mentioned E_0 SCFT. Thus, the resolved orbifold singularity corresponds to this theory deformed away from its fixed point, along its Coulomb branch. Due to its significance to the situation at hand, it is worthwhile to explore some of the features of this theory in more detail.

7.2 The E_0 SCFT

The E_0 SCFT is difficult to study due to its isolated nature. There is no gauge theory that flows to the E_0 SCFT by itself. The best we can do is

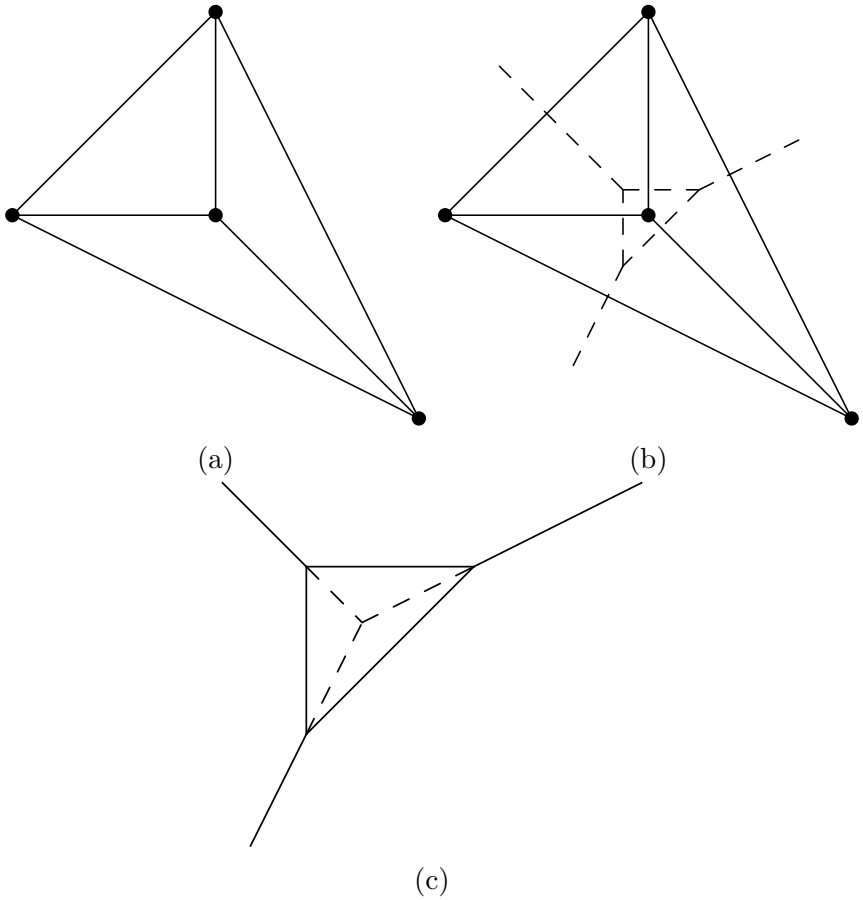

Figure 7.4: Converting the toric diagram to a brane web: (a) the toric diagram, (b) an overlay of the conversion, and (c) the brane web with blow down indicated by the dashed line.

flow to it with the assistance of additional matter. To see this, consider $SU(2)$ SYM with $\theta = \pi$ along its Coulomb branch with brane web in Fig. 5.4b. The theory has two parameters to vary: the breathing mode corresponding to the modulus ϕ that breaks the gauge symmetry $SU(2) \to U(1)$ for $\phi \neq 0$ and the width of the D5-branes at $\phi = 0$ corresponding to the bare coupling/mass of the $SU(2)$ instanton t_0. We can vary these parameters and explore the

different limits that result. Starting at $t_0 > 0$, $\phi > 0$ as in Fig. 7.5a, we can let $t_0 \to 0$. At $t_0 = 0$, the quantum corrected coupling is still positive, so the theory is still $SU(2)$ SYM with $\theta = \pi$, as in Fig. 7.5b. Continuing into negative t_0[3], we eventually reach a point $t_0 = t_{flop}$ where the coupling diverges and a quark becomes massless (the mass depends on the length of the bottom brane, which goes to zero at t_{flop}, Fig. 7.5c). Past this point, there is a flop transition as seen in Fig. 7.5d. This new phase has a massive quark with a mass proportional to t_0. In the low energy effective theory, we only care about the massless spectrum, so we neglect this massive quark. The resulting theory represented by the brane web in Fig. 7.5e is the E_0 theory along its Coulomb branch. Its massless spectrum consists of a single $U(1)$ vector multiplet whose scalar field $\hat{\phi}$, a linear combination of ϕ and t_0, characterizes the breathing mode of the resulting triangle. There is no possible global deformation, so there is no global symmetry in the E_0 theory, as stated earlier. When $\hat{\phi} = 0$ as in Fig. 7.5f, the coupling diverges and we reach the E_0 SCFT point in the moduli space.

7.3 Deconstructing the Fixed Point Theory

From above, we can see that to make contact with the E_0 SCFT, we will need to deconstruct $SU(2)$ SYM with $\theta = \pi$. We've already mentioned that, unlike for $N_c > 2$, their is no cubic invariant for $SU(2)$, so there is no

[3]There is no inconsistency in letting t_0 go negative here. One way to have $\theta = \pi$ is to add a flavor to $SU(2)$ with $\theta = 0$, let it become heavy ($m > \phi$), and then integrate it out. Then our "bare coupling" has the form $t_0 - 2m$, i.e., it can be negative.

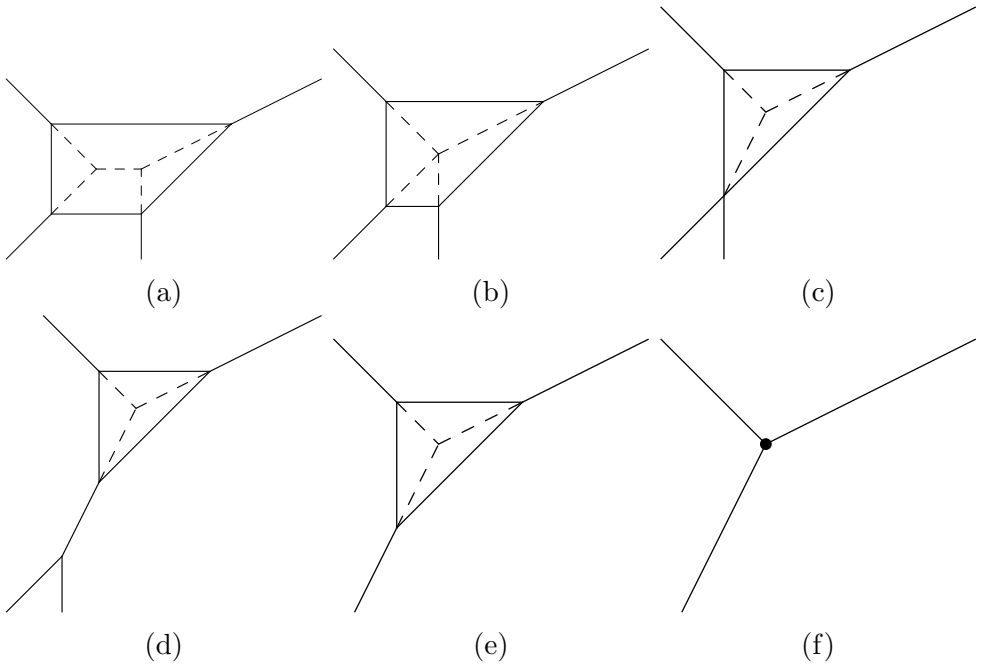

Figure 7.5: Brane webs for $SU(2)$ SYM with $\theta = \pi$. (a) $t_0 > 0$, $\phi > 0$, (b) $t_0 = 0$, $\phi > 0$, (c) $t_0 = t_{flop} < 0$, $\phi > 0$, (d) $t_0 < t_{flop} < 0$, $\phi > 0$, (e) E_0 SCFT along its Coulomb branch, $\hat{\phi} > 0$, (f) E_0 SCFT, $\hat{\phi} = 0$.

Chern-Simons term. However, by starting with $SU(3)$ SQCD and Higgsing down to $SU(2)$, it is easy to see that the $SU(2)$ θ-angle is related to the $SU(3)$ Chern-Simons coupling (mod 2) [25]. Thus, the proper quiver theory to deconstruct E_0 will have $N_c = 2$, $N_f = 0$, and $\Delta F = 1$.

The chiral ring of this quiver has already been analyzed in [24] and the Seiberg-Witten spectral curve in [25], so we will focus instead on the relevant results. According to the deconstruction dictionary, the coupling at the origin of the Coulomb branch has the following form:

$$t_0 \equiv \frac{3}{a} \log \left(\frac{v}{|\gamma|^{\frac{1}{3}} \Lambda} \right), \tag{7.4}$$

where Λ is the dimensional transmutant introduced by instanton effects. For $t_0 > 0$, the low energy effective gauge coupling along the Coulomb branch has the proper form with $N_f = 0$ [17]

$$t_{eff} = 2t_0 + 8\phi, \tag{7.5}$$

with $SU(2)$ restoration at $\phi = 0$.[4]

For $t_0 < 0$ the structure of the Coulomb branch is more complicated. In the regime $\phi > (-t_0) > 0$, the gauge coupling still has the same form as for $t_0 > 0$, eq. (7.5). As $\phi \to -t_0$, a quark is becoming light and becomes massless at $\phi = -t_0$. This is reflected in the fact that the gauge coupling abruptly transitions to

$$t_{eff} = 3t_0 + 9\phi \tag{7.6}$$

for $(-t_0) > \phi > (-t_0/3)$. In this regime, it is convenient to define $\hat{\phi} = \phi + (t_0/3)$ so that we can rewrite eq. (7.6) as $t_{eff} = 9\hat{\phi}$ and consider what happens as $\hat{\phi} \to 0$. It is clear that the theory is approaching a fixed point, $t_{eff} \to 0$, and it can be identified as the E_0 fixed point. In light of this, it becomes clear that the regime $(-t_0) > \phi > (-t_0/3)$ deconstructs the Coulomb branch of the E_0 theory. Note that all of these phases identified in the deconstructed theory match the phases identified using the brane web techniques illustrated in Fig. 7.5. The last regime, $(-t_0/3) > \phi > 0$, has no corresponding brane

[4]This is true up to some arbitrary redefinitions of parameters that we neglect in order to keep with [25].

web because it is a nongeometric phase that disappears as the fifth dimension is decompactified.

Let us examine this E_0 modulus $\hat{\phi}$ in more detail. We rewrite the VEV's of the link fields in the form

$$\langle \Phi \rangle = v \begin{pmatrix} e^{a\varphi} & 0 \\ 0 & e^{-a\varphi} \end{pmatrix} = \begin{pmatrix} \omega_1 & 0 \\ 0 & \omega_2 \end{pmatrix}. \tag{7.7}$$

Since $\phi = \mathrm{Re}(\varphi) \propto \log(|\omega_1/v|)$, for our current purposes we can simply consider ω_1 to be real. This allows us to cleanly write $\hat{\phi}$ in the form:

$$\begin{aligned} \hat{\phi} &= \frac{1}{a} \log\left(\frac{\omega_1}{v}\right) + \frac{1}{3}\left(\frac{3}{a}\log\left(\frac{v}{|\gamma|^{\frac{1}{3}}\Lambda}\right)\right) \\ &= \frac{1}{a}\log\left(\frac{\omega_1}{|\gamma|^{\frac{1}{3}}\,\Lambda}\right). \end{aligned} \tag{7.8}$$

Written in this way, it becomes evident that the Coulomb modulus $\hat{\phi}$ is actually independent of v! Originally, v was necessarily nonzero in order to deconstruct the $SU(2)$ SYM theory. After the flop transition, however, the sole parameter, namely the modulus $\hat{\phi}$, does not depend on v, signalling that $v > 0$ is really just a relic from the fact that we approached the E_0 fixed point from this parent theory. By sending $v \to 0$, we are sending $t_0 \to -\infty$ according to eq. (7.4), isolating the E_0 theory from the $SU(2)$ SYM phase as we did with the brane webs. Thus, we will proceed to set $v = 0$ for the remainder of this section.

7.4 Spectrum at Blow-down

Consider the first gauged node, $\ell = 1$. The superpotential terms that contain fields charged under $SU(2)_2$ are

$$W_{tree,\ell=1} = \widetilde{Q}_1 \Phi_0 Q_0 + \sigma_0 \det(\Phi_0) + \widetilde{Q}_2 \Phi_1 Q_1 + \sigma_1 \det(\Phi_1), \tag{7.9}$$

where we have rescaled $\gamma \widetilde{Q}_\ell \to \widetilde{Q}_\ell$, $\beta \sigma_\ell \to \sigma_\ell$ for simplicity. Let us now temporarily relax the constraint that all gauge couplings be equal and, in the spirit of [30], assume that $\Lambda_1 \gg \Lambda_\ell \ \forall \ell \neq 1$. In this limit, the effective theory looks like $SU(2)_1$ gauge theory with $SU(2)_2$ a global symmetry (the fields at all other nodes are decoupled singlets under the gauge symmetry so we neglect them). Thus, the $SU(2)_1 \times SU(2)_2$ bifundamental field $\Phi_{1(\alpha\dot{\alpha})}$, $\alpha = 1, 2$ and $\dot{\alpha} = 1, 2$, now represents two doublets under the gauge group just like $\Phi_{0(\alpha\dot{\alpha})}$. Additionally, $\widetilde{Q}_{1(\dot{\alpha})}$ now represents two singlets of the gauge group. Noting that $\det(\Phi_\ell) = \frac{1}{2}\Phi_{\ell(\alpha\dot{\alpha})}\epsilon^{\alpha\beta}\epsilon^{\dot{\alpha}\dot{\beta}}\Phi_{\ell(\beta\dot{\beta})}$, we can repackage the fields as

$$\mathcal{Q}_{1(\alpha)} = \begin{pmatrix} \Phi_{1(\alpha 1)} \\ \Phi_{1(\alpha 2)} \\ Q_{1(\alpha)} \end{pmatrix}, \qquad \mathcal{S}_1 = \begin{pmatrix} \widetilde{Q}_{2(1)} \\ \widetilde{Q}_{2(2)} \\ \sigma_1 \end{pmatrix}. \tag{7.10}$$

Similarly, we can make the definitions

$$\widetilde{\mathcal{Q}}_{1(\alpha)} = \begin{pmatrix} \widetilde{Q}_{1(\alpha)} \\ \Phi_{0(\alpha 1)} \\ \Phi_{0(\alpha 2)} \end{pmatrix}, \qquad \widetilde{\mathcal{S}}_1 = \begin{pmatrix} \sigma_0 \\ Q_{0(1)} \\ Q_{0(2)} \end{pmatrix} \tag{7.11}$$

so that we can cleanly write

$$W_{tree,\ell=1} = \epsilon_{ijk} \mathcal{S}_1^i \mathcal{Q}_1^j \mathcal{Q}_1^k + \epsilon_{ijk} \widetilde{\mathcal{S}}_1^i \widetilde{\mathcal{Q}}_1^j \widetilde{\mathcal{Q}}_1^k. \tag{7.12}$$

Thus, we have an effective theory with gauge group $SU(2)$ and $N_f = 3$. As in [29], we see that this induces an effective superpotential:

$$W_{eff} = \frac{1}{\Lambda_1^3}\left(\det \mathcal{M}_1 - \mathcal{B}_{1,i}\mathcal{M}_1^{ij}\widetilde{\mathcal{B}}_{1,j}\right), \tag{7.13}$$

where $\mathcal{B}_{1,i} = \epsilon_{ijk}\mathcal{Q}_1^j\mathcal{Q}_1^k$, $\widetilde{\mathcal{B}}_{1,i} = \epsilon_{ijk}\widetilde{\mathcal{Q}}_1^j\widetilde{\mathcal{Q}}_1^k$, and $\mathcal{M}_1^{ij} = \mathcal{Q}_1^i\widetilde{\mathcal{Q}}_1^j$.

In this form, the $\mathcal{S}_1$'s and $\widetilde{\mathcal{S}}_1$'s act as Lagrange multipliers, imposing the moduli constraint $\mathcal{B}_1 = \widetilde{\mathcal{B}}_1 = 0$. Thus, the superpotential takes the form

$$W_{eff} \sim \frac{1}{\Lambda_1^3}\det \mathcal{M}_1. \tag{7.14}$$

F-flatness requires that $\frac{\partial W_{eff}}{\partial \mathcal{M}_1} = 0$ at this fixed point, or in other words

$$\frac{\partial}{\partial(\mathcal{M}_1)_{ij}}\det \mathcal{M}_1 = (\text{adj } \mathcal{M}_1)_{ji} = 0. \tag{7.15}$$

This constraint is only possible if the rank of $\mathcal{M}_1$ is at most 1. Also, the D-terms constrain the VEV's of $\mathcal{Q}_1$ and $\widetilde{\mathcal{Q}}_1$ to be equal up to a flavor symmetry transformation, taking the form

$$\mathcal{Q}_1^1 = \begin{pmatrix} h \\ 0 \end{pmatrix}, \quad \widetilde{\mathcal{Q}}_1^1 = \begin{pmatrix} h & 0 \end{pmatrix} \tag{7.16}$$

with all other $\mathcal{Q}_1^i, \widetilde{\mathcal{Q}}_1^i = 0$ so that

$$\mathcal{M}_1 = \begin{pmatrix} h^2 & 0 & 0 \\ 0 & 0 & 0 \\ 0 & 0 & 0 \end{pmatrix}, \tag{7.17}$$

i.e., only $\mathcal{M}_1^{11}$ is nonzero. In the region $\mathcal{M}_1^{11} < \mathcal{O}(\Lambda_1^2)$ (we want to send $h \to 0$), the theory confines and the appropriate degrees of freedom to consider

are the composite fields. In the absence of $W_{tree,\ell=1}$, the mesons, baryons, and antibaryons transform together under the antisymmetric **15** representation of $SU(6)$. However, $W_{tree,\ell=1}$ breaks $SU(6)$ to $SU(3) \times SU(3)$ and gives masses to $\mathcal{B}_{1,i}$, $\widetilde{\mathcal{B}}_{1,i}$, $\mathcal{S}_1^i$, and $\widetilde{\mathcal{S}}_1^i$. Thus, the only massless degrees of freedom are the $\mathcal{M}_1$'s.

Assume now that $\Lambda_2 \gg \Lambda_\ell$, so that $SU(2)_2$ is gauged while the other $SU(2)$'s are global symmetries. We can see that the $\mathcal{M}_1$'s do not have the same charge under $SU(2)_2$. In terms of the constituent fields, the mesons $(\Phi_1 \widetilde{\mathcal{Q}}_1^i)$ are doublets under $SU(2)_2$ while the remaining mesons $(Q_1 \widetilde{\mathcal{Q}}_1^i)$ are singlets. Thus, in the effective field theory the second gauged node appears to be the first gauged node, with three doublets

$$\widetilde{\mathcal{Q}}_2^i = \frac{1}{\Lambda_1}(\Phi_1 \widetilde{\mathcal{Q}}_1^i) \tag{7.18}$$

and three singlets

$$\widetilde{\mathcal{S}}_2^i = \frac{1}{\Lambda_1}(Q_1 \widetilde{\mathcal{Q}}_1^i). \tag{7.19}$$

By repackaging the remaining fields in the same fashion as eqn. (7.10)

$$\mathcal{Q}_2 = \begin{pmatrix} \Phi_{2(\alpha 1)} \\ \Phi_{2(\alpha 2)} \\ Q_2 \end{pmatrix}, \qquad \mathcal{S}_2 = \begin{pmatrix} \widetilde{Q}_{3(1)} \\ \widetilde{Q}_{3(2)} \\ \sigma_2 \end{pmatrix}, \tag{7.20}$$

we see that we have the same situation we started with for the first gauged node. Integrating out the massive fields from the first gauged node gives an effective tree-level superpotential for the second gauged node:

$$W_{tree,\ell=2} = \epsilon_{ijk} \mathcal{S}_2^i \mathcal{Q}_2^j \mathcal{Q}_2^k + \epsilon_{ijk} \widetilde{\mathcal{S}}_2^i \widetilde{\mathcal{Q}}_2^j \widetilde{\mathcal{Q}}_2^k, \tag{7.21}$$

and the previous analysis can be carried out again. This is performed inductively from node to node until finally we reach the last gauged node, $\ell = L$, in which we are left with a composite field:

$$\mathcal{M}_L = \left(\widetilde{\mathcal{Q}}_1 \prod_{\ell=1}^{L-1} \Phi_\ell \mathcal{Q}_L \right), \tag{7.22}$$

where we have conveniently defined

$$\mathcal{Q}_L = \begin{pmatrix} Q_L \\ \Phi_{L(\alpha 1)} \\ \Phi_{L(\alpha 2)} \end{pmatrix}. \tag{7.23}$$

This field transforms in the bifundamental representation of an $SU(3) \times SU(3)$ global symmetry (for $h = 0$) with an effective superpotential of the form

$$W_{eff} \sim \frac{1}{\Lambda^{3L}} \det \mathcal{M}_L. \tag{7.24}$$

By the same argument in eq. (7.15), $\mathcal{M}_L$ must be rank 1. Thus, it appears that $\mathcal{M}_L/\Lambda^L$ has the properties we seek for the twisted state at the fixed point for the model of interest.

If instead we were in the regime $\mathcal{M}_1^{11} = h^2 > \mathcal{O}(\Lambda_1^2)$, the effective theory would be perturbative and the constituent fields would be the proper degrees of freedom to consider. As it turns out, all of the singlet fields become massive due to quantum effects. Consider, for instance, the first node. By perturbing the superpotential with a baryon mass term $W_{mass} = b\mathcal{B}_{1,1} + \widetilde{b}\widetilde{\mathcal{B}}_{1,1}$, integrating them out, and taking $b, \widetilde{b} \to 0$, we find an effective potential term of the form

$$W_{\mathcal{S}} = \frac{\Lambda_1^3}{h^2} \mathcal{S}_1^1 \widetilde{\mathcal{S}}_1^1. \tag{7.25}$$

Remembering that $\mathcal{S}_1^1 = \widetilde{Q}_{2(1)}$ and $\widetilde{\mathcal{S}}_1^1 = \sigma_0$, we see that these constituent fields gain masses. At a general node, this can also be achieved by adding mass terms $W_{mass,\ell} = \Phi_\ell M_\ell Q_\ell + \widetilde{Q}_{\ell+1}\widetilde{M}_{\ell+1}\Phi_{\ell+1}$, integrating out the singlet composite fields, and taking $M_\ell, \widetilde{M}_{\ell+1} \to 0$. Along with the Higgs mechanism eating or giving mass to fields, we find that the only remaining massless fields in the spectrum for $h > \mathcal{O}(\Lambda)$ are the modulus h, link fields $\Phi_{0(\alpha 1)}$ and $\Phi_{0(\alpha 2)}$, and link fields $\Phi_{L(\alpha 1)}$ and $\Phi_{L(\alpha 2)}$. These fields have the same transformation properties as the fields in eq. (7.32). Hence, we see the same symmetry breaking pattern conjectured in [20].

In fact, we can actually see this transition by considering the Kähler potential. We do not have a firm grasp on the quantum corrections, but assuming they are reasonably under control we can qualitatively analyze the Kähler potential, which should have the form

$$K \sim (L+1)\left(\left(\overline{\Lambda}\Lambda\right)^{L+1} + \mathrm{tr}\left(\mathcal{M}_L^\dagger \mathcal{M}_L\right)\right)^{\frac{1}{L+1}}. \tag{7.26}$$

We see from eq. (7.22) that $\langle \mathcal{M}_L \rangle = h^{L+1}$.Thus, the two regimes of interest, $h > \mathcal{O}(\Lambda)$ and $h < \mathcal{O}(\Lambda)$, correspond to drastically different Kähler potentials. This is important because the corresponding Kähler metric Z corrects the effective superpotential (7.24). This superpotential gives the $\mathcal{M}_L$ components containing $\Phi_{0(\alpha 1)}$, $\Phi_{0(\alpha 2)}$, $\Phi_{L(\alpha 1)}$ and $\Phi_{L(\alpha 2)}$ a bare mass

$$m_{bare} = \frac{|h|^{L+1}}{\Lambda^{3L}}. \tag{7.27}$$

For $h > \mathcal{O}(\Lambda)$,

$$K \sim (L+1)\left(\mathrm{tr}\left(\mathcal{M}_L^\dagger \mathcal{M}_L\right)\right)^{\frac{1}{L+1}} \Rightarrow Z = \frac{1}{\left(\overline{h}h\right)^L}, \tag{7.28}$$

and we see that the physical mass,

$$m_{phys} = \frac{m_{bare}}{Z} = \frac{|h|^{L+1}}{|\Lambda|^{3L}} \times |h|^{2L} = \frac{|h|^{3L+1}}{|\Lambda|^{3L}}, \tag{7.29}$$

is very large. On the other hand, for $h < \mathcal{O}(\Lambda)$,

$$K \sim (L+1)\left(\overline{\Lambda}\Lambda\right) + \frac{\mathrm{tr}\left(\mathcal{M}_L^\dagger \mathcal{M}_L\right)}{\left(\overline{\Lambda}\Lambda\right)^L} \Rightarrow Z = \frac{1}{\left(\overline{\Lambda}\Lambda\right)^L}, \tag{7.30}$$

and the physical mass,

$$m_{phys} = \frac{m_{bare}}{Z} = \frac{|h|^{L+1}}{|\Lambda|^{3L}} \times |\Lambda|^{2L} = \frac{|h|^{L+1}}{|\Lambda|^{L}}, \tag{7.31}$$

is very small. Thus, for large $\mathcal{M}_L^{11}/\Lambda^L$ ($\mathcal{M}_L^{11}/\Lambda^L = h^{L+1}/\Lambda^L > \mathcal{O}(\Lambda)$), there are no light composite fields involving $\Phi_{0(\alpha 1)}$, $\Phi_{0(\alpha 2)}$, $\Phi_{L(\alpha 1)}$ and $\Phi_{L(\alpha 2)}$, and the only massless field across the bulk is $\mathcal{M}_L^{11}/\Lambda^L$, which we can associate with the E_0 modulus $\hat{\phi}$. At $\mathcal{M}_L^{11}/\Lambda^L \sim \mathcal{O}(\Lambda)$, there is a sharp transition, and below this point the $\mathcal{M}_L$'s involving $\Phi_{0(\alpha 1)}$, $\Phi_{0(\alpha 2)}$, $\Phi_{L(\alpha 1)}$ and $\Phi_{L(\alpha 2)}$ are light, becoming massless at $\mathcal{M}_L^{11}/\Lambda^L = 0$. This is where there is symmetry restoration $SU(2)_L \times SU(2)_R \times U(1) \to SU(3)_L \times SU(3)_R$ with the massless state $\Psi = \mathcal{M}_L/\Lambda^L$ transforming bifundamentally.

7.5 Interpretation

With the construction of the state complete, we can now discuss how it is applied to the theory in question. In the continuum limit, the product of bifundamental fields forms a Wilson line stretched from one boundary to the other. Thus, the state at each fixed point is a bound state of quarks from

either boundary with a Wilson line connecting them. Because the $U(1)$ gauge field in the Coulomb branch originates from the 11D supergravity three-form C, it appears that supergravity somehow mediates the interaction between the two boundaries, becoming strongly coupled and, hence, confining at the blow-down limit to generate the composite state. Also, note that this state is nonlocal in 5D, and is only localized in the 4D limit where the extra dimension shrinks to zero size and the heterotic string description is restored.

Now, let us discuss the symmetry breaking pattern in more detail. We've shown that the deconstructed theory predicts that chiral fields at the boundaries confine and form a bifundamental field charged under (at the very least) a global symmetry, $SU(3)_{global} \times SU(3)_{global}$. When the E_0 theory is deformed away from its fixed point, however, we see that the theory is no longer confined and there is a doublet at either boundary charged under individual $SU(2)_{global}$'s. These doublets are also oppositely charged under the $U(1)_{gauge}$ that is present in the Coulomb branch of E_0. Thus we have states with charges

$$X : (2,1)_{\frac{3}{2}}, \qquad\qquad Y : (1,2)_{-\frac{3}{2}} \tag{7.32}$$

under $SU(2)_{global} \times SU(2)_{global} \times U(1)_{gauge}$.[5]

This decomposition seems highly irregular; somehow a global $SU(3)_{global} \times SU(3)_{global}$ is broken to a mixed global-gauge $SU(2)_{global} \times SU(2)_{global} \times U(1)_{gauge}$.

[5]The original symmetry breaking is to $SU(2)_{global} \times SU(2)_{global} \times U(1)_{global} \times U(1)_{gauge}$. However, the VEV in the perturbative regime is not invariant under $U(1)_{global}$ but a mixture of $U(1)_{global}$ and $U(1)_{gauge}$ which we refer to simply as $U(1)_{gauge}$ above. See [20] for more detail.

The issue is that anomaly consistency at the fixed point is satisfied with only a global symmetry, but the blow-up procedure is not. The E_0 Coulomb branch is one-dimensional, so in order to blow up the fixed point along the Coulomb branch, there must necessarily be a $U(1)$ gauge field. The only symmetry breaking consistent with the superpotential is the one above, so this particular resolution of the orbifold requires that the boundary $SU(3)$'s be gauged. Thus, we are led to the conclusion that the state with the above symmetry breaking pattern will occur uniquely for the orbifold with $E_6 \times SU(3) \times E_6' \times SU(3)'$ gauge symmetry, as this is the only orbifold with $SU(3)$ gauge symmetries on both boundaries.

It is important to note that the presence of the bound state alone does not require that the $SU(3)$'s be gauged; it is the symmetry-breaking pattern that requires gauged $SU(3)$'s. The state is simply the product of an E_0 SCFT, necessarily present at the blow-down limit of a $\mathbb{CP}^2$, being compactified on $S^1/\mathbb{Z}_2$. These blown-down $\mathbb{CP}^2$'s describe the fixed points of any $T^6/\mathbb{Z}_3$ orbifold, regardless of how the gauge symmetries are broken. However, if there are no $SU(3)$ gauge groups following the orbifold symmetry breaking, then there is no way to charge the state under the boundary gauge fields. Thus, we believe the state decouples from the boundaries and is not present when deriving the spectrum using heterotic string theory.

Following our line of reasoning, there may in fact be another instance of this state. Specifically, the spectrum of the $E_6 \times SU(3) \times E_8'$ orbifold theory contains an interesting twisted state, with charge $3(\mathbf{1}, \mathbf{3}; \mathbf{1})$. The presence

of this state might indicate that the global symmetries of the state we have created are capable of being gauged on any boundary where the E_8 there is broken to an $SU(3)$ subgroup. As only one side has its gauge symmetry broken in such a way, the other $SU(3)$ remains global. Note, however, that this state is not consistent with the superpotential derived above that breaks the symmetry to $SU(2) \times SU(2) \times U(1)$. Thus, while a fixed point of the orbifold can be resolved, it will not be along the Coulomb branch of E_0. Other scalar fields present in the spectrum must be given nonzero VEV's to resolve it, and the analysis above is not applicable.

Chapter 8

$\mathbb{Z}_4$ Orbifold

From Table 2.1, the root lattice needed to build the necessary torus for the $\mathbb{Z}_4$ orbifold is $SO(5) \times SO(5) \times SU(2) \times SU(2)$. Similar to the case of $\Lambda_{SU(3)}$, we can plot $\Lambda_{SO(5)}$ and $\Lambda_{SU(2)\times SU(2)}$ since they both have rank 2. This is done in Fig. 8.1. On the first two dimensions z^1, z^2, the root lattice of $SO(5)$ identifies points on $\mathbb{C}$ by

$$z^i \sim z^i + 1, \quad z^i \sim z^i + \tau, \tag{8.1}$$

where $\tau = \frac{1}{\sqrt{2}} e^{\frac{\pi}{4} i}$. On z^3 the $SU(2) \times SU(2)$ root lattice identifies points on $\mathbb{C}$ by

$$z^3 \sim z^3 + 1, \quad z^3 \sim z^3 + e^{\frac{\pi}{2} i} = z^3 + i. \tag{8.2}$$

This torus can then be orbifolded by acting with the $\mathbb{Z}_4$ twist listed in Table 2.1:

$$z^i \to e^{(2\pi i) r_i / 4} z^i. \tag{8.3}$$

The necessary twist vector for the $\mathbb{Z}_4$ orbifold is $\vec{r} = (1, 1, -2)$. Unlike in the $\mathbb{Z}_3$ case, the coordinates here are not treated uniformly by the twist; the first two coordinates receive a quarter-twist, while the third receives a half-twist. The first two coordinates have fixed points at

$$z^i_{fixed} = 0, \frac{1}{2}, \quad i = 1, 2. \tag{8.4}$$

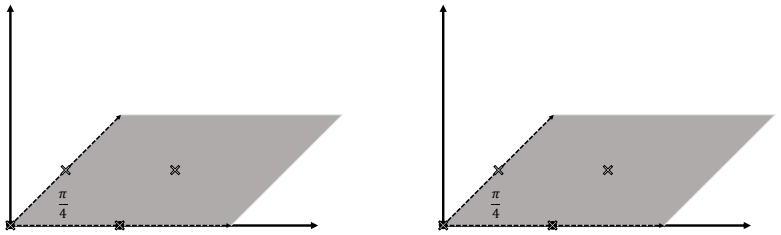

(a) $SO(5)$ (b) $SO(5)$

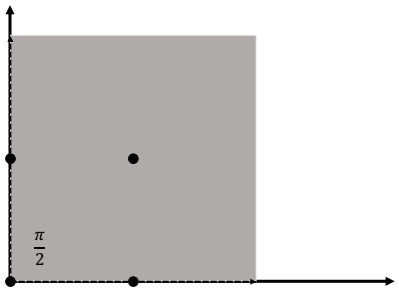

(c) $SU(2) \times SU(2)$

Figure 8.1: The root lattice for each coordinate z^i. The gray region signifies the fundamental domain of the torus in each complex dimension. The solid points are the fixed points of the $\mathbb{Z}_4$ action on each T^2, while the lightly colored x's mark the $\mathbb{Z}_2$ fixed points of the 2-twist. Note that the entire $SU(2) \times SU(2)$ root lattice is fixed under the 2-twist.

The third coordinate has fixed points at

$$z^3_{fixed} = 0, \frac{1}{2}, \frac{i}{2}, \frac{1+i}{2} \tag{8.5}$$

There are thus $2 \times 2 \times 4 = 16$ fixed points on this orbifold.

The $\mathbb{Z}_3$ orbifold only had one independent twisted sector, as the 1-twisted sector and 2-twisted sector are conjugates. In the $\mathbb{Z}_4$ case, however, the

1-twisted sector is conjugate to the 3-twisted sector, and there is an additional self-conjugate 2-twisted sector. We thus have two twisted sectors that we must consider. The 2-twisted sector will have twist vector $\vec{r}_2 = 2(1,1,-2) = (2,2,-4)$. This then acts on the coordinates as

$$\left(z^1, z^2, z^3\right) \to \left(e^{\pi i} z^1, e^{\pi i} z^2, e^{-2\pi i} z^3\right) = \left(-z^1, -z^2, z^3\right). \tag{8.6}$$

The 2-twist acts like a $\mathbb{Z}_2$ twist on z^1 and z^2, while acting trivially on z^3. This is essentially just a compactification on $T^4/\mathbb{Z}_2 \times T^2$, and so we are really dealing with a 6D orbifold compactified to 4D on a T^2! On $T^4/\mathbb{Z}_2$, there are 16 fixed points corresponding to $z^1_{fixed}, z^2_{fixed} \in \{0, 1/2, \tau/2, (1+\tau)/2\}$. Upon compactification to 4D, these become the location of fixed tori corresponding to the z^3-direction. However, we cannot neglect the action of the entire $\mathbb{Z}_4$ on these fixed tori. Four of them are invariant under the twist, $z^1_{fixed}, z^2_{fixed} \in \{0, 1/2\}$. This is only possible if they are in fact orbifolded themselves, $T^2/\mathbb{Z}_2$. Each of these has four $\mathbb{Z}_4$ fixed points corresponding to those in the z^3-direction.

The remaining 12 tori have $z^1_{fixed}, z^2_{fixed} \in \{\tau/2, (1+\tau)/2\}$. The 1-twist identifies $\tau/2 \to (1+\tau)/2$, so these tori are pairwise identified with each other. This creates a much more complicated fixed point structure than in the $\mathbb{Z}_3$ case. There are four fixed $T^2/\mathbb{Z}_2$'s with four $\mathbb{Z}_4$ fixed points each. There are no isolated fixed points; all fixed points are located on these smaller-dimensional fixed surfaces. Additionally, there are $12/2 = 6$ independent fixed T^2's with no fixed points.

On the fixed surfaces, the 2-twist on the coordinates must be met with

a similar double action in the gauge shift. The only possible gauge groups on $T^4/\mathbb{Z}_2$ are E_8, $E_7 \times SU(2)$, and $SO(16)$, and so every possible $\mathbb{Z}_4$ gauge group found from shifting by $\vec{s}$ must be a subgroup of the corresponding $\mathbb{Z}_2$ gauge group found after shifting by $2\vec{s}$. These gauge groups for all consistent shift vectors are listed in Table 8.1. The untwisted spectra of these groups consist of the untwisted spectra from 6D (in representations of the 4D gauge group), as well as the residual states from the breaking of the 6D gauge group to the subgroup in 4D.

Going further, the total gauge groups consistent with eq. (2.12) must also be consistent in the 6D gauge groups. Specifically, the allowed combinations of gauge groups on $T^6/\mathbb{Z}_4$ must descend from one of the allowed combinations of gauge groups on the $T^4/\mathbb{Z}_2$ orbifold, $E_7 \times SU(2) \times E_8'$ or $E_7 \times SU(2) \times SO(16)'$. The 2-twisted spectra are simply derived from the twisted spectra of the corresponding 6D model, in appropriate representations of the broken gauge group. The 1-twisted spectra, however, must be calculated using the methods alluded to earlier. The results are tabulated in Table 8.2. We can once again identify peculiar states charged across the bulk. In the 1-twisted sector, models 4, 9, and 12 all contain such states. In the case of model 4, however, there is an anomalous $U(1)$ gauge symmetry so, as discussed earlier, we will not consider it any further. In addition, there are 2-twisted states in models 5 and 6 that are charged across the bulk. Unlike the 1-twisted states, however, these are not localized at the fixed points. Rather, they propogate across all of the fixed T^2's and $T^2/\mathbb{Z}_2$'s. Due to the individual nature

Normalized Shift Vector	$T^6/\mathbb{Z}_4$ Gauge Group	$T^4/\mathbb{Z}_2$ Gauge Group	Untwisted Spectrum
$\frac{1}{4}(0^8)$	E_8	E_8	$\emptyset$
$\frac{1}{4}(2^2,0^6)$	$E_7 \times SU(2)$	E_8	$(\mathbf{56},\mathbf{2})$
$\frac{1}{4}(1^2,0^6)$	$E_7 \times U(1)$	$E_7 \times SU(2)$	$2(\mathbf{56})_1 + (\mathbf{1})_2 + (\mathbf{1})_{-2}$
$\frac{1}{4}(2,1^2,0^5)$	$E_6 \times SU(2) \times U(1)$	$E_7 \times SU(2)$	$2[(\overline{\mathbf{27}},\mathbf{2})_1 + (\mathbf{1},\mathbf{2})_{-3}] + (\overline{\mathbf{27}},\mathbf{1})_{-2} + (\mathbf{27},1)_2$
$\frac{1}{4}(4,0^7)$	$SO(16)$	E_8	$\mathbf{128}_c$
$\frac{1}{4}(2,0^7)$	$SO(14) \times U(1)$	$SO(16)$	$2(\mathbf{64}_s)_1 + (\mathbf{14}_v)_2 + (\mathbf{14}_v)_{-2}$
$\frac{1}{4}(3,1,0^6)$	$SO(12) \times SU(2) \times U(1)$	$E_7 \times SU(2)$	$2[(\mathbf{32}_s,\mathbf{1})_{-1} + (\mathbf{12}_v,\mathbf{2})_1] + (\mathbf{32}_c,\mathbf{1})_0 + (\mathbf{1},\mathbf{1})_2 + (\mathbf{1},\mathbf{1})_{-2}$
$\frac{1}{4}(2^3,0^5)$	$SO(10) \times SU(4)$	$SO(16)$	$2(\mathbf{16}_c,\overline{\mathbf{4}}) + (\mathbf{10}_v,\mathbf{6})$
$\frac{1}{4}(3,1^5,0^2)$	$SU(8) \times SU(2)$	$E_7 \times SU(2)$	$2(\overline{\mathbf{28}},\mathbf{2}) + (\mathbf{70},\mathbf{1})$
$\frac{1}{4}(1^7,-1)$	$SU(8) \times U(1)$	$SO(16)$	$2[(\overline{\mathbf{56}})_1 + (\mathbf{8})_{-3}] + (\mathbf{28})_2 + (\overline{\mathbf{28}})_{-2}$

Table 8.1: Possible normalized shift vectors satisfying the constraint in eq. (2.11). For each normalized shift vector, the gauge group and the original 6D gauge group in the 2-twisted sector are listed, along with the untwisted spectrum.

of these situations, we shall consider them separately. First let's analyze the 1-twisted states using our devised scheme.

	Gauge Group	1-Twisted (T_1)	2-Twisted (T_2)	Anomalous
1	$E_7 \times U(1) \times SO(14)' \times U(1)'$	$(\mathbf{1};\mathbf{14}_v)_{\frac{1}{2};\text{-}1} + (\mathbf{1};\mathbf{1})_{\text{-}\frac{3}{2};1} + 5(\mathbf{1};\mathbf{1})_{\frac{1}{2};1}$	$(\mathbf{1};\mathbf{14}_v)_{1;0} + (\mathbf{1};\mathbf{1})_{\text{-}1,2} + (\mathbf{1};\mathbf{1})_{\text{-}1,\text{-}2}$	Yes
2	$E_7 \times U(1) \times SO(10)' \times SU(4)'$	$(\mathbf{1};\mathbf{16}_c,\mathbf{1})_{\frac{1}{2}} + 2(\mathbf{1};\mathbf{1},\mathbf{4})_{\frac{1}{2}}$	$(\mathbf{1};\mathbf{10}_v,\mathbf{1})_{\text{-}1} + (\mathbf{1};\mathbf{1},\mathbf{6})_1$	Yes
3	$SO(12) \times SU(2) \times U(1) \times SO(14)' \times U(1)'$	$(\mathbf{12}_v,\mathbf{1};\mathbf{1})_{\frac{1}{2};1} + 2(\mathbf{1},\mathbf{2};\mathbf{1})_{\text{-}\frac{1}{2};1}$	$(\mathbf{1},\mathbf{1};\mathbf{14}_v)_{1;0} + (\mathbf{1},\mathbf{1};\mathbf{1})_{\text{-}1;2} + (\mathbf{1},\mathbf{1};\mathbf{1})_{\text{-}1;\text{-}2}$	Yes
4	$SO(12) \times SU(2) \times U(1) \times SO(10)' \times SU(4)'$	$(\mathbf{1},\mathbf{2};\mathbf{1},\mathbf{4})_{\frac{1}{2}}$	$(\mathbf{1},\mathbf{1};\mathbf{10}_v,\mathbf{1})_{\text{-}1} + (\mathbf{1},\mathbf{1};\mathbf{1},\mathbf{6})_1$	Yes
5	$E_6 \times SU(2) \times U(1) \times SU(8)' \times U(1)'$	$(\mathbf{1},\mathbf{2};\mathbf{1})_{\text{-}\frac{3}{2};2} + (\mathbf{1},\mathbf{1};\mathbf{8})_{\frac{3}{2};\text{-}1} + 2(\mathbf{1},\mathbf{1};\mathbf{1})_{\frac{3}{2};2}$	$(\mathbf{1},\mathbf{2};\overline{\mathbf{8}})_{0;\text{-}1}$	Yes
6	$SU(8) \times SU(2) \times SU(8)' \times U(1)'$	$(\mathbf{8},\mathbf{1};\mathbf{1})_2$	$(\mathbf{1},\mathbf{2};\mathbf{8})_1$	Yes
7	$E_6 \times SU(2) \times U(1) \times E_8'$	$2(\mathbf{1},\mathbf{2};\mathbf{1})_{\text{-}\frac{3}{2}} + (\overline{\mathbf{27}},\mathbf{1};\mathbf{1})_{\text{-}\frac{1}{2}} + 5(\mathbf{1},\mathbf{1};\mathbf{1})_{\frac{3}{2}}$	$(\overline{\mathbf{27}},\mathbf{1};\mathbf{1})_1 + (\mathbf{1},\mathbf{1};\mathbf{1})_{\text{-}3} + 2(\mathbf{1},\mathbf{2};\mathbf{1})_0$	No
8	$E_6 \times SU(2) \times U(1) \times SO(16)'$	$(\mathbf{1},\mathbf{1};\mathbf{16}_v)_{\frac{3}{2}}$	$(\overline{\mathbf{27}},\mathbf{1};\mathbf{1})_1 + (\mathbf{1},\mathbf{1};\mathbf{1})_{\text{-}3} + 2(\mathbf{1},\mathbf{2};\mathbf{1})_0$	Yes
9	$E_6 \times SU(2) \times U(1) \times E_7' \times SU(2)'$	$(\mathbf{1},\mathbf{2};\mathbf{1},\mathbf{2})_{\text{-}\frac{3}{2}} + 2(\mathbf{1},\mathbf{1};\mathbf{1},\mathbf{2})_{\frac{3}{2}}$	$(\mathbf{27},\mathbf{1};\mathbf{1},\mathbf{1})_{\text{-}1} + (\mathbf{1},\mathbf{1};\mathbf{1},\mathbf{1})_3 + 2(\mathbf{1},\mathbf{2};\mathbf{1},\mathbf{1})_0$	No
10	$SU(8) \times SU(2) \times E_8'$	$2(\mathbf{8},\mathbf{1};\mathbf{1}) + (\overline{\mathbf{8}},\mathbf{2};\mathbf{1})$	$(\mathbf{28},\mathbf{1};\mathbf{1}) + 2(\mathbf{1},\mathbf{2};\mathbf{1})$	No
11	$SU(8) \times SU(2) \times SO(16)'$	$\emptyset$	$(\mathbf{28},\mathbf{1};\mathbf{1}) + 2(\mathbf{1},\mathbf{2};\mathbf{1})$	No
12	$SU(8) \times SU(2) \times E_7' \times SU(2)'$	$(\mathbf{8},\mathbf{1};\mathbf{1},\mathbf{2})$	$(\overline{\mathbf{28}},\mathbf{1};\mathbf{1},\mathbf{1}) + 2(\mathbf{1},\mathbf{2};\mathbf{1},\mathbf{1})$	No

Table 8.2: Twisted spectra of all $\mathbb{Z}_4$ models. Each model has 16 T_1 states (one at each fixed point), 6 T_2 and 6 $\overline{T}_2$ states (from the fixed T^2's), and an additional 4 T_2 states (from the fixed $T^2/\mathbb{Z}_2$'s). The other 4 $\overline{T}_2$ states are projected out by the $\mathbb{Z}_2$ action. The $U(1)$ gauge anomalies are also indicated.

8.1 Deriving the Brane Web

The resolution of the fixed points for the $\mathbb{Z}_4$ orbifold is a Hirzebruch surface, $\mathbb{F}_2$, with a toric diagram of the form in Fig. 8.2. The dual brane

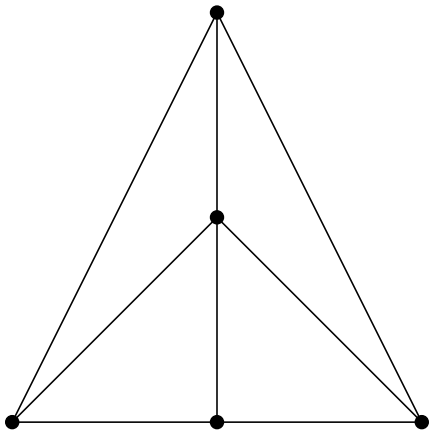

Figure 8.2: The toric diagram for the $\mathbb{C}^3/\mathbb{Z}_4$ (resolved) fixed point.

web is derived in Fig. 8.3. This brane web corresponds to $SU(2)$ SYM with $\theta = 2\pi$. This is the theory we discussed before with "maximum Chern-Simons number" for $SU(2)$. From a field theory point of view, it should flow to a 5D fixed point with $E_1 = SU(2)$ global symmetry. However, the point at which this occurs in the moduli/parameter space, namely $\phi = t_0 = 0$, is also the point at which the parallel seminfinite legs in Fig. 8.3c become coincident, and the 6D physics here is nontrivial as strings become tensionless. The nontrivial 6D physics occurring in our model at this point is the blow-down of 6D $\mathbb{Z}_2$ fixed points, and so we see t_0 corresponds with this blow-down parameter, while ϕ corresponds to the blow-down of the 4D $\mathbb{Z}_4$ fixed points on these fixed surfaces upon compactification from 6D to 4D. The deconstruction data gathered from

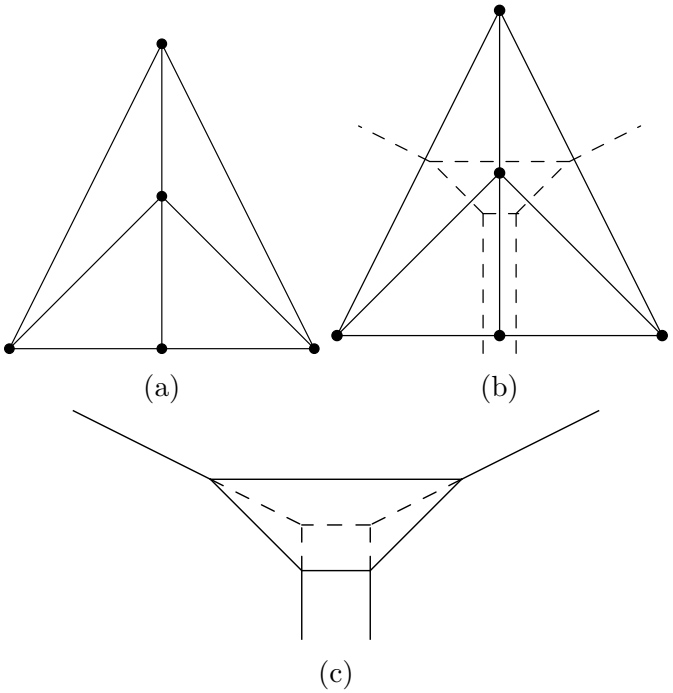

Figure 8.3: Converting the toric diagram to a brane web: (a) the toric diagram, (b) an overlay of the conversion, and (c) the brane web with blow down indicated by the dashed line.

this brane web indicates the model will have $N_c = 2$, $N_f = 0$, and $\Delta F = 0$.

8.2 Deconstructing the Fixed Point Theory

Using the data from above, we know that the appropriate quiver for the 5D theory at the $\mathbb{Z}_4$ fixed point must have the form in Fig. 8.4. The lines between nodes in the quiver represent bifundamental fields Φ_ℓ in the $(2, 2)$ of $SU(2)_\ell \times SU(2)_{\ell+1}$. The spectral curve for this theory was analyzed in [23], so we will focus on the relevant results. According to the deconstruction dictionary, the bare coupling at the origin of the Coulomb branch has the

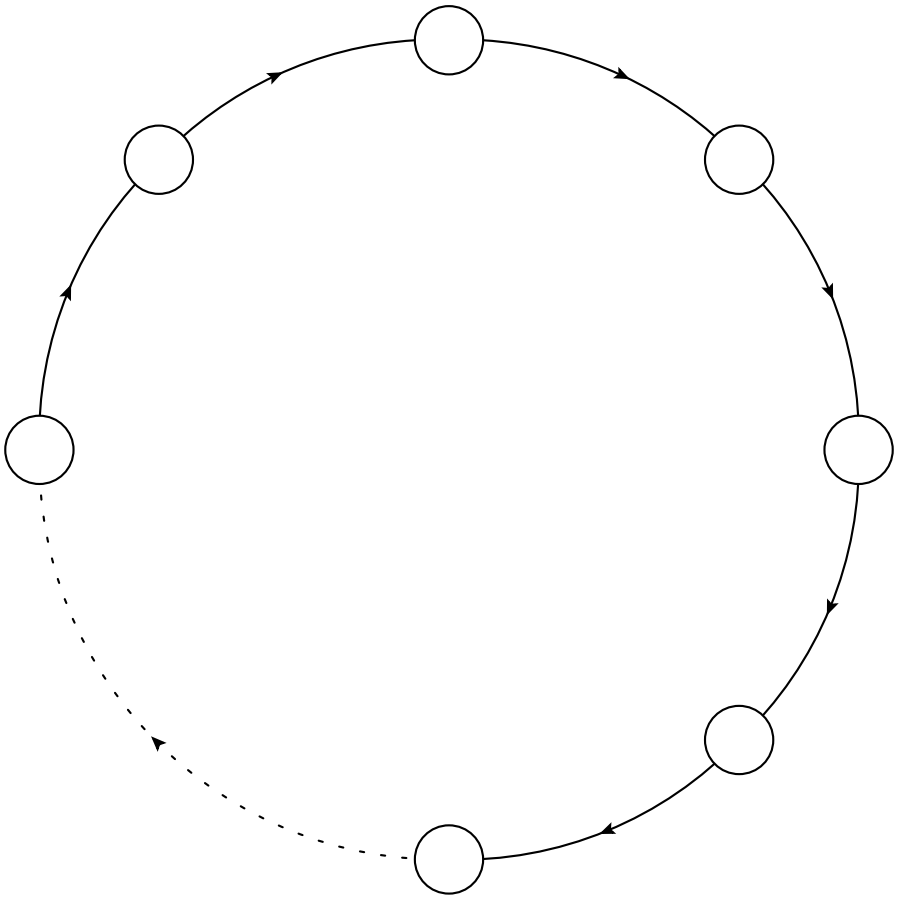

Figure 8.4

form[1]

$$t_0 = \frac{4}{a} \log \left| \frac{v}{\Lambda} \right|, \tag{8.7}$$

where again Λ is the dimensional transmutant introduced by instanton effects. We will be interested in the theory in the blow-down limit $t_0 \to 0$, so eq. (8.7) implies that we will be considering $v \to \Lambda$.

[1]Technically, $h = \frac{4}{a} \log \left| \frac{V}{\Lambda_2} \right|$, where $V = v + \mathcal{O}(\Lambda_2^4)$. In the continuum limit, however, the quantum correction is overwhelmed and the relation $V = v$ becomes exact.

Similar to the previous analysis for $\mathbb{Z}_3$, we would like to deconstruct this theory on an interval. Boundary conditions dictate that the quiver should look like:

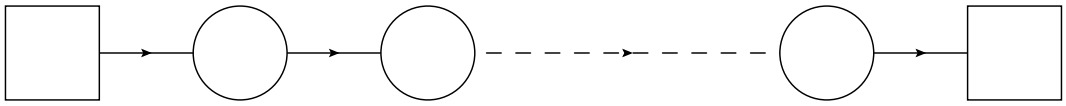

8.3 Spectrum at Blow-down

Relaxing the condition that all of the gauge couplings be equal, we can consider the limit in which $\Lambda_1 \gg \Lambda_\ell \ \forall \ell \neq 1$. In this regime, only the symmetry on the $\ell = 1$ node is gauged, and the rest are global. Neglecting all noninteracting singlets under this gauge symmetry, our matter content consists of gauge doublets Φ_0, Φ_1 charged under individual global symmetries $SU(2)_0$, $SU(2)_2$, as well as their companion singlets σ_0, σ_1. Upon rescaling $\beta\sigma_\ell \to \sigma_\ell$, the superpotential in eq. (6.4) takes the form

$$\begin{aligned} W_{tree,\ell=1} &= \sigma_0 \left(\det \Phi_0 - v^2\right) + \sigma_1 \left(\det \Phi_1 - v^2\right) \\ &= \sigma_0 \left(\mathcal{B}_1 - v^2\right) + \sigma_1 \left(-\widetilde{\mathcal{B}}_1 - v^2\right), \end{aligned} \tag{8.8}$$

where we have defined $\mathcal{Q}_{1\alpha}^T = \left(\Phi_{0(1)(\alpha)} \ \Phi_{0(2)(\alpha)}\right)$, $\widetilde{\mathcal{Q}}_{1\alpha}^T = \left(\Phi_{1(\alpha)(2)} \ \Phi_{1(\alpha)(1)}\right)$, $\mathcal{B}_1 = \mathcal{Q}_1\mathcal{Q}_1$, and $\widetilde{\mathcal{B}}_1 = \widetilde{\mathcal{Q}}_1\widetilde{\mathcal{Q}}_1$. We thus have an effective theory with gauge group $SU(2)$ and $N_f = 2$. We can use the analysis in [29] to determine an effective superpotential

$$W_{eff} = \mathcal{A}_1 \left(\det \mathcal{M}_1 - \mathcal{B}_1\widetilde{\mathcal{B}}_1 - \Lambda_1^4\right), \tag{8.9}$$

where $\mathcal{M}_1 = \mathcal{Q}_1\widetilde{\mathcal{Q}}_1$ and $\mathcal{A}_1$ is simply a singlet field introduced as a Lagrange multiplier. Along with eq. (8.8), this superpotential imposes the following constraints on the VEV's:

$$\langle \mathcal{B}_1 \rangle = -\left\langle \widetilde{\mathcal{B}}_1 \right\rangle = v^2, \tag{8.10}$$

$$\langle \det \mathcal{M}_1 \rangle = \Lambda_1^4 - v^4. \tag{8.11}$$

In general, these VEV's result in chiral symmetry breaking: $SU(2)_0 \times SU(2)_2 \times U(1)_B \to U(1)_V$. As mentioned before, though, we are interested in driving the 5D theory to strong coupling. This is achieved when $v = \Lambda_1$, at which point the constraints take the convenient form

$$\langle \mathcal{B}_1 \rangle = -\left\langle \widetilde{\mathcal{B}}_1 \right\rangle = \Lambda_1^2, \tag{8.12}$$

$$\det \langle \mathcal{M}_1 \rangle = 0. \tag{8.13}$$

Up to global symmetry transformations, this constrains $\mathcal{M}_1$ to take the form

$$\langle \mathcal{M}_1 \rangle = \begin{pmatrix} h^2 & 0 \\ 0 & 0 \end{pmatrix}, \tag{8.14}$$

where h is the modulus. For $h^2 = 0$, the theory confines and the composite fields $\mathcal{M}_1$, $\mathcal{B}_1$, and $\widetilde{\mathcal{B}}_1$ are the appropriate degrees of freedom. There is now chiral symmetry breaking (there always is in the quantum-corrected theory), but it is only $SU(2)_0 \times SU(2)_2 \times U(1)_B \to SU(2)_0 \times SU(2)_2$. The total effective superpotential at $v = \Lambda_1$ looks like

$$W_{tot} \sim \mathcal{A}_1 \det \mathcal{M}_1. \tag{8.15}$$

Now assume $\Lambda_2 \gg \Lambda_\ell$ so that the composite fields $\mathcal{M}_1$ form two gauge doublets under $SU(2)_2$ with global symmetry $SU(2)_0$. Since we will be interested in the limit in which $v \to \Lambda_2$ now, we no longer have $v = \Lambda_1$, but $v \gg \Lambda_1$. Thus, the constraint in eq. (8.11) is once again general, and we can impose it with an effective superpotential for $\mathcal{M}_1$ of the form

$$W_{tot} \sim \mathcal{A}_1 \left(-\frac{1}{v^2} \det \mathcal{M}_1 + \frac{\Lambda_1^4}{v^2} - v^2 \right) \underset{v \gg \Lambda_1}{\to} \mathcal{A}_1 \left(-\mathcal{B}_2 - v^2 \right), \tag{8.16}$$

where $\mathcal{Q}_{2\alpha}^T = \frac{1}{v^2} \left(\mathcal{M}_{1(1)(\alpha)} \ \mathcal{M}_{1(2)(\alpha)} \right)$ and $\mathcal{B}_2 = \mathcal{Q}_2 \mathcal{Q}_2$. We can also define $\widetilde{\mathcal{Q}}_{2\alpha}^T = \left(\Phi_{2(\alpha)(2)} \ \Phi_{2(\alpha)(1)} \right)$, and $\widetilde{\mathcal{B}}_2 = \widetilde{\mathcal{Q}}_2 \widetilde{\mathcal{Q}}_2$ so that the total effective superpotential for fields charged under $SU(2)_2$ can be written similar to eq. (8.8):

$$\begin{aligned} W_{tree,\ell=2} &= \mathcal{A}_1 \left(-\mathcal{B}_2 - v^2 \right) + \sigma_2 \left(\det \Phi_2 - v^2 \right) \\ &= \mathcal{A}_1 \left(-\mathcal{B}_2 - v^2 \right) + \sigma_2 \left(\widetilde{\mathcal{B}}_2 - v^2 \right). \end{aligned} \tag{8.17}$$

We can then set $v = \Lambda_2$ and repeat the previous analysis. This procedure can be performed inductively from node to node until finally we reach the last gauge node, $\ell = L$, in which we are left with a composite field at the strong coupling threshold $v = \Lambda$:

$$\mathcal{M} = \frac{1}{v^{L+1}} \prod_{\ell=0}^{L} \Phi_\ell = \frac{1}{\Lambda^{L+1}} \prod_{\ell=0}^{L} \Phi_\ell. \tag{8.18}$$

This final composite state $\mathcal{M}$ has charge $SU(2)_L \times SU(2)_R$, one $SU(2)$ at each boundary. It has an effective superpotential

$$W_{eff} \sim \mathcal{A} \det \mathcal{M}, \tag{8.19}$$

which imposes the constraint

$$\det \langle \mathcal{M} \rangle = 0. \tag{8.20}$$

Up to a global transformation, $\langle \mathcal{M} \rangle$ thus has the form

$$\langle \mathcal{M} \rangle = \begin{pmatrix} \phi^2 & 0 \\ 0 & 0 \end{pmatrix}. \tag{8.21}$$

For $\phi^2 \neq 0$, the symmetry is broken $SU(2)_L \times SU(2)_R \to U(1)_V$, while it is restored at $\phi^2 = 0$. Following similar arguments from the $\mathbb{Z}_3$ case, in the broken phase the theory is perturbative and there are no light composite fields aside from the modulus. the constituent fields for this modulus, $\Phi_{1(1)}$ and $\Phi_{L(1)}$, are charged under the residual $U(1)_{gauge} \times U(1)_V$ symmetry as

$$\Phi_{1(1)} : \ (1,1), \quad \Phi_{L(1)} : \ (-1,-1). \tag{8.22}$$

In the blown-up phase corresponding to this broken symmetry, the VEV's of Φ_1 and Φ_L are not invariant under $U(1)_V$. We can compensate it with a gauge transformation, defining a new gauge charge $Q_{new} = Q_{gauge} - Q_V$; the states are then singlets under $U(1)_{new}$. As with the $\mathbb{Z}_3$ case, we see that we now have global-to-gauge symmetry breaking, which seems to indicate that while the symmetries at the boundaries need only be global for the sake of deconstruction, they should be gauged to consistently blow up the fixed points alon the VEV of this scalar.

8.4 Interpretation

Looking at the models in Table 8.2 it is pretty simple to see the potential for this state. For instance, model 9 has a $(\mathbf{2};\mathbf{2})$ state in it from the $SU(2)$'s in $E_6 \times SU(2) \times U(1) \times E_7' \times SU(2)'$. This is an obvious candidate for the

composite state we have built. Additionally, model 12 there is an $(\mathbf{8};\mathbf{2})$ state charged under $SU(8) \times SU(2) \times E_7' \times SU(2)'$. While this theory does not have the precise state in which we are interested, it is still possible that this could be related to the composite state. To see this, consider the non-Abelian anomalies as in [39]. The only gauge group that is not automatically anomaly free is the $SU(8)$. The local 4D contributions to its anomaly come from uniquely 4D untwisted states, 2-twisted states, and 1-twisted states. The first of these is local to the M9-brane, while the second is simply inherited from the 6D orbifold theory. In order to cancel these anomalies, it is required that there be two states charged under the $\mathbf{8}$ of $SU(8)$. Assume the states formed a doublet localized on the M9-brane, $(\mathbf{8},\mathbf{2};\mathbf{1},\mathbf{1})$. Then along with the $(\mathbf{2};\mathbf{2})$ composite state, at this boundary there would be $8 + 2 = 10$ total $SU(2)$ doublets. This would have the low energy effective theory of $SU(2)$ gauge theory with $N_f = 5$ flavors. For $N_f = 5$, the theory is conjectured to flow into an interacting conformal field theory [29]. The physics in this case is highly nontrivial, but the gauge singlet state formed from these would then transform under the remaining gauge symmetries as $(\mathbf{8},\mathbf{1};\mathbf{1},\mathbf{2})$, as desired. This is only a conjecture, and would not be applicable if the states were not charged under $SU(2)$, but it is still promising. There are currently no other "obvious" mechanisms with which to impart $SU(8)$ charge on the $(\mathbf{2};\mathbf{2})$ in a natural way.

There are also 2-twisted states that seem to be charged across the bulk, namely those in models 5 and 6. These 2-twisted states descend from the 6D

orbifold theory on $T^4/\mathbb{Z}_2$. In both cases, the 6D theory has gauge group $E_7 \times SU(2) \times SO(16)'$. In fact, this is simply the 6D theory we considered earlier with a state charged across the bulk, the $(\mathbf{1}, \mathbf{2}; \mathbf{16}_v)$ half-hypermultiplet. This state has been explained using brane engineering and so poses no quandry. Upon compactification to 4D, the 6D 1-twisted state S_1 decomposes as

$$S_1 \to T_2 + \overline{T}_2. \tag{8.23}$$

In both cases, the 2-twisted state in T_2 is charged under $SU(2) \times SU(8)'$, either $(\mathbf{2}; \mathbf{8})$ or $(\mathbf{2}; \overline{\mathbf{8}})$. This is consistent with eq. (8.23), where

$$(\mathbf{2}; \mathbf{16}_v) \to (\mathbf{2}; \mathbf{8}) + (\mathbf{2}; \overline{\mathbf{8}}). \tag{8.24}$$

These states are thus uninteresting from 4D point of view.

Chapter 9

$\mathbb{Z}_{6-I}$ Orbifold

There are two $\mathbb{Z}_6$ orbifolds that yield consistent 4D theories, labeled $\mathbb{Z}_{6-I}$ and $\mathbb{Z}_{6-II}$. The first of these orbifolds, $\mathbb{Z}_{6-I}$, requires a torus built from the $G_2 \times G_2 \times SU(3)$ root lattice acting on $\mathbb{C}^3$. The fundamental domains for this construction are given in Fig. 9.1. On z^1 and z^2 the G_2 root lattice identifies points on $\mathbb{C}$ by

$$z^i \sim z^i + 1, \quad z^i \sim z^i + \tau, \tag{9.1}$$

where here $\tau = \frac{1}{\sqrt{3}} e^{\frac{\pi}{6} i}$. As before, the $SU(3)$ root lattice identifies points on $\mathbb{C}$ for z^3 by

$$z^3 \sim z^3 + 1, \quad z^3 \sim z^3 + e^{\frac{\pi}{3} i}. \tag{9.2}$$

The orbifold action on this T^6 is a $\mathbb{Z}_6$ twist:

$$z^i \to e^{(2\pi i) r_i / 6} z^i. \tag{9.3}$$

The appropriate twist vector for this orbifold is $\vec{r} = (1, 1, -2)$. Like the $\mathbb{Z}_4$ case before, the coordinates are not treated equally under the twist. The first two receive a 1/6-twist, under which only the origin is fixed:

$$z^i_{fixed} = 0 \quad i = 1, 2. \tag{9.4}$$

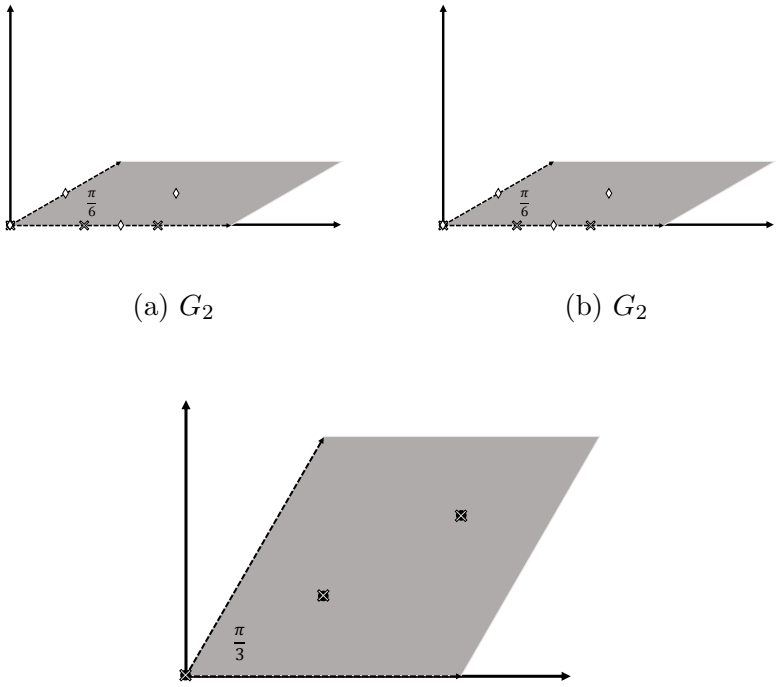

(a) G_2 (b) G_2

(c) $SU(3)$

Figure 9.1: The root lattice for each coordinate z^i. The gray region signifies the fundamental domain of the torus in each complex dimension. There is only one fixed point of the $\mathbb{Z}_{6-I}$ action on each G_2 torus and three on the $SU(3)$ torus, symbolized with solid points, while the lightly colored x's mark the $\mathbb{Z}_3$ fixed points of the 2-twist. The white diamonds mark the $\mathbb{Z}_2$ fixed points of the 3-twist. Note that the entire $SU(3)$ root lattice is fixed under the 3-twist.

For z^3, however, the orbifold only acts as a 1/3-twist, which on the $SU(3)$ root lattice has fixed points as in the $\mathbb{Z}_3$ case:

$$z^3_{fixed} \in \{0, \frac{1}{\sqrt{3}}e^{\frac{\pi i}{6}}, \frac{2}{\sqrt{3}}e^{\frac{\pi i}{6}}\}. \tag{9.5}$$

There is thus a total of $1 \times 1 \times 3 = 3$ fixed points of the total action on the T^6.

Under two twists, the normalized twist vector becomes $\vec{\phi} = 2\times(\frac{1}{6}, \frac{1}{6}, -\frac{2}{6}) = (\frac{1}{3}, \frac{1}{3}, -\frac{2}{3})$. In other words, the 2-twist is simply the $\mathbb{Z}_3$ orbifolding that we discussed earlier! On the G_2 root lattice, this $\mathbb{Z}_3$ twist has fixed points at

$$z^i_{fixed} \in \{0, \frac{1}{3}, \frac{2}{3}\}. \tag{9.6}$$

The 2-twist action on z^3 has the same fixed points as the 1-twist action, as they are just conjugate actions:

$$z^3_{fixed} \in \{0, \frac{1}{\sqrt{3}}e^{\frac{\pi i}{6}}, \frac{2}{\sqrt{3}}e^{\frac{\pi i}{6}}\}. \tag{9.7}$$

This would naively give $3 \times 3 \times 3 = 27$ fixed points again. However, as in the $\mathbb{Z}_4$ case we must see how the 1-twist acts on these fixed points. On the $SU(3)$ root lattice, these points are still distinct since the 1-twist and 2-twist produce identical fixed points. On the G_2 root lattice the $\mathbb{Z}_6$ action identifies the fixed point at $z = 1/3$ with the one at $z = 2/3$. These points are thus not distinct. The fixed point at the origin is not identified with another fixed point and remains distinct. Thus, of the original 27 fixed points, three distinct points remain at the origin while the remaining 24 fixed points are pairwise identified with each other, for a total of $3 + 24/2 = 15$ fixed points.

Finally, there is a 3-twist with normalized twist vector $\vec{r} = 3\times(\frac{1}{6}, \frac{1}{6}, -\frac{2}{6}) = (\frac{1}{2}, \frac{1}{2}, -2)$. This acts on the coordinates as

$$\left(z^1, z^2, z^3\right) \to \left(e^{\pi i}z^1, e^{\pi i}z^2, e^{-4\pi i}z^3\right) = \left(-z^1, -z^2, z^3\right), \tag{9.8}$$

i.e., this is the same action as the 2-twist of the $\mathbb{Z}_4$ orbifold in the previous section! Specifically, this acts as a $\mathbb{Z}_2$ twist on the first two coordinates while leaving the third invariant. This has the appearance of a $T^4/\mathbb{Z}_2$ orbifold that is further compactified on a torus. On the G_2 root lattice, the $\mathbb{Z}_2$ action has four fixed points:

$$z^i_{fixed} \in \{0, \frac{1}{2}, \frac{\tau}{2}, \frac{1+\tau}{2}\}, \tag{9.9}$$

while the entire $SU(3)$ root lattice is fixed under the twist. This naively gives $4 \times 4 = 16$ fixed points of the $T^4/\mathbb{Z}_2$ which then become fixed tori on $T^6/\mathbb{Z}_{6-I}$. Once again, however, we must check how the full $\mathbb{Z}_6$ twist acts on the fixed structures. On the G_2 root lattice, the fixed point at $z = 0$ is invariant under the full twist. This implies that the torus present at $z^{1,2} = 0$ must itself be orbifolded, $T^2/\mathbb{Z}_3$. There are three fixed points of this orbifold, and in fact we have already seen what it looks like in Table 7.2. The fixed points of this 2D orbifold are actually simultaneously $\mathbb{Z}_3$ and $\mathbb{Z}_6$ fixed points in the full 6D orbifold, further complicating the singular structure.

The remaining 15 tori are not invariant under the full twist. There is a sequence of identities for the $\mathbb{Z}_2$ fixed points on the G_2 root lattice under the full $\mathbb{Z}_6$ action,

$$z : \frac{1}{2} \to \frac{1+\tau}{2} \to \frac{\tau}{2} \to \frac{1}{2} \tag{9.10}$$

so that the fixed tori form triplets under identification. Thus, there are only $15/3 = 5$ independent fixed T^2's in addition to the fixed $T^2/\mathbb{Z}_3$. The total fixed structure is given in Table 9.1.

k-twist	Fixed Structures	Independent #
$k = 1$	3 $\mathbb{Z}_6$ fixed point	1
$k = 2$	27 $\mathbb{Z}_3$ fixed point	15
$k = 3$	15 $\mathbb{Z}_2$ fixed T^2	5
	1 $\mathbb{Z}_2$ fixed $T^2/\mathbb{Z}_3$	1

Table 9.1

As with the $\mathbb{Z}_4$ case, the fixed tori mentioned above support 6D fields from the original $\mathbb{Z}_2$ theory on them in appropriate representations of the unbroken gauge groups. For $\mathbb{Z}_6$ orbifolds, there are 26 such 4D gauge groups with appropriate gauge shift vectors, but all of these gauge groups descend from either E_8, $SO(16)$, or $E_7 \times SU(2)$ in the 6D $\mathbb{Z}_2$ orbifold. In fact, each $\mathbb{Z}_6$ gauge group also has a corresponding $\mathbb{Z}_3$ gauge group from the 2-twist sector, corresponding to the gauge groups in Table 7.1. Rather than listing all of these groups or all of the spectra for the consistent $E_8 \times E_8$ subgroups (there are 58 of them), we will simply mention interesting examples as they become relevant. For tables with all of these models (with $U(1)$ charges largely neglected), consult [38]. For a more in-depth exploration of individual models, the orbifolder has proven quite useful as well [40].

9.1 Deriving the Brane Web

The resolution of the fixed points for the $\mathbb{Z}_{6-I}$ orbifold has a toric diagram of the form in Fig. 9.2.

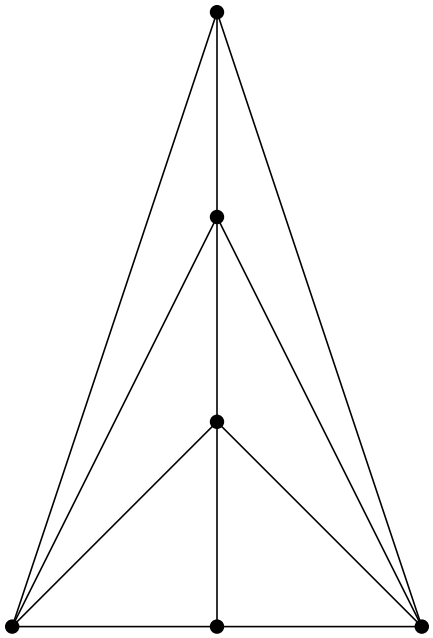

Figure 9.2: The toric diagram for the $\mathbb{C}^3/\mathbb{Z}_{6-I}$ (resolved) fixed point.

This has a dual brane web as derived in Fig. 9.3. The brane web is that of $SU(3)$ SYM with maximal Chern-Simons number $k = 3$. There are three parameters in this theory corresponding to the bare coupling t_0 and the two moduli of the $SU(3)$ gauge group ϕ_1, ϕ_2. As with the $\mathbb{Z}_4$ case, driving the parameter $t_0 \to 0$ corresponds to blowing down the fixed tori in the 3-twist sector, while $\phi_1, \phi_2 \to 0$ corresponds to the $\mathbb{Z}_{6-I}$ and $\mathbb{Z}_3$ fixed points. The superconformal theories at the fixed points of generic $SU(N)$ gauge theories

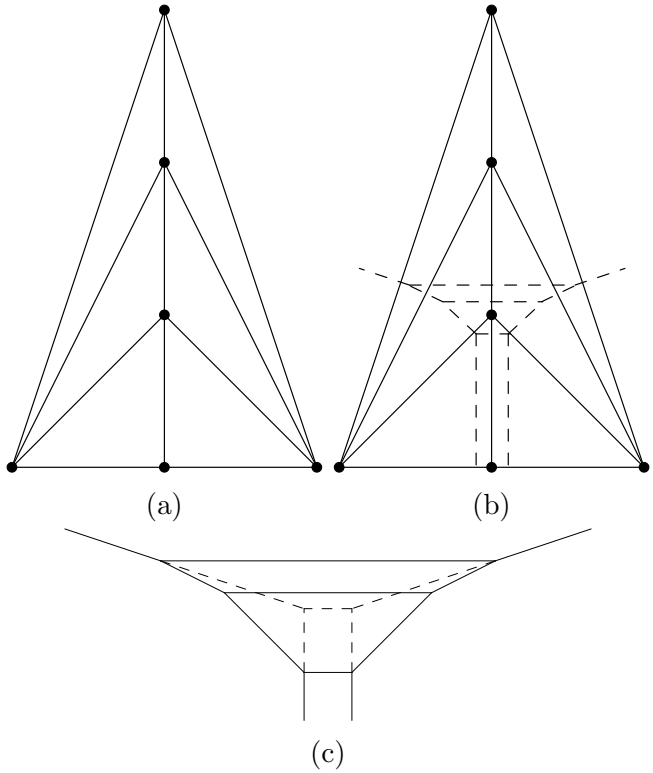

Figure 9.3: Converting the toric diagram to a brane web: (a) the toric diagram, (b) an overlay of the conversion, and (c) the brane web with blow down indicated by the dashed line.

were discussed in [41], but we will not need much of this content so we can instead focus on the deconstruction of this theory. The brane web corresponds to a deconstruction with $N_c = 3$, $N_f = 0$, and $\Delta F = 0$.

9.2 Deconstructing the Fixed Point Theory

Using the data from above, we know that the appropriate quiver for the 5D theory at the $\mathbb{Z}_{6-I}$ fixed point must have the form in Fig. 9.4. The

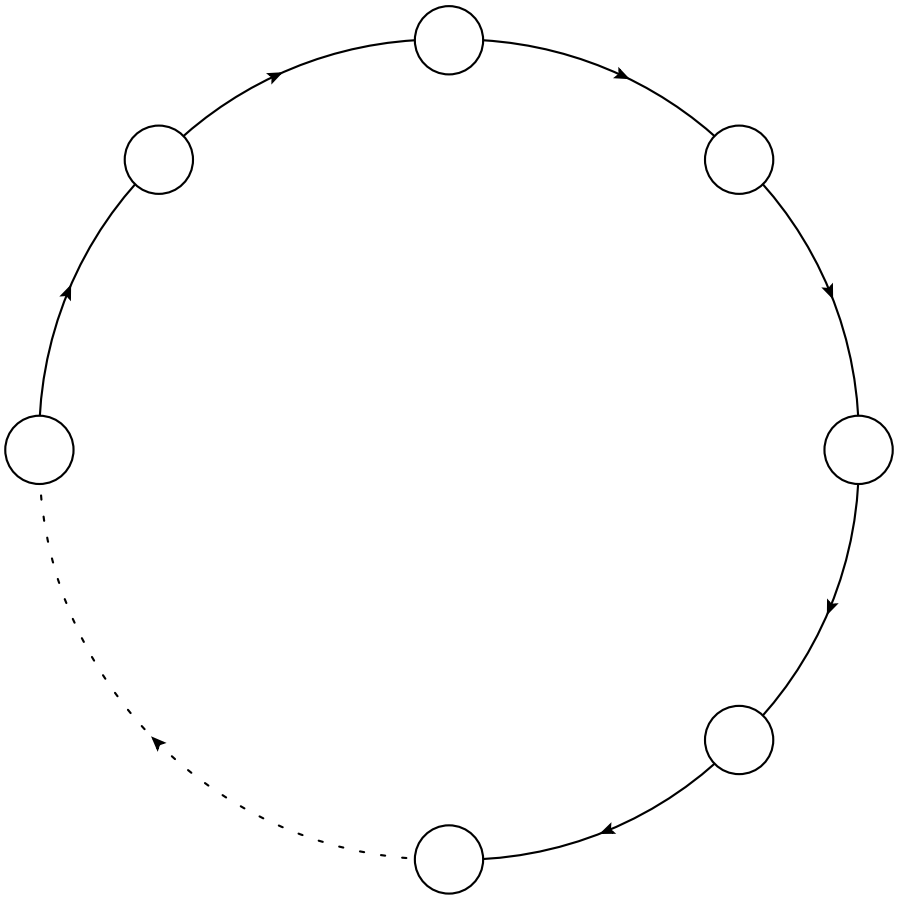

Figure 9.4

nodes represent $SU(3)$ gauge symmetries, and the lines between nodes represent bifundamental fields $(\mathbf{3}, \overline{\mathbf{3}})$ charged under $SU(3)_\ell \times SU(3)_{\ell+1}$. Through analysis of the spectral curve [23], we find that the bare coupling t_0 takes the form

$$t_0 = \frac{6}{a} \log \left| \frac{v}{\Lambda} \right|, \tag{9.11}$$

and the 6D $\mathbb{Z}_2$ blow-down at $t_0 = 0$ corresponds to $v = \Lambda$.

We modify the quiver in the same fashion as before to deconstruct com-

pactification on an interval. The quiver corresponds to

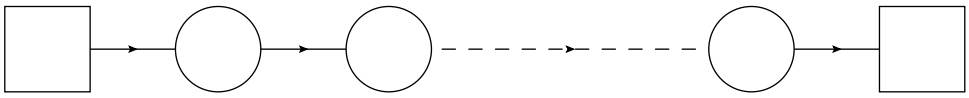

where the circular nodes are gauged $SU(3)$'s, while the squares represent global $SU(3)$'s.

9.3 Spectrum at Blow-down

The analysis that follows is very reminiscent of that for the $\mathbb{Z}_4$ orbifold. Relaxing the condition that all of the gauge couplings be equal, we can consider the limit in which $\Lambda_1 \gg \Lambda_\ell \ \forall \ell \neq 1$. In this regime, only the symmetry on the $\ell = 1$ node is gauged, and the rest are global. Neglecting all non-interacting singlets under this gauge symmetry, our matter content consists of gauge triplets Φ_0, Φ_1 charged under individual global symmetries $SU(3)_0$, $SU(3)_2$, as well as their companion singlets σ_0, σ_1. Upon rescaling $\beta\sigma_\ell \to \sigma_\ell$, the superpotential in eq. (6.4) takes the form

$$\begin{aligned} W_{tree,\ell=1} &= \sigma_0 \left(\det \Phi_0 - v^3\right) + \sigma_1 \left(\det \Phi_1 - v^3\right) \\ &= \sigma_0 \left(\mathcal{B}_1 - v^3\right) + \sigma_1 \left(-\widetilde{\mathcal{B}}_1 - v^3\right), \end{aligned} \tag{9.12}$$

following similar definitions to the $\mathbb{Z}_4$ example. This is another case with $N_f = N_c$, so we once again have an effective superpotential

$$W_{eff} = \mathcal{A}_1 \left(\det \mathcal{M}_1 - \mathcal{B}_1 \widetilde{\mathcal{B}}_1 - \Lambda_1^6\right), \tag{9.13}$$

where $\mathcal{A}_1$ is simply a singlet field introduced as a Lagrange multiplier. Along with eq. (9.12), this superpotential imposes the following constraints on the VEV's:

$$\langle \mathcal{B}_1 \rangle = -\left\langle \widetilde{\mathcal{B}}_1 \right\rangle = v^3, \tag{9.14}$$

$$\langle \det \mathcal{M}_1 \rangle = \Lambda_1^6 - v^6. \tag{9.15}$$

In general, these VEV's result in chiral symmetry breaking: $SU(3)_0 \times SU(3)_2 \times U(1)_B \to U(1)_V$. As mentioned before, though, we are interested in driving the 5D theory to strong coupling. This is achieved when $v = \Lambda_1$, at which point the constraints take the convenient form

$$\langle \mathcal{B}_1 \rangle = -\left\langle \widetilde{\mathcal{B}}_1 \right\rangle = \Lambda_1^3, \tag{9.16}$$

$$\det \langle \mathcal{M}_1 \rangle = 0. \tag{9.17}$$

Up to global symmetry transformations, this constrains $\mathcal{M}_1$ to take the form

$$\langle \mathcal{M}_1 \rangle = \begin{pmatrix} h_1^2 & 0 & 0 \\ 0 & h_2^2 & 0 \\ 0 & 0 & 0 \end{pmatrix}, \tag{9.18}$$

where h_1, h_2 are the moduli. For $h_1^2 = h_2^2 = 0$, the theory confines and the composite fields $\mathcal{M}_1$, $\mathcal{B}_1$, and $\widetilde{\mathcal{B}}_1$ are the appropriate degrees of freedom. There is now chiral symmetry breaking, but it is only $SU(3)_0 \times SU(3)_2 \times U(1)_B \to SU(3)_0 \times SU(3)_2$. The total effective superpotential at $v = \Lambda_1$ looks like

$$W_{tot} \sim \mathcal{A}_1 \det \mathcal{M}_1. \tag{9.19}$$

Now assume $\Lambda_2 \gg \Lambda_\ell$ so that the composite fields $\mathcal{M}_1$ form three gauge triplets under $SU(3)_2$ with global symmetry $SU(3)_0$. Since we will be

interested in the limit in which $v \to \Lambda_2$ now, we no longer have $v = \Lambda_1$, but $v \gg \Lambda_1$. Thus, the constraint in eq. (9.15) is once again general, and we can impose it with an effective superpotential for $\mathcal{M}_1$ of the form

$$W_{tot} \sim \mathcal{A}_1 \left(-\frac{1}{v^3} \det \mathcal{M}_1 + \frac{\Lambda_1^6}{v^3} - v^3 \right) \underset{v \gg \Lambda_1}{\to} \mathcal{A}_1 \left(-\mathcal{B}_2 - v^3 \right), \tag{9.20}$$

where $\mathcal{Q}_2$ is built from the $\mathcal{M}_1$'s as in the $\mathbb{Z}_4$ case and $\mathcal{B}_2 = \mathcal{Q}_2 \mathcal{Q}_2 \mathcal{Q}_2$. We can also define $\widetilde{\mathcal{Q}}_2$ with the Φ_2's so that the total effective superpotential for fields charged under $SU(3)_2$ can be written similar to eq. (9.12):

$$\begin{aligned} W_{tree,\ell=2} &= \mathcal{A}_1 \left(-\mathcal{B}_2 - v^3 \right) + \sigma_2 \left(\det \Phi_2 - v^3 \right) \\ &= \mathcal{A}_1 \left(-\mathcal{B}_2 - v^3 \right) + \sigma_2 \left(\widetilde{\mathcal{B}}_2 - v^3 \right). \end{aligned} \tag{9.21}$$

We can then set $v = \Lambda_2$ and repeat the previous analysis. This procedure can be performed inductively from node to node until finally we reach the last gauge node, $\ell = L$, in which we are left with a composite field at the strong coupling threshold $v = \Lambda$:

$$\mathcal{M} = \frac{1}{v^{L+1}} \prod_{\ell=0}^{L} \Phi_\ell = \frac{1}{\Lambda^{L+1}} \prod_{\ell=0}^{L} \Phi_\ell. \tag{9.22}$$

Thus, we have a final composite state $\mathcal{M}$ with charge $SU(3)_L \times SU(3)_R$, one $SU(3)$ at each boundary.

9.4 Interpretation

The effective superpotential for this composite state looks similar to that of the $\mathbb{Z}_4$ case,

$$W_{eff} \sim \mathcal{A} \det \mathcal{M}, \tag{9.23}$$

but the implications in this case are quite different. This superpotential imposes the constraint

$$\det \langle \mathcal{M} \rangle = 0, \tag{9.24}$$

so that $\langle \mathcal{M} \rangle$ must have the form (up to global transformations)

$$\langle \mathcal{M} \rangle = \begin{pmatrix} \phi_1^2 & 0 & 0 \\ 0 & \phi_2^2 & 0 \\ 0 & 0 & 0 \end{pmatrix}, \tag{9.25}$$

i.e., it must be at most rank 2. As it turns out, this rank has an interpretation in terms of the fixed structures of the orbifold. We have already mentioned that letting $t_0 \to 0$ as we have corresponds to blowing down the fixed tori of the 3-twist, but we can also consider the case where $\phi_2 \to 0$ along with t_0 while ϕ_1 remains arbitrary. At this locus of the moduli space, the theory looks just like the $\mathbb{Z}_3$ model along its Coulomb branch. The VEV of $\mathcal{M}$ is rank 1, so the global symmetry is $SU(2)_L \times SU(2)_R \times U(1)_V$ for $\phi_1 \neq 0$ and enhances to $SU(3)_L \times SU(3)_R$ for $\phi_1 = 0$ as before. This is a reflection of the fact that there are $\mathbb{Z}_3$ fixed points coincident with the $\mathbb{Z}_{6-I}$ fixed points under study. For generic $\phi_1, \phi_2 \neq 0$, The symmetry is broken to $U(1)_{V'} \times U(1)_V$ with enhancement to the full $SU(3)_L \times SU(3)_R$ when $\phi_1 = \phi_2 = 0$.

Unfortunately, the increased fixed structure complexity comes with increased complexity in the spectra of these models as well. One such occurence is the $E_7 \times SU(2) \times SO(16)'$ model with twisted spectrum in Table 9.2. The 3-twist spectrum consists of $5(\mathbf{1}, \mathbf{2}; \mathbf{16}_v)$, one for each of the 5 fixed tori. This is a reflection of the origin of these $(\mathbf{2}; \mathbf{16}_v)$ twisted states. One would expect an additional state for the remaining independent fixed point of the 6D $\mathbb{Z}_2$

action. However, this is not simply a torus but is instead an orbifolded torus, $T^2/\mathbb{Z}_3$. This $\mathbb{Z}_3$ action on the torus projects out the 6D states everywhere but at the fixed points where it acts invariantly. At these points, the states seem to survive as 1-twisted states at the fixed points. This suggests that the origin of these twisted spectra is more intricate than in the previous cases.

Gauge Group	1-twist	2-twist	3-twist
$E_7 \times SU(2) \times SO(16)'$	$3(\mathbf{1},\mathbf{2};\mathbf{16}_v)$	$123(\mathbf{1},\mathbf{1};\mathbf{1})$	$5(\mathbf{1},\mathbf{2};\mathbf{16}_v)$

Table 9.2

Perhaps more perplexing than the example above is the fact that no single model has a 1-twisted spectrum with a charge $(\mathbf{3};\mathbf{3})$ state! The simplest model to illustrate this is the $E_7 \times SU(2) \times E_6' \times SU(3)'$ model in Table 9.3. This model is clearly a $\mathbb{Z}_2$ twist on the first E_8 with the second left alone and a $\mathbb{Z}_3$ twist on the second E_8 with the first left alone. It thus has no obvious states from its 2-twisted or 3-twisted sectors to lend to its 1-twisted sector, and so we expect its 1-twisted state charged across the bulk to be explained by the composite state constructed above. This state, however, does not have charge $(\mathbf{3};\mathbf{3})$ as we would expect from the state we built, but $(\mathbf{2};\mathbf{3})$ instead. Focusing on just a single fixed point, we see that we have the spectrum

$$2(\mathbf{1},\mathbf{3};\mathbf{1},\mathbf{2}) + (\mathbf{27},\mathbf{1};\mathbf{1},\mathbf{1}) + (\mathbf{1},\overline{\mathbf{3}};\mathbf{1},\mathbf{1}) + 2(\mathbf{1},\mathbf{1};\mathbf{1},\mathbf{2}). \tag{9.26}$$

The composite state above cannot explain this on its own and is open to further investigation.

Gauge Group	1-twist	2-twist	3-twist
$E_6 \times SU(3) \times E_7' \times SU(2)'$	$6(\mathbf{1},\mathbf{3};\mathbf{1},\mathbf{2})$	$15(\mathbf{27},\mathbf{1};\mathbf{1},\mathbf{1})+$ $39(\mathbf{1},\overline{\mathbf{3}};\mathbf{1},\mathbf{1})$	$5(\mathbf{1},\mathbf{1};\mathbf{56},\mathbf{1})+$ $22(\mathbf{1},\mathbf{1};\mathbf{1},\mathbf{2})$

Table 9.3

The last model worth mentioning is in Table 9.4. This model has a lot of features similar to the $\mathbb{Z}_4$ model with the $(\mathbf{2};\mathbf{8})$ state. Namely, there is $SU(3) \times SU(3)'$ gauge symmetry present but a state in the $(\mathbf{6},\mathbf{1};\mathbf{3})$ of $SU(6) \times SU(3) \times SU(3)'$. This may have a potential bound state interpretation like that conjectured for the $\mathbb{Z}_4$ model, but would require further analysis beyond what was presented here through deconstruction.

Gauge Group	1-twist	2-twist	3-twist
$E_6 \times SU(3) \times SU(6)' \times$ $SU(3)' \times SU(2)'$	$3(\mathbf{1},\mathbf{3};\mathbf{6},\mathbf{1},\mathbf{1})$	$15(\mathbf{1},\overline{\mathbf{3}};\mathbf{1},\overline{\mathbf{3}},\mathbf{1})$	$5(\mathbf{1},\mathbf{1};\mathbf{20},\mathbf{1},\mathbf{1})+$ $5(\mathbf{1},\mathbf{1};\mathbf{6},\overline{\mathbf{3}},\mathbf{1})+$ $6(\mathbf{1},\mathbf{1};\overline{\mathbf{6}},\mathbf{3},\mathbf{1})+$ $22(\mathbf{1},\mathbf{1};\mathbf{1},\mathbf{1},\mathbf{2})$

Table 9.4

With this level of obscurity, it is important to emphasize that while these spectra are not simply described by the composite state as in the previous orbifolds, it is still in fact present. It is a product of blowing down the $\mathbb{Z}_{6-I}$ fixed point regardless of the gauge groups present at the boundaries. It may be a question of boundary conditions with this state and these gauge fields,

or perhaps some nontrivial combination of this state and the compactified 6D twisted state.

Chapter 10

Z_7 Orbifold

The final orbifold that we consider is the $\mathbb{Z}_7$ orbifold. There is still much to be done with it, but it is extremely interesting so we will discuss current progress. To start, we need a root lattice of rank 6 on which to wrap $\mathbb{C}^3$ for the initial torus; in this case the lattice of choice is $SU(7)$. Unlike the previous cases, this root lattice does not decompose into three lattices of rank 2, so it cannot be simply represented on individual complex dimensions. In terms of $x^i \in \mathbb{R}^6$, this root lattice acts as

$$\begin{aligned} x^i &\to x^{i+1}, \quad i = 1, ..., 5 \\ x^6 &\to -x^1 - x^2 - x^3 - x^4 - x^5 - x^6. \end{aligned} \tag{10.1}$$

To orbifold this torus, we apply the appropriate twist vector, $\vec{r} = (1, 2, -3)$. Like the $\mathbb{Z}_3$ case, the $\mathbb{Z}_7$ orbifold is a prime orbifold and the only fixed structures are isolated fixed points, seven in all. However, unlike the $\mathbb{Z}_3$ case, there are multiple twisted sectors for the $\mathbb{Z}_7$ orbifold. Conventionally, the twisted sectors considered are the 1-twist, the 2-twist, and the 4-twist[1], with the other k-twisted sectors being conjugate to these.

[1]The 4-twist is the chiral conjugate of the 3-twist, but has nicer properties with the 1-twist and 2-twist

10.1 Deriving the Brane Web

The resolution of the fixed points for the $\mathbb{Z}_7$ orbifold has a toric diagram of the form in Fig. 10.1. It has a dual brane web as in Fig. 10.2. The toric

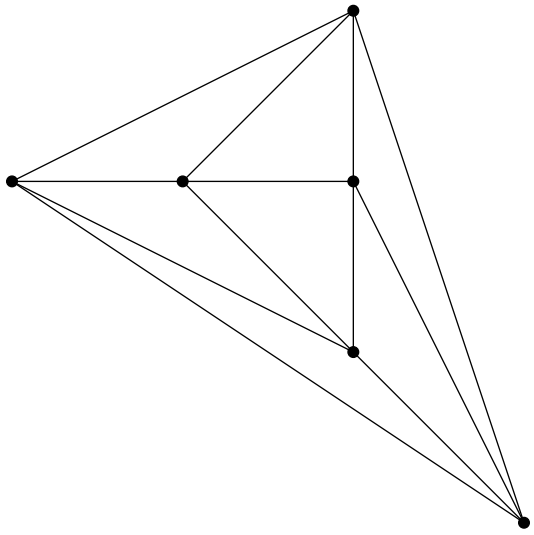

Figure 10.1: The toric diagram for the $\mathbb{C}^3/\mathbb{Z}_7$ (resolved) fixed point.

diagram and brane web are full of interesting features. First, the brane web clearly has three semi-infinite external branes. This corresponds to $3-3=0$ global symmetries at the fixed point. Thus, the theory appears to be isolated like the other prime orbifold $\mathbb{Z}_3$, but there is more structure present. The toric diagram reveals that the three internal points are actually Hirzebruch surfaces $\mathbb{F}_2$ as in the $\mathbb{Z}_4$ case, and this is reflected in the dual brane web. as Fig. 10.3 demonstrates, the same brane web present in the $\mathbb{Z}_4$ fixed point resolution is present three times in the $\mathbb{Z}_7$ resolution (up to an $SL(2,\mathbb{Z})$ transformation). The major difference is that the global parameter associated to the bare coupling in the $\mathbb{Z}_4$ case now acts as the VEV of the modulus along the Coulomb

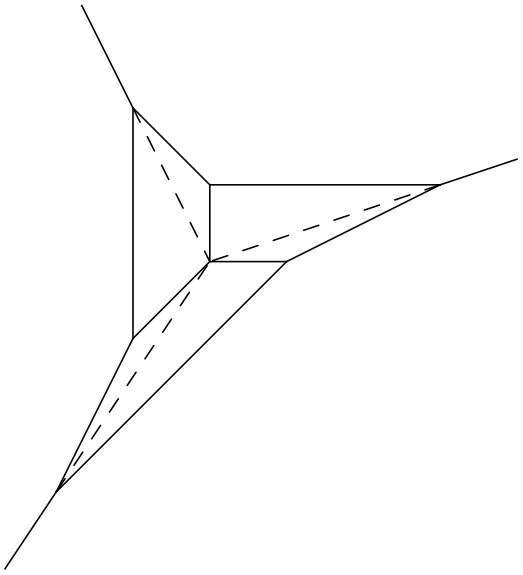

Figure 10.2: The brane web corresponding to the$\mathbb{Z}_7$ fixed point toric diagram.

branch of another $SU(2)$ gauge symmetry! In the end, this demonstrates an $SU(2) \times SU(2) \times SU(2)$ gauge theory along its Coulomb branch with no global symmetry, so there is no way to un-Higgs the individual $SU(2)$'s. Instead, the coupling associated with each $SU(2)$ is a combination of all three VEV's, and the theory does not have enhanced gauge symmetry before reaching the superconformal fixed point at the origin of the moduli space. Additionally, consider the different k-twisted sectors. The 1-twist has twist vector $\vec{r} = (1, 2, -3)$, so acting repeatedly with it gives

$$\begin{aligned} \vec{r} &= (1, 2, -3), \\ \vec{r}^{\,2} &= (2, 4, -6) = (2, -3, 1), \\ \vec{r}^{\,4} &= (4, 8, -12) = (-3, 1, 2). \end{aligned} \tag{10.2}$$

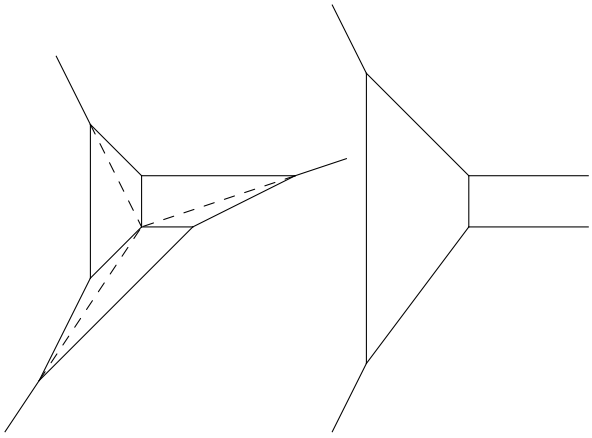

(a) (b)

Figure 10.3: The brane web for (a) the $\mathbb{Z}_7$ fixed point compared to that of (b) the $\mathbb{Z}_4$ fixed point.

We see then that the various k-twists just rotate the $\mathbb{Z}_7$ action on $\mathbb{C}^3$! This is reflected in the E_8 breaking as well [38], where the shift vectors form triplets with identical untwisted spectra.[2] The individual shift vectors in these triplets pair with different shift vectors to consistently break the full $E_8 \times E_8$, however, so they produce unique twisted spectra. In fact, no two shift vectors from one triplet will ever simultaneously pair with two shift vectors from another triplet. There can only be at most one shift vector from a triplet that pairs with at most one shift vector from another triplet.

Unfortunately, we have yet to build a means with which to deconstruct this theory; it may be the case that the addition of matter that is then made

[2]There are a few exceptions to this. The triplets actually exchange which untwisted states have $\sum R^i s_i/7 = 1/7$, $2/7$, or $4/7$ (mod 1). The exceptions are shift vectors which have the same states for each $\sum R^i s_i/7$, and so are self-dual in this regard.

heavy is necessary, as in the $\mathbb{Z}_3$ case. In that instance, the field was necessary to set a scale for the deconstruction threshold and could be discarded following the phase transition to the isolated E_0 SCFT. There is still a lot of analysis necessary to devise a similar strategy, as all of the 5D $SU(2)$ gauge groups must still be tangled with each other no matter how much matter is added to the model. It is important to note, however, that there is no model that has states charged across the bulk without an anomalous $U(1)$. It is not obvious what an analysis of this fixed point will uncover, but the theory there is certainly interesting and worthy of exploration regardless.

Chapter 11

Future Directions

We would like to conclude this work with a collection of open problems that encourage future research.

- As the $\mathbb{Z}_{6-I}$ orbifold demonstrated, the complexity of the fixed structures can quickly become overwhelming. There are models with twisted states charged across the bulk for this orbifold, and yet none of them seem to have a simple explanation in line with the $\mathbb{Z}_3$ and $\mathbb{Z}_4$ orbifolds. The fact that there are $\mathbb{Z}_{6-I}$, $\mathbb{Z}_3$, and compactified 6D $\mathbb{Z}_2$ states all present at these fixed points certainly lends plenty of intricacy with which to investigate further and attempt to substantiate all relevant models.

- The final orbifold that we studied, the $\mathbb{Z}_7$ orbifold, had a particularly interesting 5D field theory. As $\mathbb{Z}_3$ and $\mathbb{Z}_7$ are the only allowable prime orbifolds, it is easy to see that fixed points that are isolated and do not rest on 6D fixed tori correspond to SCFT's that are isolated and do not exist as limits of 5D gauge theories (without the addition of matter). Unlike the E_0 SCFT at the $\mathbb{Z}_3$ fixed point, however, there appears to be little study of this $\mathbb{Z}_7$ SCFT. Simply learning anything about this SCFT would be worthwhile, but we would be particularly interested

in designing the proper deconstruction quiver and studying the moduli space in some detail. In this light, our treatment of it here has been more of a "tip of the iceberg" than a comprehensive analysis.

- The orbifolds with multiple resolutions ($\mathbb{Z}_{6-II}$, $\mathbb{Z}_{8-I}$, $\mathbb{Z}_{8-II}$, $\mathbb{Z}_{12-I}$, and $\mathbb{Z}_{12-II}$) are also open fields for study.In these cases, the difficulties arising from overlapping fixed structures in the $\mathbb{Z}_{6-I}$ orbifold will only be magnified. For instance, for the $\mathbb{Z}_{6-II}$ orbifold there are $\mathbb{Z}_6$ fixed points located at the intersections of $\mathbb{Z}_2$ fixed tori in the z^3 direction with $\mathbb{Z}_3$ fixed tori in the z^2 direction. Thus, the theory has to account for intersecting compactified 6D states and 4D fixed point states. It would likely be advantageous to first solve the issues with the $\mathbb{Z}_{6-I}$ orbifold so that the interaction of these fixed structures is better understood before tackling the models with multiple resolutions.

Bibliography

[1] E. Witten, Nucl. Phys. B **443**, 85 (1995) doi:10.1016/0550-3213(95)00158-O [hep-th/9503124].

[2] M. Dine, P. Y. Huet and N. Seiberg, Nucl. Phys. B **322**, 301 (1989). doi:10.1016/0550-3213(89)90418-5

[3] J. Dai, R. G. Leigh and J. Polchinski, Mod. Phys. Lett. A **4**, 2073 (1989). doi:10.1142/S0217732389002331

[4] L. J. Dixon, J. A. Harvey, C. Vafa and E. Witten, Nucl. Phys. B **261**, 678 (1985). doi:10.1016/0550-3213(85)90593-0

[5] L. J. Dixon, J. A. Harvey, C. Vafa and E. Witten, Nucl. Phys. B **274**, 285 (1986). doi:10.1016/0550-3213(86)90287-7

[6] M. B. Green and J. H. Schwarz, Phys. Lett. B **149**, 117 (1984). doi:10.1016/0370-2693(84)91565-X

[7] W. Fischler, H. P. Nilles, J. Polchinski, S. Raby and L. Susskind, Phys. Rev. Lett. **47**, 757 (1981). doi:10.1103/PhysRevLett.47.757

[8] P. Fayet and J. Iliopoulos, Phys. Lett. B **51**, 461 (1974). doi:10.1016/0370-2693(74)90310-4

[9] P. K. Townsend, *The eleven-dimensional supermembrane revisited*,' Phys. Lett. B 350, 184 (1995) [arXiv:hep-th/9501068].

[10] E. Witten, Nucl. Phys. B **471**, 195 (1996) doi:10.1016/0550-3213(96)00212-X [hep-th/9603150].

[11] A. C. Cadavid, A. Ceresole, R. D'Auria and S. Ferrara, Phys. Lett. B **357**, 76 (1995) doi:10.1016/0370-2693(95)00891-N [hep-th/9506144].

[12] S. Ferrara, R. R. Khuri and R. Minasian, Phys. Lett. B **375**, 81 (1996) doi:10.1016/0370-2693(96)00270-5 [hep-th/9602102].

[13] S. Ferrara, R. Minasian and A. Sagnotti, Nucl. Phys. B **474**, 323 (1996) doi:10.1016/0550-3213(96)00268-4 [hep-th/9604097].

[14] P. Hořava and E. Witten, Nucl. Phys. B **460**, 506 (1996) doi:10.1016/0550-3213(95)00621-4 [hep-th/9510209].

[15] P. Hořava and E. Witten, Nucl. Phys. B **475**, 94 (1996) doi:10.1016/0550-3213(96)00308-2 [hep-th/9603142].

[16] E. Witten, Nucl. Phys. B **460**, 541 (1996) doi:10.1016/0550-3213(95)00625-7 [hep-th/9511030].

[17] D. R. Morrison and N. Seiberg, Nucl. Phys. B **483**, 229 (1997) doi:10.1016/S0550-3213(96)00592-5 [hep-th/9609070].

[18] O. Aharony, A. Hanany and B. Kol, JHEP **9801**, 002 (1998) doi:10.1088/1126-6708/1998/01/002 [hep-th/9710116].

[19] B. Kol and J. Rahmfeld, JHEP **9808**, 006 (1998) doi:10.1088/1126-6708/1998/08/006 [hep-th/9801067].

[20] O. J. Ganor and J. Sonnenschein, JHEP **0205**, 018 (2002) doi:10.1088/1126-6708/2002/05/018 [hep-th/0202206].

[21] V. Kaplunovsky, J. Sonnenschein, S. Theisen and S. Yankielowicz, Nucl. Phys. B **590**, 123 (2000) doi:10.1016/S0550-3213(00)00460-0 [hep-th/9912144].

[22] E. Gorbatov, V. S. Kaplunovsky, J. Sonnenschein, S. Theisen and S. Yankielowicz, JHEP **0205**, 015 (2002) doi:10.1088/1126-6708/2002/05/015 [hep-th/0108135].

[23] A. Iqbal and V. S. Kaplunovsky, JHEP **0405**, 013 (2004) doi:10.1088/1126-6708/2004/05/013 [hep-th/0212098].

[24] E. Di Napoli, V. S. Kaplunovsky and J. Sonnenschein, JHEP **0406**, 060 (2004) doi:10.1088/1126-6708/2004/06/060 [hep-th/0406122].

[25] E. Di Napoli and V. S. Kaplunovsky, JHEP **0703**, 092 (2007) doi:10.1088/1126-6708/2007/03/092 [hep-th/0611085].

[26] C. T. Hill, S. Pokorski and J. Wang, Phys. Rev. D **64**, 105005 (2001) doi:10.1103/PhysRevD.64.105005 [hep-th/0104035].

[27] H. C. Cheng, C. T. Hill, S. Pokorski and J. Wang, Phys. Rev. D **64**, 065007 (2001) doi:10.1103/PhysRevD.64.065007 [hep-th/0104179].

[28] E. Witten, Phys. Lett. B **117**, 324 (1982). doi:10.1016/0370-2693(82)90728-6

[29] N. Seiberg, Phys. Rev. D **49**, 6857 (1994) doi:10.1103/PhysRevD.49.6857 [hep-th/9402044].

[30] K. A. Intriligator, R. G. Leigh and N. Seiberg, Phys. Rev. D **50**, 1092 (1994) doi:10.1103/PhysRevD.50.1092 [hep-th/9403198].

[31] N. Arkani-Hamed, A. G. Cohen and H. Georgi, Phys. Rev. Lett. **86**, 4757 (2001) doi:10.1103/PhysRevLett.86.4757 [hep-th/0104005].

[32] S. Groot Nibbelink, M. Trapletti and M. Walter, JHEP 0703, 035 (2007) doi:10.1088/1126-6708/2007/03/035 [arXiv:hep-th/0701227].

[33] J. Polchinski and E. Witten, Nucl. Phys. B **460**, 525 (1996) doi:10.1016/0550-3213(95)00614-1 [hep-th/9510169].

[34] N. Seiberg, Phys. Lett. B **388**, 753 (1996) doi:10.1016/S0370-2693(96)01215-4 [hep-th/9608111].

[35] O. Aharony and A. Hanany, Nucl. Phys. B **504**, 239 (1997) doi:10.1016/S0550-3213(97)00472-0 [hep-th/9704170].

[36] Y. H. He, hep-th/0209230.

[37] T. Kobayashi and N. Ohtsubo, Phys. Lett. B **257**, 56 (1991). doi:10.1016/0370-2693(91)90858-N

[38] Y. Katsuki, Y. Kawamura, T. Kobayashi, N. Ohtsubo, Y. Ono and K. Tanioka, DPKU-8904.

[39] S. Groot Nibbelink, M. Hillenbach, T. Kobayashi and M. G. A. Walter, Phys. Rev. D **69**, 046001 (2004) doi:10.1103/PhysRevD.69.046001 [hep-th/0308076].

[40] H. P. Nilles, S. Ramos-Sanchez, P. K. S. Vaudrevange and A. Wingerter, Comput. Phys. Commun. **183**, 1363 (2012) doi:10.1016/j.cpc.2012.01.026 [arXiv:1110.5229 [hep-th]].

[41] K. A. Intriligator, D. R. Morrison and N. Seiberg, Nucl. Phys. B **497**, 56 (1997) doi:10.1016/S0550-3213(97)00279-4 [hep-th/9702198].